THESIS APPROVAL

GRADUATE SCHOOL, KASETSART UNIVERSITY

Master of Engineering (Chemical Engineering)
DEGREE

Chemical Engineering   Chemical Engineering
FIELD   **DEPARTMENT**

TITLE: Simulation and Design of Ammonia Process from Natural Gas Reforming

NAME: Mr. Nithi Russamee

THIS THESIS HAS BEEN ACCEPTED BY

_____ **THESIS ADVISOR**
(Associate Professor Thongchai Srinophakun, Ph.D.   )

_____ **THESIS CO-ADVISOR**
(Mr. Chanin Panjapornpon, Ph.D.   )

_____ **DEPARTMENT HEAD**
(Associate Professor Phungphai Phanawadee, D.Sc.   )

APPROVED BY THE GRADUATE SCHOOL ON _____

_____ **DEAN**
(Associate Professor Gunjana Theeragool, D.Agr.   )

THESIS

SIMULATION AND DESIGN OF AMMONIA PROCESS FROM
NATURAL GAS REFORMING

NITHI RUSSAMEE

A Thesis Submitted in Partial Fulfillment of
the Requirements for the Degree of
Master of Engineering (Chemical Engineering)
Graduate School, Kasetsart University
2009

Nithi Russamee 2009: Simulation and Design of Ammonia Process from Natural Gas Reforming. Master of Engineering (Chemical Engineering), Major Field: Chemical Engineering, Department of Chemical Engineering. Thesis Advisor: Associate Professor Thongchai Srinophakun, Ph.D. 181 pages.

A comprehensive process model is developed for ammonia process from natural gas reforming. The overall process model composes desulfurization, reforming, CO conversion, CO_2 removal, methanation, synthesis and refrigeration. The proposed model addresses reaction kinetic model using external FORTRAN subroutines. The related properties have been calculated by the SRK-BM method. This study coveres heat integration process and process dynamic and control. The model predictive control and process design are preliminary studied.

The results showed that the feed streams of process air, natural gas, process steam and combustion air are 53000, 32000, 102041 and 178220 scmh; respectively. From the proposed process, 3097 kmol/hr liquid ammonia at purity of 99.82 % can be produced. The heat integration process can improve the energy conservation up to 4.5 percent compared to the original one. The controllability analysis can be performed by changing $\pm$ 10 % of feed temperature to observe the dynamic responses. The responses are well acceptance and drive the process to the original steady-state condition.

_____   _____   ____/____/____

Student's signature   Thesis Advisor's signature

ACKNOWLEDGEMENTS

Nithi Russamee

March 2009

TABLE OF CONTENTS

Page

LIST OF TABLES

LIST OF TABLES (Continued)

LIST OF FIGURES

LIST OF FIGURES (Continued)

LIST OF FIGURES (Continued)

LIST OF ABBREVIATIONS

Ac	=	Catalyst activity
A, B and C	=	Empirical constant
AK	=	Specific rate constant
C	=	Cooler
CH_4	=	Methane
CO	=	Carbon monoxide
CO_2	=	Carbon dioxide
CP	=	Heat capacity flowrate
CSTR	=	Continuously stirred tank reactors
D	=	Diameter
dT	=	Differential temperature change
Ea	=	Activation energy
GHR	=	Gas heated reformers
H	=	Heat
H	=	Enthalpy
H_2	=	Hydrogen
H_2O	=	Water
HEN	=	Heat exchanger network
HTS	=	High temperature shift
htin	=	Inside heat transfer coeffient
htout	=	Outside heat transfer coeffient
k2	=	Reaction rate from reforming reaction
K2	=	Equilibrium constant from reforming reaction
LCA	=	Low cost ammonia process
LTS	=	Low temperature shift
MPC	=	Model predictive control
P	=	Pressure drop
Pi	=	Partial pressure
Pr	=	Prandtl number
PSA	=	Pressure swing absorption

LIST OF ABBREVIATIONS (Continued)

R	=	Gas constant
SS	=	Total number of moles of mixture per mole of methane feed
x_i	=	Mole fraction of component i
Z	=	Tube length

Subscripts

i	=	Component index
j	=	Stages index
m	=	reaction index

Superscripts

F	=	feed stream
L	=	liquid-phase
V	=	Vapor-phase

SIMULATION AND DESIGN OF AMMONIA PROCESS FROM NATURAL GAS REFORMING

INTRODUCTION

The front end of every ammonia plant is a synthesis gas plant converting either natural gas feedstock from a pipeline, typically from offshore gas production wells, naphtha feedstock, or synthetic natural gas product gas from an upstream coal gasification unit into a useful gas mixture commonly referred to as synthesis gas (or syngas) composed of hydrogen, nitrogen, carbon monoxide, carbon dioxide, water and various trace inert gases including methane and argon. In this thesis, the ammonia synthesis from natural gas reforming was considered into process simulation because it was developed to the existing ammonia process from natural gas reforming. Therefore, the ammonia production from natural gas reforming was studied for development the ammonia process.

Ammonia was synthesized from nitrogen and hydrogen by the reversible reaction, and its production was favored by high pressures and low temperatures. Common industrial ammonia synthesis processes consist of a natural gas feed stream flowing into a compressor and then into a catalytic converter bed. The effluent from the converter bed enters a heat exchanger, was cooled therefore continues into a separation device. Most of the ammonia products were removed, while some continues in a recycle loop with a purge to remove inerts. The recycle stream entered another compressor then rejoins the input stream into the reactor.

The synthesis of ammonia was a simple catalytic reaction in which three moles of hydrogen and one mole of nitrogen react to two moles of ammonia. The reaction was highly selective in that no byproducts were formed, the only concern being contaminants in the feed which might poison the catalyst, or inerts, such as methane and argon, which have to be purged from the system. Despite its simplicity, the ammonia synthesis reaction was intrinsically limited by thermodynamic

equilibrium. The equilibrium studies first carried out by Fritz Haber in the early 1900's showed that the synthesis reaction required high pressures and low temperatures, but the extent of conversion was limited and considerable recycle of unreacted gas was required. The effects of the many process variables in the synthesis reaction have been studied by many investigators. The world use Ammonia in the industry was illustrated by Figure 1. From Figure 1, the ammonia was used raw material in many industrials. Steam reforming of light hydrocarbons was the most efficient route, with about 77% of world ammonia capacity being based on natural gas.

Purple sections represent use of ammonia for production of upgraded fertilizers

Source: Fertecon
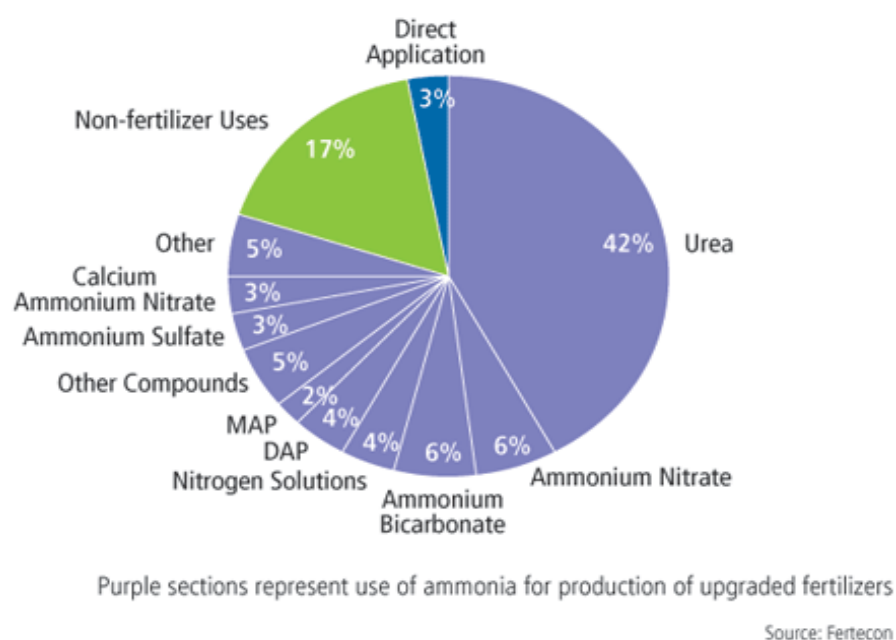
Figure 1 Ammonia is used in the industry

OBJECTIVES

1. To develop ammonia process model for ammonia production from natural gas.

2. To apply heat integration technique for ammonia process model.

3. To study preliminary of the process dynamic and control, the model predictive control, and details of process unit operations design of ammonia process model.

Scopes of work

1. The ammonia production from natural gas reforming process is modeled and simulated by ASPEN PLUS simulator version 2006.5.

2. The heat integration with ammonia process model is studied by ASPEN HX-NET simulator with the constraints of the maximum energy recovery and minimum heat transfer area.

3. The controllability of temperature is studied with ASPEN DYNAMIC simulator.

4. The model predictive control focuses on CSTR recirculation tank.

5. The ammonia process model is evaluated preliminary by ASPEN ICARUS simulator.

LITERATURE REVIEW

This section was divided into three parts. Firstly, the process description ammonia production from natural gas was described. Secondly, the chemical reactions in the process ammonia production were introduced. Finally, the heat exchanger network was used the method Pinch analysis.

1. Process Description

The simulation of Ammonia synthesis with ASPEN software was proposed by Villesca (1997). They used two types of reactor; adiabatic Gibbs and isothermal Gibbs. In Figure 2, all compositions in ammonia process model were simulated. The optimization was also performed on economics point of view.
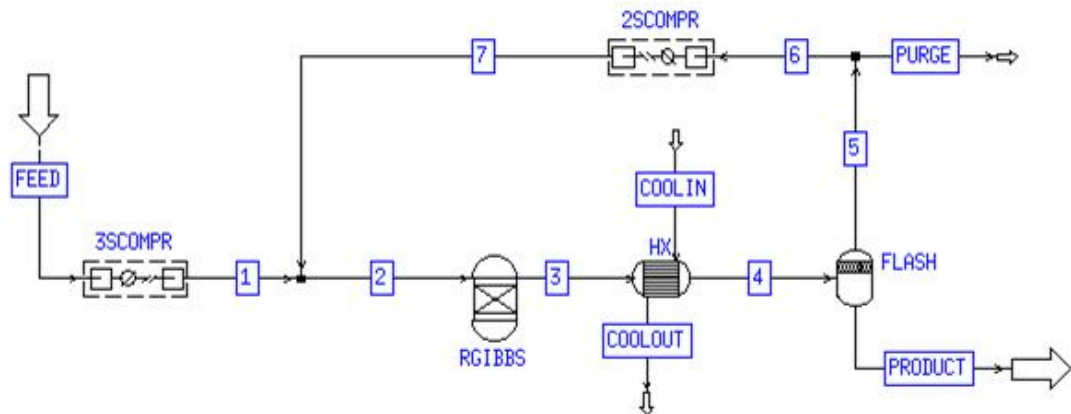
Figure 2 Ammonia process simulation using ASPEN simulator

Ammonia was primarily produced using air, natural gas and water. The process was illustrated by Figure 3. It was called a Steam Reforming Process, and it was utilized by about 75 to 80 percent of ammonia plants worldwide. The step of ammonia production from natural gas reforming was follows these. It consisted of the following five steps: 1) desulfurization, 2) primary and secondary reforming, 3) shift

conversion, 4) carbon dioxide removal and synthesis gas purification, and 5) ammonia synthesis and recovery.

The natural gas was delivered as dry gas containing a maximum of 40 ppm by weight of sulfur, which was a poison for the reformer catalyst. In the first step, sulfur compounds in the natural gas were removed to avoid a potential threat to catalysts that were used in the remaining part of the process. Two reforming steps, these steps were designed to break down CH_4 (methane) in the natural gas into H_2, CO_2, and carbon monoxide (CO). Before ammonia was produced, the CO and CO_2 must be removed from the gas mixture. This was accomplished in a two-step shift conversion, which converted the CO to CO_2, followed by a CO_2 removal step. Water vapor in the gas mixture often reacted with some of the CO to produce more H_2 and CO_2. The gas mixture then was fed to a low temperature shift converter that operates at temperatures range from 200 to 250º C. Here, most of the remaining CO was converted to CO_2. The CO_2 removal operation also was done in two steps: A) a bulk CO_2 removal in which the CO_2 concentration was reduced to a few parts per million, and B) a final purification step. The most common bulk CO_2 removal operation was performed by scrubbing the gas with a methyldiethanolamine or monoethanolamine solution. The remaining CO_2 and CO were removed from the gas stream by converting the CO_2 and CO back to CH_4 by introducing H_2 gas with a nickel catalyst. Cryogenic purification was used to remove the methane from the gas stream. In cryogenic purification, the gas was dried to a very low dew point, and then cooled and expanded in a turbine to liquefy a portion of the stream. The vapor from the partially liquefied stream was scrubbed in a rectifying column to remove almost all CH_4 and about one-half of any unreacted CO_2. At this point the gas was compressed to between 136 and 340 atm (2,000 and 5,000 psi) and then passed over an iron catalyst where the nitrogen and hydrogen react to form ammonia. The design of the ammonia synthesis section varied from plant to plant and dependent upon such factors as pressure chosen for synthesis, capacity of the plant, and thermal requirements for process operation. During the ammonia synthesis, not all the nitrogen and hydrogen were converted to ammonia. The unreacted gases were separated from the ammonia and recycled to the

compressor. The ammonia then was chilled to liquid phase and stored in tanks at atmospheric pressure.
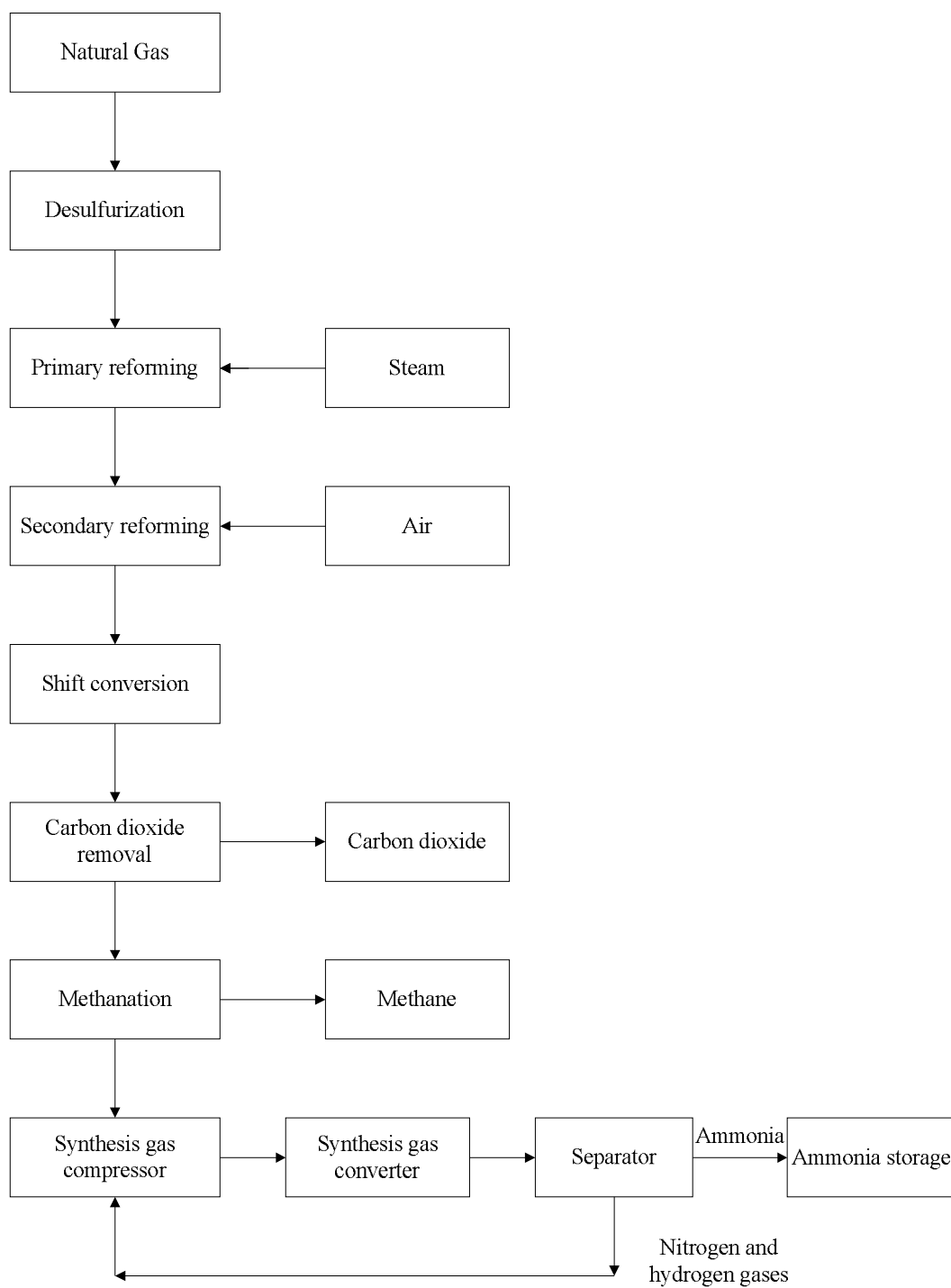
Figure 3 Process ammonia productions from natural gas

1.1 Ammonia process

1.1.1 Reforming Section

In the conventional process, steam reforming was carried out in a fired furnace of the side fired or top fired type. Both needed large surface areas for uniform heat distribution along the length of the catalyst tubes. This process had several disadvantages. For example, it was a thermally inefficient process (about 90% including the convection zone) and there were mechanical and maintenance issues. The process was difficult to control and reforming plants require a large capital investment. Future technologies included the use of Gas Heated Reformers (GHR), which were tubular gas-gas exchangers. In the GHR, the secondary reformer outlet gases supply the reforming heat. Though it was not presently being used widely, GHR had certain advantages over fired furnaces. Kellogg's Reforming Exchanger System is an example of GHR technology. Although GHR results in reduced energy consumption, a comprehensive energy conservation network should be established to maximize the benefits of a GHR system.

1.1.2 Shift Section

The water-gas shift reaction was favorable for producing carbon dioxide which was used as a raw material for urea production. Presently, most plants use a combination of conventional High/Low Temperature Shift (HTS/LTS) or High/Medium/Low Temperature Shift (HTS/MTS/LTS) technology. Another option was a combination of HTS/LTS/Selectoxo technology. While not as common as the other combinations, this arrangement offers advantages that will be discussed later. The most important objectives for this section were a low pressure drop and efficient heat recovery from the process gas.

1.1.3 Carbon Dioxide Removal Section

The removal of carbon dioxide had been performed with solvent absorption and distillation since the inception of ammonia production processes. This section of the ammonia plant was the largest consumer of energy after the cooling water system. The energy consumption was due to thermally inefficient distillation, dissipation of huge amounts of low level heat into the cooling water via product carbon dioxide, and pressurization and depressurization of absorbents. Chemical absorption in the isobaric manufacturing of ammonia can be unattractive because of the very high pressure (100 atm). Therefore, major changed in the existing carbon dioxide removal technologies may be necessary. Replacement technologies may include cryogenic condensation or pressure swing absorption (PSA). Carbon dioxide separation through PSA was offered in the Low Cost Ammonia Process (LCA). PSA was scalable may be more economical because of efficient carbon dioxide recovery at higher pressures. However, further development in this direction was essential for the recovery of high purity carbon dioxide as desired in urea production. Carbon dioxide separation via condensation may also become more attractive due to an increased concentration of carbon dioxide which can be realized with successful hydrogen separation through membranes. This would allow the concentration of carbon dioxide to be increased by 18 to 36 mole percent. This would allow carbon dioxide concentrations in the gas to be reduced to 15% by chilling of the 100 atm front end gases. This method also provides high pressure carbon dioxide for urea production which will reduce the power consumption in the carbon dioxide compressor of the urea plant substantially. The remaining product carbon dioxide gas can be recovered via PSA. A combined PSA and condensation process may solve the problem of carbon dioxide purity from the PSA process.

1.1.4 Final Purification of Synthesis Gases

Methanation process was used conventionally. However, methanation process could result in the loss of hydrogen.

1.1.5 Ammonia Synthesis

Several developments in ammonia synthesis had been made in this part, these developments revolve around the basic principles of reaction, heat recovery, cooling, production ammonia separation, and recycling of synthesis gas.

1.1.5.1 Synthesis Catalyst

After almost 90 years of a monopoly in the ammonia synthesis market, iron catalyst has not been replaced by a precious metal (ruthenium) based catalyst used in the KAAP developed by Kellogg. The KAAP catalyst was reported to be 40% more active than iron catalysts. Research work on low temperature and low pressure catalysts to produce ammonia at 20-40 kg/cm^2g and 100 ^{o}C was being performed at Project and Development India Ltd. (PDIL) according to their in-house magazine. The catalyst being studied was based on cobalt and ruthenium metals and has exhibited few encouraging results.

1.1.5.2 Ammonia Separation

The removal of product ammonia was accomplished via mechanical refrigeration or absorption/distillation. The choice was made by examining the fixed and operating costs. Typically, refrigeration was more economical at synthesis pressures of 100 atm or greater. At lower pressures, absorption/distillation was usually favored.

2. Chemical Reactions in Ammonia Process

2.1 Reforming Unit

The main reaction occurring in the reformer was the conversion of methane to a mixture of CO, CO_2 and H_2:

$$CH_4 + H_2O \rightarrow CO + 3H_2 \qquad \text{(Endothermic)} \qquad (1)$$

$$CO + H_2O \rightarrow CO_2 + H_2 \qquad \text{(Exothermic)} \qquad (2)$$
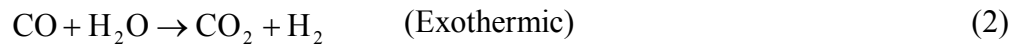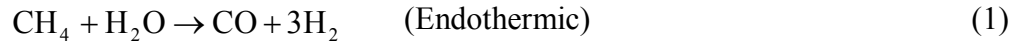
The kinetics expression for Reaction 1, the reforming reaction, (Moe *et al.,* 1965) was as follows:

$$R = k_2 \frac{K_2 P_{CH_4} P_{H_2O}^2 - P_{H_2}^4 P_{CO_2}}{379} \qquad (3)$$

The partial pressures were converted to expressions of molar quantities by assuming ideal gas behavior. The factor 379 was needed to convert the units from SCF to moles.

$$R = \frac{k_2 P^3}{SS^3 379}[K_2(CH_4)(H_2O)^2 - \frac{(H_2)^4(CO_2)}{SS^2}P^2] \qquad (4)$$

SS is the total number of moles of mixture per mole of methane fed.

Moe and Gerhard (1965) arbitrarily set the P^3 term to 1.0 in order to correlate their data taken from pressures above atmospheric. Therefore, the final form of the model did not have a P^3 term, but was lumped in with the specific rate constant k_2 as:

$$k_2 = A_c e^{(\frac{31720}{T+460} - 7.912)} \qquad (5)$$

The factor A_c, catalyst activity, was used in the model to give a reasonable reactor performance for the methane conversion. It may be adjusted such that reactor performance matches plant data. The equilibrium constant, K_2, with units of atm^2, is equal to $K_1 K_3$. (Hyman *et al.,* 1967)

$$K_1 = \exp(-\frac{49,435}{T(F)+460} + 30.707) \text{ atm}^2 \qquad (6)$$

$$K_3 = \exp(\frac{8,240}{T(F)+460} - 4.335) \text{ below } 1,100 \text{ }^O\text{F} \qquad (7)$$

$$K_3 = \exp(\frac{7,351.24}{T(F)+460} - 3.765) \text{ above } 1,100 \text{ }^O\text{F} \qquad (8)$$

where, T(F) was the temperature in °F.

Chemical equilibrium was assumed for the water shift reaction for which the following holds:

$$K_3 = \frac{(H_2)(CO_2)}{(H_2O)(CO)} \qquad (9)$$

The kinetic reactions have been implemented in user kinetics Fortran subroutines of the RPlug model. The Fortran subroutines are REFKIN, DRATE, and KFORMC. Subroutines REFKIN and KFORMC are interface routines necessary to communicate to the Aspen Plus RPlug model with DRATE. This Fortran kinetics subroutine was developed by Mok *et al.,* (1982).

The pressure drop expression adopted was as follows:

$$\frac{dP}{dz} = -P_{fact}(0.04183 + 0.003292Z - 0.0000395Z^2) \qquad (10)$$

where,

Z = tube length (ft)

P = pressure (atm)

P_{fact} = pressure drop factor (a function of catalyst characteristics)

or

$$\Delta P = -P_{fact}(0.04183Z + \frac{1}{2}0.003292Z^2 - \frac{1}{3}0.0000395Z^3) \tag{11}$$

The pressure drop expression had been implemented as a user pressure drop Fortran subroutine of RPlug model. The Fortran subroutine was REFPD. Since the net reaction in the primary reformer was endothermic, the heat-transfer rate was critical to the rate of reaction in the tube. The heat-transfer rate was determined by the tube inside and outside heat-transfer coefficients, the flame temperature, and the gas temperature. The heat transfer from the flame to the outside of the tube occurs primarily by radiation. Here an outside heat transfer coefficient was defined for ease of calculation.

$$\text{Flux} = ht_{in}(T_w - T) = ht_{out}(T_f - T_w) \tag{12}$$

The tube-wall temperature T_w is calculated

$$T_w = \frac{ht_{out}T_f + ht_{in}T}{ht_{out} + ht_{in}} \tag{13}$$

The flux was in units of BTU/hr/ft^2 of inside tube area. The ht_{in} and ht_{out} were the inside and outside heat-transfer coefficients in units of BTU/hr/°F/ft^2 of inside tube-wall area. Both coefficients vary with gas temperature T. The inside heat-transfer coefficient was an overall physical coefficient determined only by the properties of the fluid. Beck *et al.*, (1962) gave the following correlation for estimating ht_{in}:

$$ht_{in}\frac{D_P}{k_f} = 0.4[2.58(Re_p)^{\frac{1}{3}}(Pr)^{\frac{1}{3}} + 0.094(Re_p)^{0.8}(Pr)^{0.8}] \tag{14}$$

Hyman *et al.*, (1967) reported that the factor 0.4 was needed to account for the smaller value of ht_{in} when ring-shaped catalyst was used instead of the pellets used

by Beck *et al.,* (1962). The calculation of the thermal conductivity k_f, viscosity, and heat capacity were taken from Mok *et al.,* (1982).

The heat-transfer rate outside the tube was assumed to be governed by a radiant heat-transfer mechanism:

$$\text{Flux} = \frac{D_{out}}{D_{in}} c(T_{f,r}^4 - T_{w,r}^4) = ht_{out}(T_f - T_w) \tag{15}$$

Where D_{in} and D_{out} are the inside and outside diameters of the tube, c is the product of the Stefan-Boltzman constant and the effective emissivity, $T_{f,r}$ and $T_{w,r}$ are the flame temperature and tube-wall temperature in degrees Rankine.

The heat transfer rate was implemented as user heat transfer Fortran subroutines of RPlug model. The Fortran subroutines are REFHT, KFORMC, HTCOEF, TWALL, BPARM, and RKEQ. Subroutines REFHT and KFORMC are interface routines necessary to interface Aspen Plus RPlug model with other Fortran subroutines developed by Mok *et al.,* (1982) HTCOEF computes the heat transfer coefficient. TWALL computes the tube wall temperature. BPARM and RKEQ are physical property routines used to compute transport properties needed in HTCOEF and TWALL.

The primary reformer was generally represented by 1-3 RPlug reactors in series, representing the number of firing zones of the unit in the plant. This allows the fuel requirements of each fired zone to be calculated separately.

The fuel fed to the reformer contains hydrocarbons higher than methane, whereas equation (1) only represents the reforming of methane. These higher hydrocarbons, however, were rapidly converted to methane and are thus accurately modeled using a simple RSTOIC block prior to the reformer tube with the following reactions:

$$3C_2H_6 + H_2O \rightarrow 5CH_4 + CO \tag{16}$$

$$3C_3H_8 + 2H_2O \rightarrow 7CH_4 + 2CO \tag{17}$$

$$3n\text{-}C_4H_{10} + 3H_2O \rightarrow 9CH_4 + 3CO \tag{18}$$

$$3i\text{-}C_4H_{10} + 3H_2O \rightarrow 9CH_4 + 3CO \tag{19}$$

$$3C_5H_{12} + 4H_2O \rightarrow 11CH_4 + 4CO \tag{20}$$

$$3C_6H_{14} + 5H_2O \rightarrow 13CH_4 + 5CO \tag{21}$$

$$3C_7H_{16} + 6H_2O \rightarrow 15CH_4 + 6CO \tag{22}$$
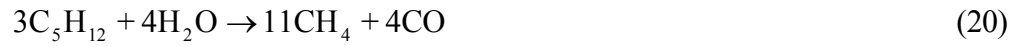
The reformer burners were described by RSTOIC blocks in which the combustion was complete. The burner temperature sets the radiant heat-transfer temperature for the reformer tubes; and the heat generated in the burner was equal to the heat absorbed in the reformer tubes. The combination of the RPlug blocks for the reformer tubes and RSTOIC blocks for the burners provided an accurate simulation of the reformer unit.

2.2 Carbon Monoxide Conversion

2.2.1 Low-Temperature Shift Reactor

The low-temperature shift reactor was modeled as a plug flow reactor, RPlug.

The reaction stoichiometry considered was:

$$CO + H_2O \rightarrow CO_2 + H_2 \qquad (23)$$

The kinetics expression (Slack *et al.,* 1974) was as follows:

$$r_{CO} = A_c \frac{T_{ref}}{T} \left[\frac{k_{LT} Y_{CO} Y_{H_2O}^{1/2} (1 - \frac{K_F}{K_3})}{\frac{1}{P} + k_A Y_{CO} + k_B Y_{CO_2}} \right] \qquad (24)$$

$$K_F = \frac{(Y_{CO_2})(Y_{H_2})}{(Y_{CO})(Y_{H_2O})} \qquad (25)$$

where:

A_c = catalyst activity

k_{LT} = exp (3620/T - 4.32126)

= standard LT catalyst activity in lb-mol/hr/ft^3/atm

K_3 = exp (8240/(T(F)+459.7) - 4.33)

k_A = exp (4580/T - 7.4643)   atm^{-1}

k_B = exp (1500/T - 2.623)   atm^{-1}

T_{ref} = 513.13 K

The reaction kinetics had been implemented in a user kinetics Fortran subroutine under the RPlug model. The Fortran rate subroutine called LTKIN, which called KFORMC for obtaining the component locations.

2.2.2 High-Temperature Shift Reactor

The high-temperature shift reactor was modeled as a plug flow reactor, RPlug.

The reaction stoichiometry considered was:

$$CO + H_2O \rightarrow CO_2 + H_2 \tag{26}$$

The kinetics expression (Slack *et al.,* 1974) was as follows:

$$CO + H_2O \rightarrow CO_2 + H_2 \tag{27}$$

$$r_{CO} = A_c K_{HT} P^{\frac{1}{2}} Y_{CO} \left(\frac{K_f}{K_3}\right) \tag{28}$$

$$K_3 = \exp\left(\frac{8,240}{T(F) + 459.7} - 4.33\right) \text{ below } 1,100 \text{ }^{\circ}F \tag{29}$$

$$K_F = \frac{(Y_{CO_2})(Y_{H_2})}{(Y_{CO})(Y_{H_2O})} \tag{30}$$

where:

A_c = catalyst activity

k_{HT} = exp (10.3375 - 5787.62/T) standard HT catalyst activity in lb- mol/hr/ft^3/atm$^{1/2}$

T = temperature in K

T(F) = temperature in °F

The reaction kinetics was implemented in a user kinetics Fortran subroutine under the RPlug model. The Fortran rate subroutine was HTKIN, which calls KFORMC for obtaining the component locations.

2.3 Carbon Dioxide Removal

The electrolyte solution chemistry had been modeled with a chemistry model. Chemical equilibrium was assumed with all the ionic reactions. In addition, a kinetic REACTION model named NH_3 had been created. In NH_3, all reactions were assumed to be in chemical equilibrium except the reactions of CO_2 with OH^- and the reactions of CO_2 with NH_3.

A. Chemistry

$$2H_2O \leftrightarrow H_3O^+ + OH^- \tag{31}$$

$$CO_2 + 2H_2O \leftrightarrow H_3O^+ + HCO_3^- \tag{32}$$

$$HCO_3^- + H_2O \leftrightarrow H_3O^+ + CO_3^{-2} \tag{33}$$

$$NH_3 + H_2O \leftrightarrow NH_4^+ + OH^- \tag{34}$$

$$H_2NCOO^- + H_2O \leftrightarrow NH_3 + HCO_3^- \tag{35}$$

$$NH_4HCO_3(S) \leftrightarrow NH_4^+ + HCO_3^- \tag{36}$$

$$NH_4HCO_3 \rightarrow NH_4^+ + HCO_3^- \tag{37}$$

B. Reaction

$$NH_3 + H_2O \leftrightarrow NH_4^+ + OH^- \tag{38}$$

$$2H_2O \leftrightarrow H_3O^+ + OH^- \tag{39}$$

$$HCO_3^- + H_2O \leftrightarrow H_3O^+ + CO_3^{-2} \tag{40}$$

$$CO_2 + OH^- \rightarrow HCO_3^- \tag{41}$$

$$HCO_3^- \rightarrow CO_2 + OH^- \tag{42}$$

$$NH_3 + CO_2 + H_2O \rightarrow H_2NCOO^- + H_3O^+ \tag{43}$$

$$H_2NCOO^- + H_3O^+ \rightarrow NH_3 + H_2O + CO_2 \tag{44}$$

$$NH_4HCO_3(S) \leftrightarrow NH_4^+ + HCO_3^- \tag{45}$$
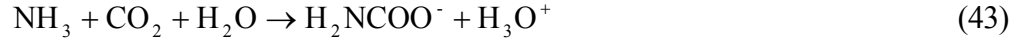
The equilibrium expressions for the reactions were taken from the work of Miles *et al.,* (1997). In addition, the power law expressions were used for the rate-controlled reactions (equation 41-44) and the general power law expression was:

$$r = k(T/T_0)^n \exp[(\frac{-E}{R})(\frac{1}{T} - \frac{1}{T_0})] \prod_{i=1}^{N} C_i^{a_i} \tag{46}$$

(1) If T_0 is not specified, the reduced power law expression was used:

$$r = kT^n \exp(-\frac{E}{RT}) \prod_{i=1}^{N} C_i^{a_i} \tag{47}$$

The kinetic parameters for reactions 41-44 in Table 1 are derived from the work of Pinsent *et al.,* (1956).

Table 1 Parameters k and E in Equation 47

Reaction No.	k	E (cal/mol)
41	4.32e+13	13249
42	2.38e+17	29451
43	1.35e+11	11585
44	4.75e+20	16529

The built-in K_{eq} expression (Equation 48) was used for the salt precipitation reaction of NH_4HCO_3,

$$\ln K_{eq} = A + B/T + C\ln(T) + DT \tag{48}$$

The parameters A, B and C were regressed against SLE data from Trypuc *et al.,* (1981).

Table 2 Parameters A, B and C in Equation 48

Reaction	A	B	C
NH_4HCO_3 salt precipitation	-914.00821	38648.2117	136.174996

2.4 Methanation Unit

The methanation reactor, which removes trace amounts of CO from H_2-rich synthesis feed mixtures, was modeled as a plug flow reactor by RPlug.

Two reactions occur in the methanation reactor:

$$CO + 3H_2 \rightarrow CH_4 + H_2O \tag{49}$$

$$CO_2 + 4H_2 \rightarrow CH_4 + 2H_2O \tag{50}$$

Yadav *et al.,* (1993) developed empirical correlations for the methanation of CO (Equation 49) as part of a laboratory data program. Their correlation, based upon a proposed Langmuir-Hinshelwood mechanism is as follows:

$$r = \frac{A P_{H_2}^{0.5} P_{CO}}{1 + B P_{CO} + C P_{H_2}^{0.5}} \tag{51}$$

Where r is the reaction rate in mol/g.s, P refers to partial pressures in kPa, and A, B and C are empirical constants determined at each temperature. Yadav *et al.,* (1993) covered a broad range of CO concentrations, but for methanation we are mainly interested in very low CO levels. At low CO concentrations, Equation 51 simplifies to the following form:

$$r = \frac{A}{C^2} \frac{P_{CO}}{P_{H_2}^{0.5}} \tag{52}$$

The data reported at 503, 513 and 529 K were fitted to a simple Arrhenius equation as follows:

$$r = 0.314 e^{(1,300[\frac{1}{T} - \frac{1}{513}])} \{ \frac{P_{CO}}{P_{H_2}^{0.5}} \} \tag{53}$$

Proper modeling of the methanation must include the effect of the backward reaction as equilibrium is approached. Hence, the complete version of Equation 53 is as follows:

$$r = A_c 0.314 e^{(1,300[\frac{1}{T} - \frac{1}{513}])} \{ \frac{P}{P_{H_2}^{0.5}} \} [y_{CO} - \frac{y_{CH_4} y_{H_2O}}{y_{H_2}^3 P^2 K_{CO}}] \tag{54}$$

where, P is the pressure in kPa, y is the component mole fraction, K_{CO} is the equilibrium constant for Equation 49 and A_c is the catalyst activity factor.

$$K_{CO} = e^{(-38.4532 + 26,270/T)} \qquad (55)$$

Kinetic data are not available for the methanation of CO_2. We use the same kinetic expression for CO_2 as for CO, recognizing the weakness of this approach, but also recognizing that the concentration of CO_2 in the process stream is very small. The rate of Reaction 50 is given as:

$$r = A_c 0.314 e^{(1,300[\frac{1}{T} - \frac{1}{513}])} \{\frac{P}{P_{H_2}^{0.5}}\} [y_{CO_2} - \frac{y_{CH_4} y_{H_2O}^2}{y_{H_2}^4 P^2 K_{CO_2}}] \qquad (56)$$

$$K_{CO_2} = e^{(-33.923 + 21,621/T)} \qquad (57)$$

2.5 Synthesis Unit

The ammonia synthesis converter beds are modeled as a plug flow reactor by RPlug.

The reaction stoichiometry considered is:

$$N_2 + 3H_2 \rightarrow 2NH_3 \qquad (58)$$

The kinetics expression Nielsen $et\ al.,$ (1968) is as follows:

$$R = A_c [\frac{AK(a_N k_{eq}^2 - \frac{a_A^2}{a_H^3})}{(1 + K_a \frac{a_A}{a_H^W})^2 \alpha}] \frac{kgmole}{m^3 hr} \qquad (59)$$

where:

A_c = catalyst activity

α = 0.654

$$w = 1.523$$

and where k_{eq} is the equilibrium constant, AK, the specific rate constant, and K_a, the adsorption equilibrium constant.

$$\text{Log}_{10} k_{eq} = -2.691122 \text{Log}_{10}(T) - 5.519265 \times 10^{-5} T + 1.848863 \times 10^{-7} T^2 \\ + \frac{2001.6}{T} + 2.6899 \tag{60}$$

$$AK = 3.945 \times 10^{10} \exp(-\frac{5,622}{T}) \tag{61}$$

$$K_a = 2.94 \times 10^{-4} \exp(\frac{12,104}{T}) \tag{62}$$

a_N, a_H, a_A, in Equation 59 are the activities of nitrogen, hydrogen and ammonia. α and w are parameters. Nielsen(1968) also gave the following formula for evaluating the activities:

$$a_i = x_i P \exp[\frac{P}{RT}(B_i - A_i/R/T - C_i/T^3 + (A_i^{0.5} - \sum x_i A_i^{0.5})^2)] \tag{63}$$

where:

R = Gas constant (=0.0826)

P - Pressure in atm

T - Temperature in K

x_i = mole fraction of component i

Table 3 The value of A's, B's and C's in Equation 63

i	A_i	B_i	C_i
H_2	0.1975	.02096	5.04×10^2
N_2	1.3445	.05046	4.20×10^4
NH_3	2.393	.03415	4.77×10^6
Ar	1.2907		
CH_4	2.2769		

3. Concepts of Pinch analysis

In this section, concepts of pinch analysis are described. Showing how it is possible to set energy targets and achieve them with a network of heat exchanger. These concepts will then be expanded for a wide variety of practical situations.

3.1 Basic concepts of heat exchanger

Consider the simple process show in Figure 4. There is a chemical reactor, which will be treated at present as a "black block". Liquid is supplied to the reactor and needs to be heated from ambient temperature to the operating temperature of the reactor. A hot liquid product from the separation system needs to be cooled down to lower temperature. There is also an additional unheated make-up stream to the reactor.

Any flow which requires to be heated or cooled, but do not change the composition, is defined as a stream. The feed, which starts cold and needs to be heated up is known as a cold stream. The hot product which must be cooled down is called a hot stream. The reaction process is not stream, because it involves a change in chemical composition; and the make-up flow is not stream, because it is not heated or cooled.
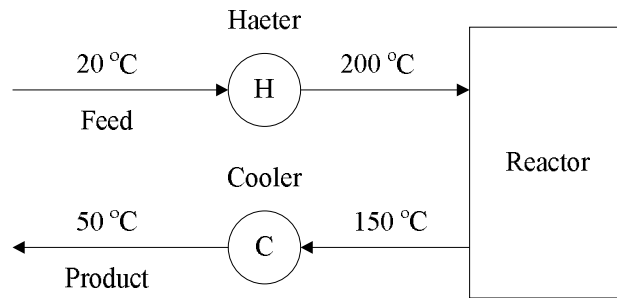
Figure 4 Simple process flowsheet for heat exchange with reactor

Table 4 Data for simple two-stream example

Streams	Mass flow rate W (kg/s)	Specific heat capacity C_p (kJ/kgK)	Heat capacity flowrate CP (kW/K)	Initial (supply) temperature T_s (^{o}C)	Final target temperature T_T (^{o}C)	Heat load H (kW)
Cold stream	0.25	4	1.0	20	200	-180
Hot stream	0.4	4.5	1.8	150	50	+180
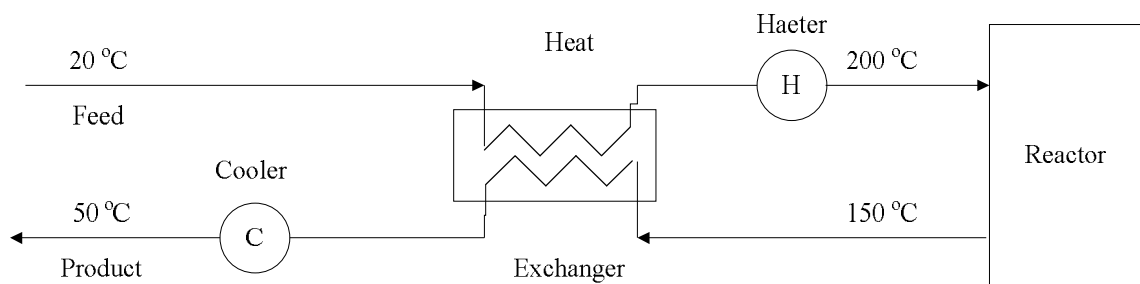
Figure 5 Simple process flowsheet with heat exchanger

To perform the heating and cooling, a stream heater could be placed on the cold stream, and a water cooler on the both stream. The flows are as given in

Table 4. Clearly, the operating process is needed to supply 180 kW of steam heating and 180 kW of water cooling.

The flowsheet will then be as in Figure 5. Ideally, the energy is recovered all 180 kW in the hot stream to heat the cold stream. However this is not possible because of temperature limitations. By the Second law of thermodynamics, the hot stream can't use to heat a cold stream at 200 ^{o}C

3.2 The temperature –enthalpy diagram

A helpful method of visualization is the temperature-heat content diagram, as illustrated in Figure 6. The heat content H of a stream (kW) is frequently calls its enthalpy; this should not be confused with the thermodynamic term, specific enthalpy (kJ/kg). Differential heat flow dQ, when added to a process stream, will increase its enthalpy (H).
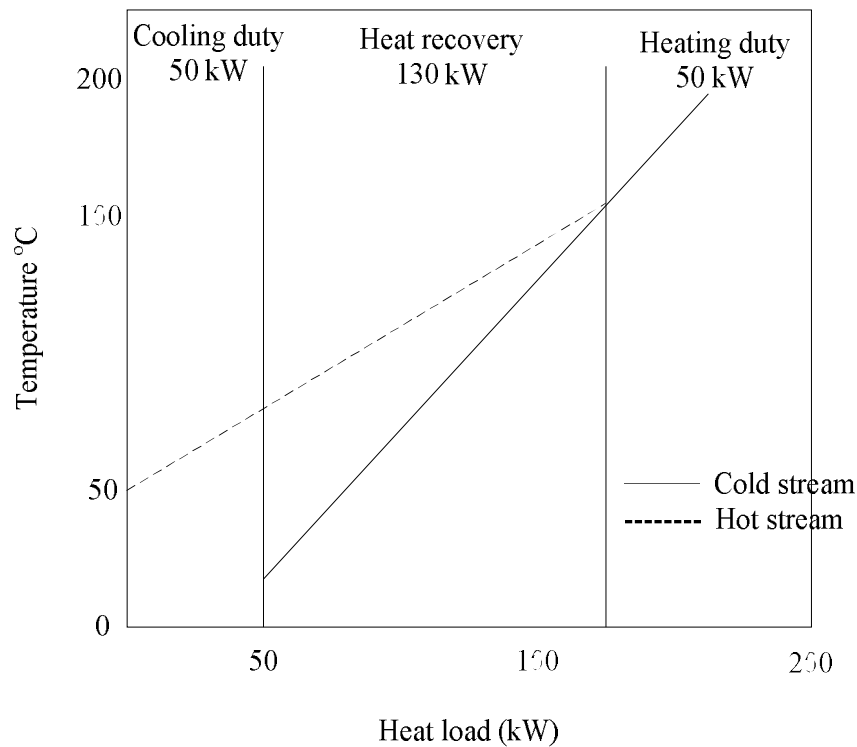
Figure 6 Stream plotted on temperature/enthalpy (T/H) diagram with $\Delta T_{min} = 0$

where;

CP = "heat capacity flowrate" (kW/K) = [mass flow W (kg/s)][specific heat C_p (kJ/kgK)]

dT = Differential temperature change

Hence, with CP assumed constant, for stream requiring heating ("cold" stream) from a "supply temperature" (T_S) to a "target temperature" (T_T), the total heat added will be equal to stream enthalpy change, i.e.

$$Q = \int_{T_S}^{T_T} CPdT = CP(T_T - T_S) = \Delta H \qquad (64)$$

and the slope of the line representing the stream is:

$$\frac{dT}{dQ} = \frac{1}{CP} \qquad (65)$$

The T/H diagram can be used to represent heat exchange, because of a very useful feature. Namely, enthalpy change of stream is interested, a given stream can be plotted anywhere on the enthalpy axis. Provided it has the same slope and runs between the same supply and target temperature, then wherever it is drawn on the H-axis.

Figure 6 shows the hot and cold streams for example plotted on the T/H diagram. Note that the hot stream is represented by the line with the arrowhead pointing to the left, and the cold stream. For feasible heat exchange the two, the hot stream must at all points be hotter than the cold stream overall temperature drop will overestimate the heat recoverable in practice from the stream. Another obvious source heat loss is from long pipe runs.

Heat exchanger network (HEN's) was first study by Linnhoff *et al.,* (1993). For synthesis of HENs, heat of process hot streams and process cold streams are exchange; it is desired to synthesize a cost effective network of heat exchangers which can transfer heat from the hot streams to the cold streams. We construct two diagrams to study. One, hot composite streams with heat lost from the hot stream and temperature, two, cold streams composite with heat gained by the cold streams and temperature. Next we construct the thermal pinch diagram. On this diagram, thermodynamic feasibility of heat exchange is gauranteed if at any heat-exchange level, the temperature of hot composite stream is located to the right of cold composite stream. Therefore, the cold stream can be slid down until it touches the hot composite stream. The point where the two composite streams touch is called the "thermal pinch point". James and Douglas (1988) said in Conceptual Design that pinch temperature is no energy transfer between temperature intervals. Then we are useful for minimizing utility usage. Above the pinch only no cooling utilities should be used while below the pinch only no heating utilities should be used. These rules can be explained by noting that above the pinch will replace a load which can be removed by a process cold stream. A similar argument can be made against using a heating utility below the pinch. The ASPEN HX-NET was favorites to perform optimal heat exchanger network design and pinch analysis.

MATERIALS AND METHODS

Materials

1. Personal Computer (PC)
   - CPU (Intel(R) Centrino Duo 1.60 GHz)
   - 2.00 GB of RAM
   - 160 GB of hard disk

2. Operating System: Microsoft Window XP Professional 2002 service pack 2

3. Softwares
   - Microsoft Visual Studio 2003
   - Microsoft Visual Studio 2005
   - Intel Fortran Compiler 9.0
   - ASPEN PLUS version 2006.5
   - ASPEN DYNAMIC version 2006.5
   - ASPEN HX-NET version 2006.5
   - ASPEN ICARUS version 2006.5
   - MATLAB Simulink^{TM} version 7.0

Methods

1. ASPEN PLUS simulation software

ASPEN PLUS is a process modelling software suitable for a variety of steady state modelling applications. The ASPEN system is based on "blocks" corresponding to unit operations as well as chemical reactors, through which most industrial operations can be simulated. By interconnecting the blocks using material, work and heat streams, a complete process flowsheet can be constructed. ASPEN PLUS includes several databases containing physical, chemical and thermodynamic data for

a wide variety of chemical compounds, as well as a selection of thermodynamic models required for accurate simulation of any given chemical system. Simulation is performed by specifying: (1) flow rates, compositions and operating conditions of the inlet streams; (2) operating conditions of the blocks used in the process, e.g. temperature, pressure, number of stages and (3) heat and/or work inputs into the process. Based on these data, ASPEN calculates flow rates, compositions and state conditions of all outlet material streams, as well as the heat and work output of all outlet heat and work streams.

Ammonia is produced basically from water, air, and energy. The energy source is usually hydrocarbons, thus providing hydrogen as well, but may also be coal or electricity. Steam reforming of light hydrocarbons is the most efficient route, with about 77% of world ammonia capacity being based on natural gas. The ammonia process model is shown in Figure 7 using ASPEN PLUS simulator.
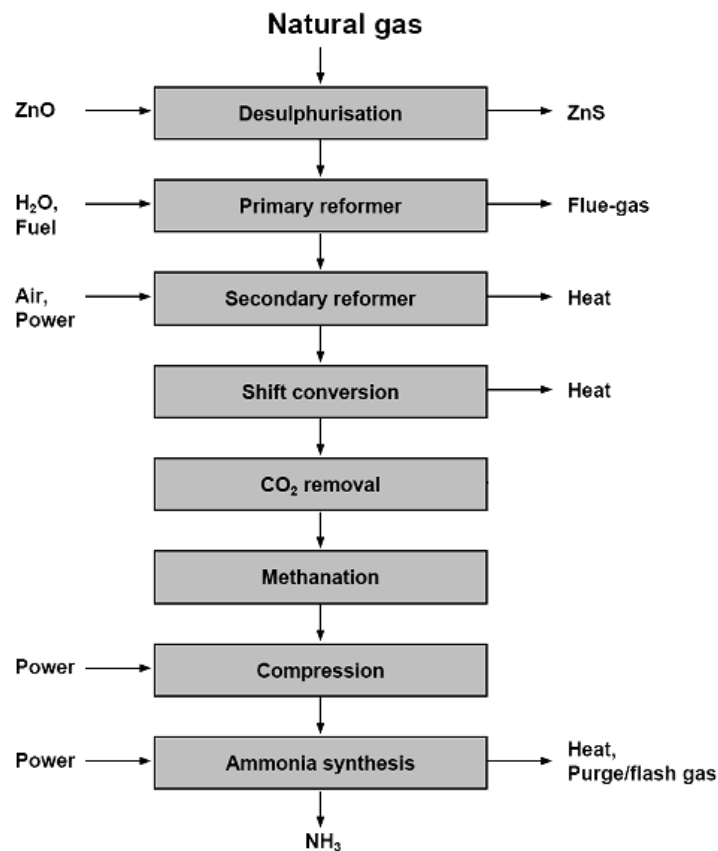
Figure 7 Block diagram of the steam/air reforming process

A typical modern ammonia-producing plant first converts natural gas (i.e., methane) or LPG (liquified petroleum gases such as propane and butane) into gaseous hydrogen. The method for producing hydrogen from hydrocarbons is referred to as "Steam Reforming" (Twygg, Martyn V. (1989)). The hydrogen is then combined with nitrogen to produce ammonia.

Starting with a natural gas feedstock, the processes used in producing the hydrogen are:

Overall conversion

The synthesis gas production and purification normally take place at $25 - 35$ bar. The ammonia synthesis pressure is in the range of $100 - 250$ bar.

$$0.88CH_4 + 1.26Air + 1.24H_2O \longrightarrow 0.88CO_2 + N_2 + 3H_2 \qquad (66)$$

$$N_2 + 3H_2 \longrightarrow 2NH_3 \qquad (67)$$
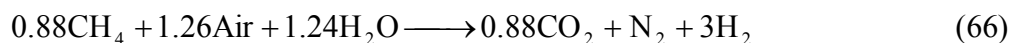
1.1 Natural Gas Desulfurization

Most of the catalysts used in the process are sensitive to S and S compounds. The feedstock normally contains up to 5 mg $S.Nm^{-3}$ as sulfur compounds. The feed-gas is preheated to $350 - 400$ ^{o}C, usually in the primary reformer convection section, and then treated in a desulfurization vessel, where the sulfur compounds are hydrogenated to H_2S.

The natural gas is delivered as dry gas containing a maximum of 40 ppm by weight of sulfur, which is a poison for the reformer catalyst. The desulfurization unit reduces the sulfur content to about 5 ppm by hydrogenating (Equation 68) it to hydrocarbons and hydrogen sulfide and then absorbing the hydrogen sulfide in zinc oxides (Equation 69).

$$H_2 + S_8 \rightarrow 8H_2S(gas) \qquad (68)$$

$$H_2S + ZnO \rightarrow ZnS + H_2O \qquad (69)$$

1.2 Reforming Unit

The gas from the desulfurizer is mixed with process steam, usually coming from an extraction turbine, and the steam/gas mixture is then heated further to

500 – 600 ^{o}C in the convection section before entering the primary reformer. In a new plant, the preheated steam/gas mixture is passed through an adiabatic pre-reformer and reheated in the convection section, before entering the primary reformer. The amount of process steam is given by the steam to carbon molar ratio (S/C ratio), which should be around 3.0 for the BAT reforming process. In new plant, the optimum S/C ratio may be lower than 3.0. The overall reaction is highly endothermic and additional heat is required to raise the temperature to 780 – 830 ^{o}C at the reformer outlet. The composition of the gas leaving the primary reformer is given by close approach to the following chemical equilibrium. The heat for the primary reforming process is supplied by burning natural gas or other gaseous fuel, in the burners of a radiant box containing the tubes. The flue gas leaving the radiant box has T in excess of 900 ^{o}C, after supplying the necessary high-level heat to the reforming process. Thus only 50 – 60% of the fuel's heat value is directly used in the process itself. The heat content (waste heat) of the flue gas is used in the reformer convection section, for various process and steam system duties. The fuel energy requirement in the conventional reforming process is 40 – 50% of the process feed-gas energy. The flue gas leaving the convection section at 100 – 200 ^{o}C is one of the main sources of emissions from the plant. These emissions are mainly CO_2, NO_x, with small amounts of SO_2 and CO.

Only 30 – 40% of the hydrocarbon feed is reformed in the primary reformer because of the chemical equilibrium at the actual operation conditions. The temperature must be raised to increase the conversion. This is done in the secondary reformer by internal combustion of part of the gas with the process air, which also provides the nitrogen for the final synthesis gas. In the conventional reforming process, the degree of primary reforming is adjusted so that the air supplied to the secondary reformer meets both the heat balance and the stoichiometric synthesis gas requirement. The process air is compressed to the reforming pressure and heated further in the primary reformer convection section to 600 ^{o}C. The process gas is mixed with the air in a burner and then passes over a nickel-containing secondary reformer catalyst. The reformer outlet T is 1000 C, and up to 99% of the HC feed (to the primary reformer) is converted, giving a residual methane content of 0.2-0.3%

(dry gas base) in the process gas leaving the secondary reformer. The process gas is cooled to 350-400 ^{o}C in a waste heat steam boiler or boiler/superheater downstream from the secondary reformer.

This unit contains two sections, one is primary reforming, and another is secondary reforming. The desulfurized hydrocarbon feed is reformed to hydrogen and carbon oxides in the presence of steam in the primary reformer, and additionally with hot air in the secondary reformer. The reformed gas contains about 0.3 vol% CH_4.

$$CH_4 + H_2O \rightarrow CO + 3H_2 \tag{70}$$

1.3 Carbon Monoxide Conversion

The process gas from the secondary reformer contains 12 – 15% CO (dry gas base) and most of the CO is converted in the shift section. In the high temperature shift (HTS) conversion, the gas is passed through a bed of iron oxide/chromium oxide catalyst at 400 ^{o}C, where the CO content is reduced to 3% (dry gas base), limited by the shift equilibrium at the actual operating temperature. There is a tendency to use copper containing catalyst for increased conversion. The gas from the HTS is cooled and passed through the low temperature shift (LTS) converter. This LTS converter is operated at 200 – 220 ^{o}C. The residual CO content in the converted gas is 0.2 -0.4% (dry gas base).

In the CO-shift conversion, the major part of the CO contained in the reformed gas is catalytically converted to CO_2 in two catalytic stages, the first at high temperature and the second at low temperature.

$$CO + H_2O \rightarrow CO_2 + H_2 \tag{71}$$

1.4 Carbon Dioxide Removal

The process gas from the LTS converter contains mainly H_2, N_2, CO_2, and the excess process steam. The gas is cooled and most of the excess steam is condensed before it enters the CO_2 removal system. The heat released during cooling/condensation is used for: the regeneration of the CO_2 scrubbing solution, driving an absorption refrigeration unit, boiler feed-water preheat. The amount of heat released depends on the process steam to carbon ratio. If all this low-level heat is used for CO_2 removal or absorption refrigeration, high-level heat has to be used for the feed-water system. An energy-efficient process should therefore have a CO_2 removal system with a low heat demand. The CO_2 is removed in a chemical or a physical absorption process. The solvents used in chemical absorption process are mainly aqueous amine solutions (MEA), aMDEA, or hot potassium carbonate solutions. Physical solvents are Selexol, propylene carbonate and others. The MEA process has a high regeneration energy consumption and is not regarded as a BAT process. The BAT processes are: aMDEA standard 2-stage process, Benfield process (HiPure, LoHeat), Selexol process. The typical range of heat consumption in the modern chemical absorption process is 30 – 60 MJ/kmol CO_2. The physical absorption processes may be designed for zero heat consumption, but for comparison with the chemical processes, the mechanical energy requirement has also to be considered.

The carbon dioxide is removed from the converted gas in the CO_2 removal. CO_2 is captured by NH_3 and it will generate ammonium hydrogen carbonate as byproduct. The purified gas with about 0.1 vol% CO_2 is called synthesis gas.

1.5 Methanation Unit

The small amounts of CO and CO_2, remaining in the synthesis gas, are poisonous for the ammonia synthesis catalyst and must be removed by conversion to CH_4. The reactions take place at 300 C in a reactor filled with a nickel containing catalyst. Methane is an inert gas in the synthesis reaction, but the water must be

removed before entering the converter. This is done firstly by cooling and condensation downstream of the methanator and finally by condensation/absorption in the product ammonia in the loop or in a make-up gas drying unit.

Even small quantities of CO (0.1 vol%) and CO_2 (0.3 vol%) are poisons for the ammonia synthesis catalyst. The residual content of $CO + CO_2$ is less than 10 ppm.

$$CO + 3H_2 \rightarrow CH_4 + H_2O \tag{72}$$

$$CO_2 + 4H_2 \rightarrow CH_4 + 2H_2O \tag{73}$$

1.6 Synthesis Unit

Modern ammonia plants use centrifugal compressors for synthesis gas compression, usually driven by steam turbines, with the steam being produced in the ammonia plant. The refrigeration compressor, needed for condensation of product ammonia, is also driven by a steam turbine. The synthesis of ammonia takes place on an iron catalyst at P of $100 - 250$ bar and T of $350 - 550$ ^{o}C. Only $20 - 30\%$ is reacted per pass in the converter due to the unfavorable equilibrium conditions. The ammonia that is formed is separated from the recycle gas by cooling/condensation, and the reacted gas is substituted by the fresh make-up synthesis gas, thus maintaining the loop pressure. In addition, extensive heat exchange is required due to the exothermic reaction and the large T range in the loop. A newly developed ammonia synthesis catalyst containing ruthenium on a graphite support has a much higher activity per unit volume and has the potential to increase conversion and lower operating pressure. Synthesis loop arrangements differ with respect to the points in the loop at which the make-up gas is delivered and the ammonia and purge gas are taken out. The best arrangement is to add the make-up gas after ammonia condensation and ahead of the converter. The loop purge should be taken out after ammonia separation and before make-up gas addition. The configuration depends on the make-up gas being treated in a drying step before entering the loop. A make-up

gas containing traces of water or CO_2 must be added before ammonia condensation, with negative effects both to ammonia condensation and energy. Conventional reforming with methanation as the final purification step, produces a synthesis gas containing inert (methane and argon) in quantities that do not dissolve in the condensed ammonia. The major part of these inert is removed by taking out a purge stream from the loop. The size of this purge steam controls the level of inert in the loop to 10-15%. The purge gas is scrubbed with water to remove ammonia before being used as fuel or before being sent for hydrogen recovery. Ammonia condensation is far from complete if the cooling is done with water or air. Vaporizing ammonia is used as a refrigerant in most ammonia plants, to achieve sufficiently low ammonia concentrations in the gas recycled to the converter. The ammonia vapor is liquefied after recompression in the refrigeration compressor.

The synthesis gas is pressurized by a centrifugal compressor to approximately 300 bar and hydrogen and nitrogen are catalytically converted to ammonia. The ammonia in the purge gas from the ammonia unit is recovered in the tailgas scrubbing unit and fed to a refrigeration unit. The treated purge gas is used as fuel for the primary reformer. The building blocks offered in this package do not model this section of the plant.

$$3H_2 + N_2 \rightarrow 2NH_3 \tag{74}$$
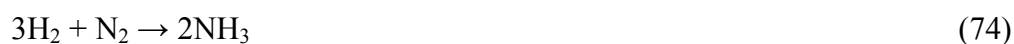
1.7 Refrigeration

The ammonia gas in the synthesis loop is liquefied by ammonia evaporation in the ammonia chiller and discharged as feed to the urea process and to ammonia storage. The building blocks offered in this package do not model this section of the plant.

2. Model Predictive Control (MPC)

Model Predictive Control, or MPC, is an advanced method of process control that has been in use in the process industries such as chemical plants and oil refineries since the 1980s. Model predictive controllers rely on dynamic models of the process, most often linear empirical models obtained by system identification. MPC is based on iterative, finite horizon optimization of a plant model. At time t the current plant state is sampled and a cost minimizing control strategy is computed (via a numerical minimization algorithm) for a relatively short time horizon in the future: [t,t + T]. Specifically, an online or on-the-fly calculation is used to explore state trajectories that emanate from the current state and find (via the solution of Euler-Lagrange equations) a cost-minimizing control strategy until time t + T. Only the first step of the control strategy is implemented, then the plant state is sampled again and the calculations are repeated starting from the now current state, yielding a new control and new predicted state path. The prediction horizon keeps being shifted forward and for this reason MPC is also called receding horizon control. Although this approach is not optimal, in practice it has given very good results. Much academic research has been done to find fast methods of solution of Euler-Lagrange type equations, to understand the global stability properties of MPC's local optimization, and in general to improve the MPC method. To some extent the theoreticians have been trying to catch up with the control engineers when it comes to MPC.

RESULTS AND DISCUSSION

This section includes the results of (1) steady-state ammonia process simulation, (2) heat integration process (3) test of controllability for ammonia process, (4) advanced control process and, (5) preliminary process design. The first part is using ASPEN PLUS 2006.5 simulator. Next part is the heat integration process using ASPEN HX-NET 2006.5 simulator. The heat integration process will also illustrate the comparison between the process with and without the integration. The third part is test of controllability for ammonia process. The fourth part, the advanced control process shows the advanced control process; Model Predictive Control (MPC), for the proposed process. Therefore, the last part will give the detail on equipments and operations.

1. Steady-state simulation of ammonia process

The process scheme for production of ammonia Profertil was proposed by H. Topsoe (2001). A capacity of 2,050 ton/day of ammonia in one single line, this is the world's largest grassroots plant. The plant is part of an ammonia/urea complex producing 3,250 ton/day of urea in one single line. My thesis ammonia simulation from natural gas reforming based on H. Toposoe (2001). The main operating parameters were shown in the Table 5.

Table 5 The process features and main operating parameters

Functions	Main Operating Parameters
Desulfurization	Hydrogenation/Absorption on ZnO
Primary Reforming	
S/C ratio	3.1
Pressure, kg/cm^2g	40
Number of tubes	264
Secondary Reforming	
CH_4 slip, %	0.3
Shift Conversion	Two steps
CO_2 Removal System	MDEA
Methanation	Yes
Ammonia Synthesis	
Pressure, kg/cm^2g	195

As mentioned the plant lay-out comprises desulfurization, primary and secondary reforming, two-step shift conversion, MDEA CO_2 removal, methanation, compression, S-200 ammonia synthesis loop. The process scheme for production of ammonia profertil was shown in the Figure 8.
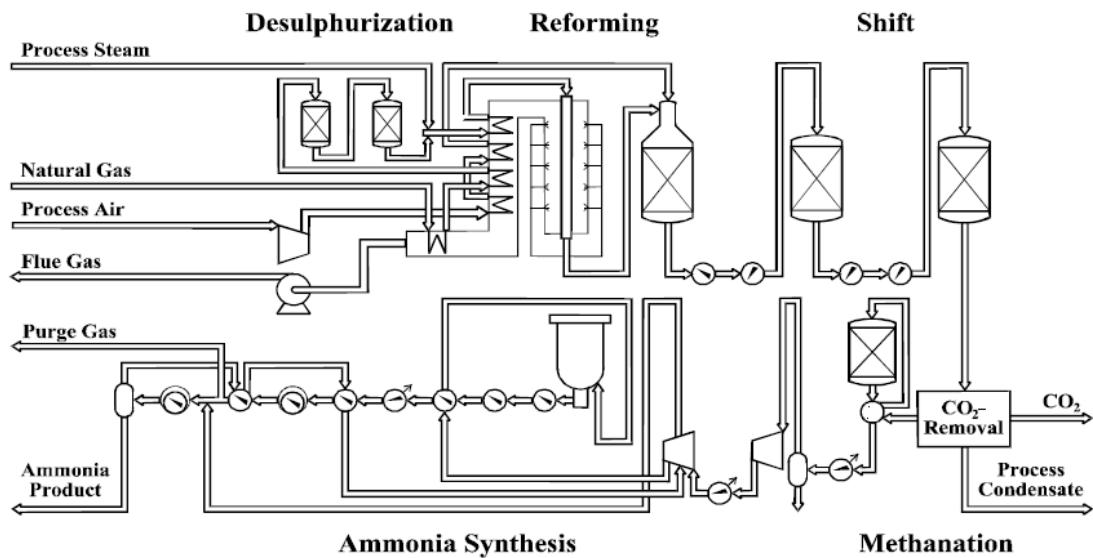
Figure 8 Process Scheme for Production of Ammonia Profertil

Source: H. Toposoe (2001).

An ammonia production process comprises steam hydrocarbon primary reforming, air secondary reforming, carbon monoxide shift conversion, carbon dioxide removal, ammonia synthesis and discarding of non-reactive gases. There were made more economical in energy consumption by using excess air in secondary reforming and treating the synthesis gas to separate a hydrogen-enriched stream and returning that stream to the synthesis. The ammonia process model flowsheet was created from Modified from USGS: Mineral Commodity Profiles – "Nitrogen" 2005 and Design and Operation of Large Capacity Ammonia Plants by H. Toposoe (2001).

The process simulation based on real process was introduced. The temperature condition was considered to simulate ASPEN PLUS in the Figure 9. The reactors in this process were used plug flow reactor. In the ASPEN PLUS simulation used RPLUG reactor but RPLUG reactor based on kinetics reaction. Therefore, some reactor that did not know kinetics reaction used Rstoic. The separation process used flash separation. The simualtion process was used Flash2 because the separation based on vapor pressure but the process vapor-vapor separation that did not have vapor-vapor equilibrium was used Sep2. The inputs conditions in ASPEN PLUS were

main operating parameters (Table 5), temperature condition based on real process (Figure 9), and key input stream condition (Table 6).
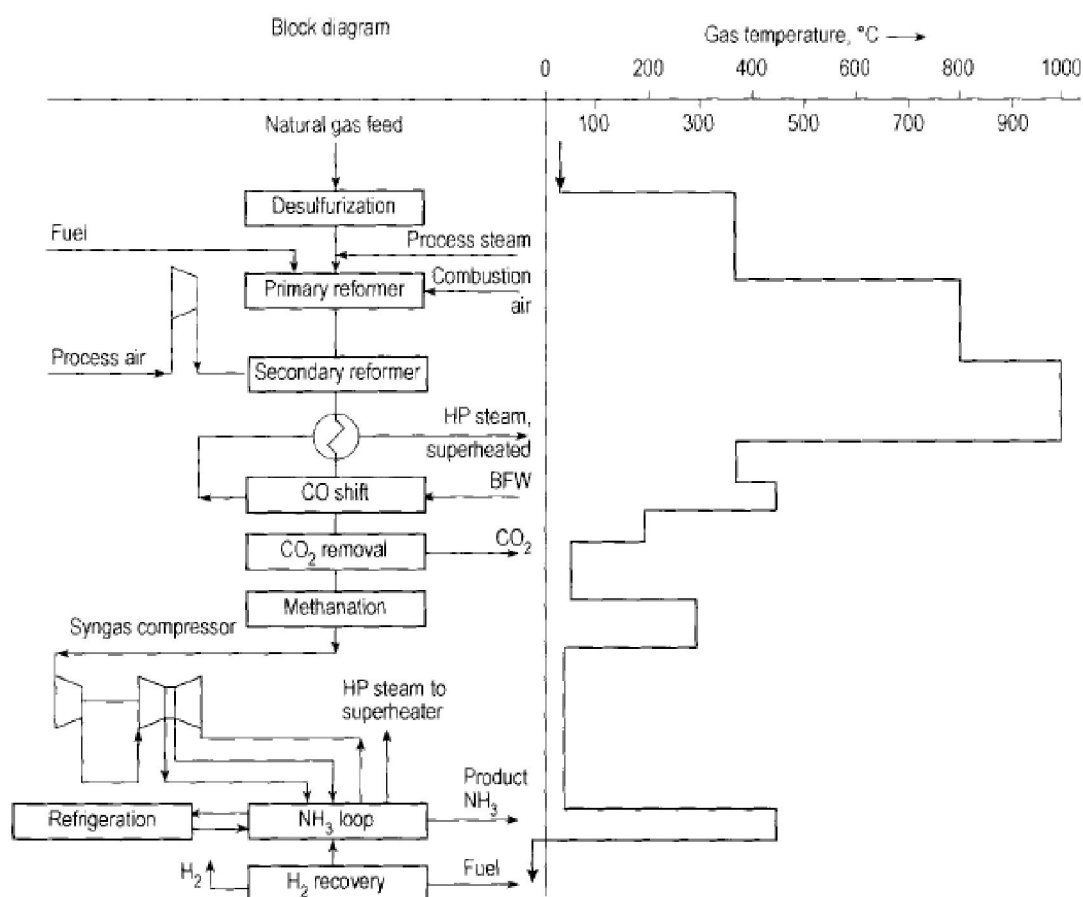
Figure 9 The temperature condition based on real process

The key input streams conditions in ASPEN PLUS simulation were shown in Table 8 and the other inputs were shown in APPENDIX C. The streams S-01, S-02, S-PA01 and S-PS1 were natural gas, hydrogen, process air, and process steam.

Table 6 The key input stream condition in ASPEN PLUS

Stream	Natural Gas (S-01)	Hydrogen (S-02)	Process Air (S-PA01)	Process Steam (S-PS1)
Temperature (^{o}C)	45	116	33	360
Pressure (bar)	38.25	38.25	2.94	35.30
Mole Flow (kmol/hr)				
CO_2	0	0	0.71	0
CO	0	0	0	0
H_2	0	62.87	0	0
N_2	11.29	21.02	1845.12	0
CH_4	1142.87	0.63	0	0
AR	0	0.25	22.46	0
NH_3	0	0	0	0
H_2O	0	0	0	5664.14
O_2	2.85	0	496.34	0
C_2H_6	252.92	0	0	0
C_3H_8	13.41	0	0	0
N-BUTANE	0.85	0	0	0
I-BUTANE	0	0	0	0
I-PENTAN	0	0	0	0
N-PENTAN	2.67	0	0	0
N-HEXANE	0.85	0	0	0
N-HEPTNE	0	0	0	0
SULFUR	0.0014	0	0	0
H_2S	0	0	0	0

The ammonia process model was created by ASPEN PLUS simulator. The ASPEN PLUS unit operation blocks in ammonia process model and specifications were shown in the Table 7. The property methods and models used the SRK-BM method. The M. Lísal proposed Monte Carlo adiabatic simulation of equilibrium reacting systems: The ammonia synthesis reaction. The M. Lisal work's used the SRK-BM.

Table 7 ASPEN PLUS Unit Operation Blocks Used in Ammonia production Model

Unit Operation	Aspen Plus "Block"	Comments / Specifications
Natural Gas Desulfurization	Sep2 + Rstoic	The sulfur is hydrogenated to hydrogen sulfide and then removed
Reforming	RStoic + RPlug	The reactions are defined in the subroutines using RPlug. The reformed gas contains about 0.3 vol% CH_4.
Carbon Monoxide Conversion	RPlug + Heater	CO converts to CO_2 in two catalytic stages, the first at high temperature and the second at low temperature.
Carbon Dioxide Removal	Flash2	CO_2 is captured by NH_3.
Methanation	RPlug + Sep2	The residual content of CO + CO_2 is less than 10 ppm.
Synthesis	RPlug + FSplit + Heater	Reacting with RPlug and high pressure.
Refrigeration	Valve + HeatX	Ammonia gas in the synthesis loop is liquefied

The overall ammonia process model was categorized into desulfurization, reforming, carbon monoxide shift conversion, carbon dioxide removal, methanation, ammonia synthesis and refrigeration according to their main functions. The first step in the process was removed sulfur compounds from the natural gas because sulfur deactivates the catalysts used in subsequent steps. Sulfur removal requires catalytic hydrogenation to convert sulfur compounds in the natural gas to gaseous hydrogen sulfide. For the simulation, the RStoic reactor was used hydrogenating to hydrogen sulfide. Then, Sep2 was used removal hydrogen sulfide. The desulfurized gas was mixed by process steam and sent to the reforming section. The process air was fed into the secondary reforming section. The purpose was to reform the desulfurized hydrocarbon to hydrogen, carbon monooxide and carbon dioxide. The main reactor was used in reforming section such as RPlug reactors (primary and secondary reforming). The side reaction was used RStoic reactor. The reformed gas was fed to CO conversion to catalytically convert from reformed gas to carbon dioxide. The simulation in part of carbon monoxide conversion was used RPlug reactor for high and low temperature shifts carbon monoxide conversion. The Heater was used to be heated up the stream. The carbon dioxide was removed from the converted gas in the carbon dioxide removal section. For the simulation, Flash2 was used removal carbon dioxide gas. The carbon dioxide gas and hydrogen were reacted to methane in methanation section. The methanation simulation was used RPlug reactor to react methane and Sep2 was used to separate methane. The synthesis section catalytically reacted from hydrogen and nitrogen to ammonia. The make-up gas was delivered into the ammonia synthesis loop for increasing ammonia conversion. The ammonia was separated and purified to vapor ammonia and liquid ammonia.

The overall process model of ammonia production from natural gas was shown in Figure 10. The feed stream composed of process air, natural gas, process steam and combustion air at 53000, 32000, 102041 and 178220 scmh; respectively, to produce the liquid ammonia at 3097 kmol/hr.
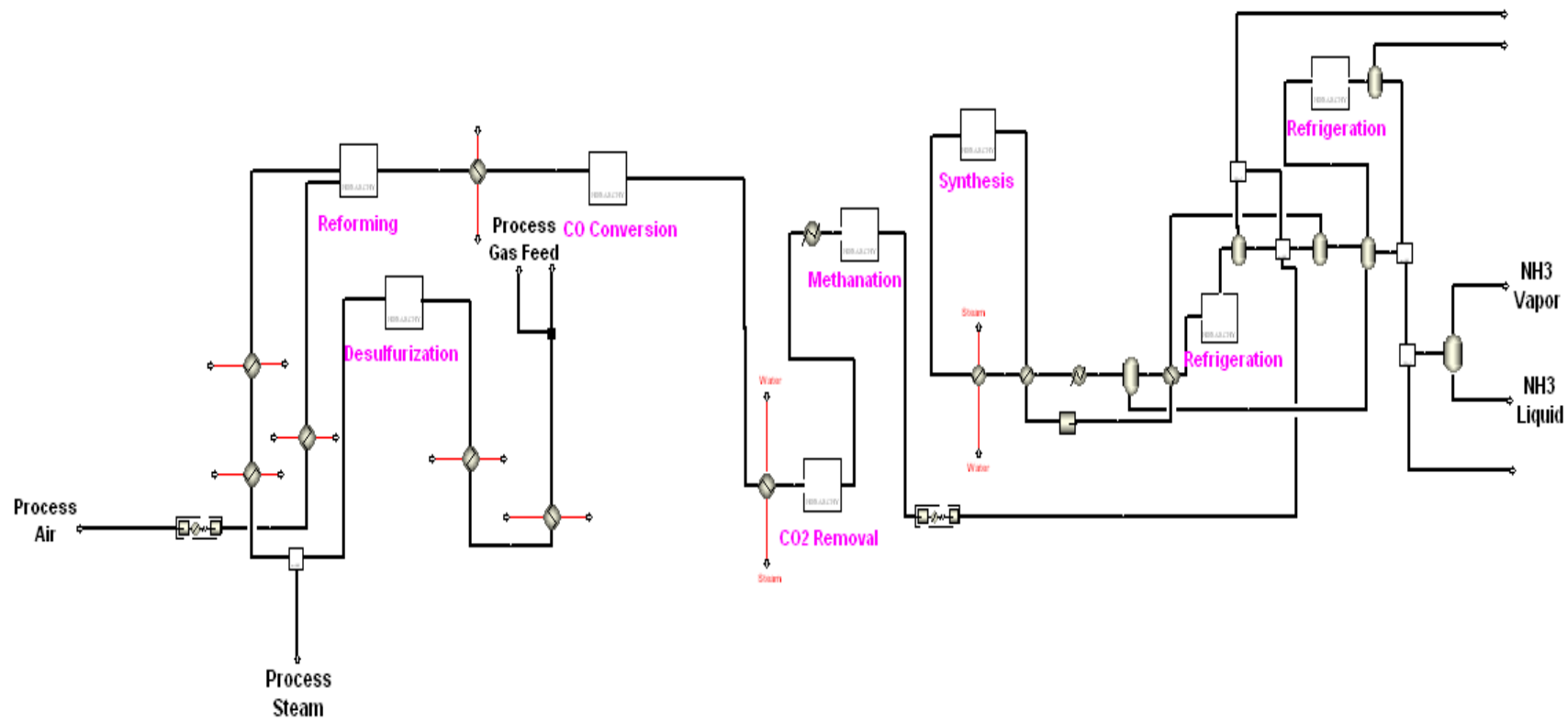
Figure 10 Overall process model ammonia production from natural gas reforming

All of components were used in ammonia process model from natural gas reforming in ASPEN PLUS. The Table 8 shows the materials detail in process model simulation by ASPEN PLUS.

Table 8 Lists the components modeled in the ammonia plant model

Component ID	Component name	Formula
NH3	AMMONIA	NH_3
H2	HYDROGEN	H_2
N2	NITROGEN	N_2
CH4	METHANE	CH_4
AR	ARGON	Ar
CO	CARBON-MONOXIDE	CO
CO2	CARBON-DIOXIDE	CO_2
H2O	WATER	H_2O
O2	OXYGEN	O_2
C2H6	ETHANE	C_2H_6
C3H8	PROPANE	C_3H_8
N-BUTANE	N-BUTANE	C_4H_{10}
I-BUTANE	ISOBUTANE	C_4H_{10}
N-PENTAN	N-PENTANE	C_5H_{12}
I-PENTAN	I-PENTANE	C_5H_{12}
N-HEXANE	N-HEXANE	C_6H_{14}
N-HEPTAN	N-HEPTANE	C_7H_{16}
SULFUR	SULFUR-8-ATOMIC-GAS	S_8
H2S	HYDROGEN-SULFIDE	H_2S
H3O+	H3O+	H_3O^+
OH-	OH-	OH^-
NH4+	NH4+	NH_4^+
NH2COO-	CARBAMATE	$NH2COO^-$
HCO3-	HCO3-	HCO_3^-
CO3--	CO3--	CO_3^{-2}
NH4HCO3S	AMMONIUM-HYDROGEN-CARBONATE	NH_4HCO_3
NH4HCO3	AMMONIUM-HYDROGEN-CARBONATE	NH_4HCO_3

Every component is not included in all the plant sections in order to keep the model as simple as possible. The higher hydrocarbons (C2-C7) are only included in the reformer section. The CO_2 Removal section only includes ions and electrolytes. The synthesis and refrigeration sections only include the components H_2, N_2, Ar, CH_4, NH_3 and H_2O.

The process flow diagram and the condition of each streams of desulfurization section were shown in Figure 11 and Table 9. The natural gas is a raw material that composes of hydrocarbon and sulfur. It was delivered as dry gas containing a maximum of 40 ppm by weight of sulfur, which was a highly poison for the reformer catalyst. The desulfurization unit can reduce the sulfur content by about 5 ppm by hydrogenating to hydrocarbons and hydrogen sulfide and then absorbing the hydrogen sulfide in zinc oxides.

The desulfurization section was composed of hydrogenating and removal hydrogen sulfide. The hydrogenating process was used RStoic reactor because stoichiometric reactor based on known fractional conversions or extents of reaction. The process sulfur was removed from a material such as coal or oil. It may involve one of many techniques including elutriation, froth flotation, laundering, magnetic separation, chemical treatment, etc (IUPAC, 1997). The removal hydrogen sulfide was used Sep2 because separate compositions into 2 outlet streams based on flows and purities. Assumption, the DESULF-R was adiabatic reactor. The input parameters of DESULF-R block (RStoic) required pressure, heat duty and reaction. The pressure and heat duty of DESULF-R block was 51 bar and 0 cal/sec. The reaction of DESULF-R block, sulfur and hydrogen were reacted to hydrogen sulfide. The DESULF-S block (Sep2) was separated the hydrogen sulfide by specification split fraction of hydrogen sulfide equal to 1.

There were 10 blocks in desulfurization section that composed two mixers, five heat exchanger, two reactors and one compressor. The natural gas (S-01) and hydrogen (S-02) were mixed to stream S-01A in MIX01 block for reacting with sulfur and hydrogen to hydrogen sulfide. The stream S-01A was heated up from 46.9 to

253.5 ^{o}C with E-204B block. The stream S-01B was heated up from 253.5 to 344.2 ^{o}C with E-204A block. The hydrogen and sulfur in stream S-01C were reacted to hydrogen sulfide in stream S-01D with DESULF-R block. The hydrogen sulfide was separated with DESULF-S block in stream S-DS01. The desulfurized gas and the process steam were mixed with STMFEED block. The stream S-01F was heated up from 347.9 to 513.5 ^{o}C with E-201 block. The stream S-01G was cooled down from 513.5 to 503.3 ^{o}C with HLOSS block. The process air was compressed from 2.94 to 32.4 bar with K-302 block. The stream S-03 was heated up from 133.1 to 482.3 ^{o}C with E-202 block. The stream S-01H and S-PA2 were delivered to reforming section.
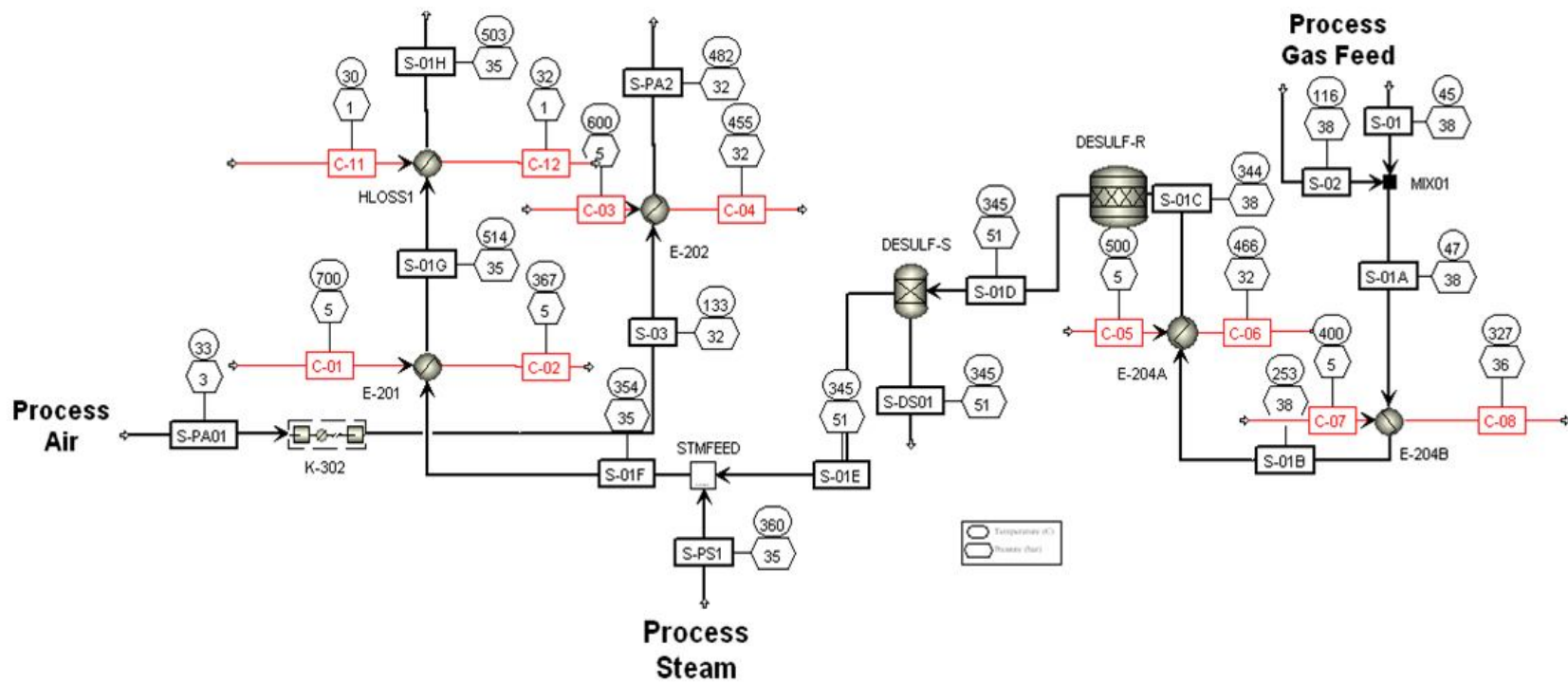
Figure 11 Process model of desulfurization section

Table 9 Operating condition of each streams of desulfurization section

Stream no.	Description	T (^{o}C)	P (bar)
S-01	Fresh process gas feed (natural gas)	45	38.2
S-01A	Mixed stream between fresh process gas and	46.9	38.2
S-01B	Heated stream with E-204B block	253.5	38.2
S-01C	Heated stream with E-204A block	344.2	38.2
S-01D	Reacted stream with DESULF-R block	344.8	51
S-01E	Reacted stream with DESULF-S block	324.8	51
S-01F	Mixed stream between S-01E and process steam	347.9	35.3
S-01G	Heated stream with E-201 block	513.5	35.3
S-01H	Heated stream with HLOSS1 block	503.3	35.3
S-02	Fresh hydrogen gas feed	116	38.2
S-03	Compressed stream with K-302 block	133.1	32.4
S-DS01	Separated stream with DESULF-S block	433.8	51
S-PS1	Fresh process steam	360	35.3
S-PA01	Fresh process air	33	2.9
S-PA2	Heated stream with E-202 block	482.3	32.4
C-01	Steam input in E-201 block	700	5
C-02	Steam output in E-201 block	355	5
C-03	Steam input in E-202 block	600	5
C-04	Steam output in E-202 block	454.6	5
C-05	Steam input in E-204A block	500	5
C-06	Steam output in E-204A block	465.6	5
C-07	Steam input in E-204B block	400	5
C-08	Steam output in E-204B block	326.9	5
C-11	Water input in HLOSS1 block	30	1
C-12	Water output in HLOSS1 block	32	1

The process flow diagram and the condition of each streams of reforming section were shown in Figure 12 and Table 10. The reforming unit contains two units;

the primary reforming and the secondary reforming. The desulfurized hydrocarbon feed was reformed to hydrogen, carbon monoxide and carbon dioxide in the presence of steam at the primary reformer, and additionally with hot air in the secondary reformer. The reformed gas contained about 0.3 vol% of CH_4.

The reforming section was composed of main and side reforming reaction. The main reforming reaction was primary and secondary reforming. The main reforming reaction was used RPLUG reactor because rigorous plug flow reactor with rate-controlled reactions based on knows kinetics. The side reactions were used RStoic reactor because stoichiometric reactor based on known fractional conversions or extents of reaction. The input parameters of PREF-S were pressure, heat duty and reactions. Assumption, the PREF-S and SREF-T were adiabatic reactor. The pressure and heat duty of PREF-S block was -1.9 bar and 0 kW. The reactions were separated two parts. The first part of reaction, ethane, propane, n-butane, i-butane, n-pentane, i-pentane, hexane, heptane and water were reacted to methane and carbon monoxide by fractional conversion of hydrocarbon equal to 1 based on hydrocarbon. The second part of reaction, methane and oxygen reacted to carbon dioxide and water. The input parameters of SREF-S block were pressure, heat duty and reaction. The pressure and heat duty of SREF-S block was 0 bar and 0 kW. The reaction, hydrogen and oxygen reacted to water by fractional conversion of oxygen equal to 1 based on oxygen. The input parameters of PREF-T and SREF-R (primary and secondary reformer) required reactor type, heat transfer specification, configuration and reaction. The primary reformer, the reactor type and heat transfer specification of PREF-T block were reactor with constant coolant temperature and heat transfer parameters U (coolant-process steam) equal to 70 kcal/hr.sqm.K. The configuration composed of number of tubes, length and diameter equal to 280, 10 meter and 0.14 meter. The secondary reformer, the reactor type and heat transfer specification of SREF-R block required reactor with constant coolant temperature and heat transfer parameters U (coolant-process steam) equal to 70 kcal/hr.sqm.K. The configuration was composed of length and diameter equal to 4.7 meter and 3 meter. The primary and secondary reformer reactions were written external fortran code from Moe (1965) reaction.

There were 4 reactor blocks in the reforming section that composed four reactors. Streams S-01H and S-PA2 from desulfurization section were fed to the reforming section. The desulfurized hydrocarbon was reformed to carbon monoxide, carbon dioxide, hydrogen, methane and water with PREF-S block. The stream S-01I was reformed from methane to hydrogen, carbon dioxide and water with PREF-T block (the primary reformer). The stream S-04 and S-PA2 (Process Air) were reacted to water with SREF-S block. The stream S-04A was from methane to hydrogen, carbon dioxide and water with SREF-R block (the secondary reformer). The stream S-05 was delivered to the carbon monoxide conversion section. Simulation result in process stream line S-05 contained carbon dioxide 541.42 and hydrogen 3543.78 kmol/hr.
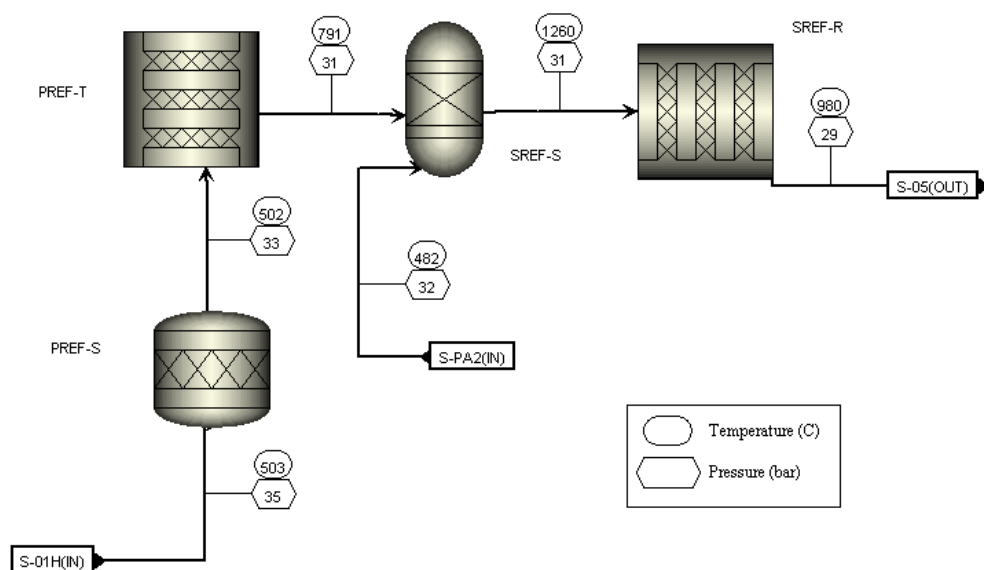
Figure 12 Process model of reforming section

Table 10 Operating condition of each streams of reforming section

Stream no.	Description	T (^{o}C)	P (bar)
S-01H	Stream is fed from desulfurization section	503.3	53.3
S-01I	Reacted stream with PREF-S block	502.2	33.4
S-04	Reacted stream with PREF-T block	790.7	30.7
S-04A	Reacted stream with SREF-S block	1260.1	30.7
S-05	Reacted stream with SREF-R block	980.3	28.7
S-PA2	Fresh process air is fed from desulfurization section	482.3	32.4

The process flow diagram and the condition of each stream of carbon monoxide conversion section were shown in Figure 13 and Table 11. In the CO-shift conversion, the major part of the CO contained in the reformed gas was catalytically converted to CO_2 in two catalytic stages; the first at high temperature and the second at low temperature.

. The carbon monoxide conversion section was composed of high and low temperature shift conversion. The carbon monoxide conversion reaction was used RPLUG reactor because rigorous plug flow reactor with rate-controlled reactions based on knows kinetics. The input parameters of HT-SHIFT and LT-SHIFT blocks (high and low temperature shift conversion) composed of reactor type, configuration and reaction. The high and low temperature shift conversion, the reactor type HT-SHIFT and LT-SHIFT block were adiabatic reactor. The configuration HT-SHIFT block composed of length and diameter equal to 15.8 and 2.2 meter. The configuration LT-SHIFT block composed of length and diameter equal to 7.7 and 3.7 meter. The high and low temperature shift conversion reactions were written external fortran code from Slack (1974) reaction.

Carbon monoxide conversion section composed into two reactors and two heat exchangers. The stream S-05 from the reforming section was fed to the carbon monoxide conversion section. The stream S-05 was cooled down from 980.3 to 380

°C with E-205 block. The heat duty of E-205 was 24.07 MMkcal/hr. The stream S-05A is reformed from carbon monoxide to carbon dioxide with HT-SHIFT (high temperature). The stream S-06 was cooled down from 447.9 to 210 °C with H block. The stream S-06F was reformed from carbon monoxide to carbon dioxide with LT-SHIFT (low temperature). The stream S-07 was delivered to the carbon dioxide removal section. Simulation result in process stream line S-06 contained carbon dioxide 1394.23 kmol/hr and line S-07 carbon dioxide 1639.98 kmol/hr. The carbon monoxide was reacted to carbon dioxide at 1014.94 kmol/hr.
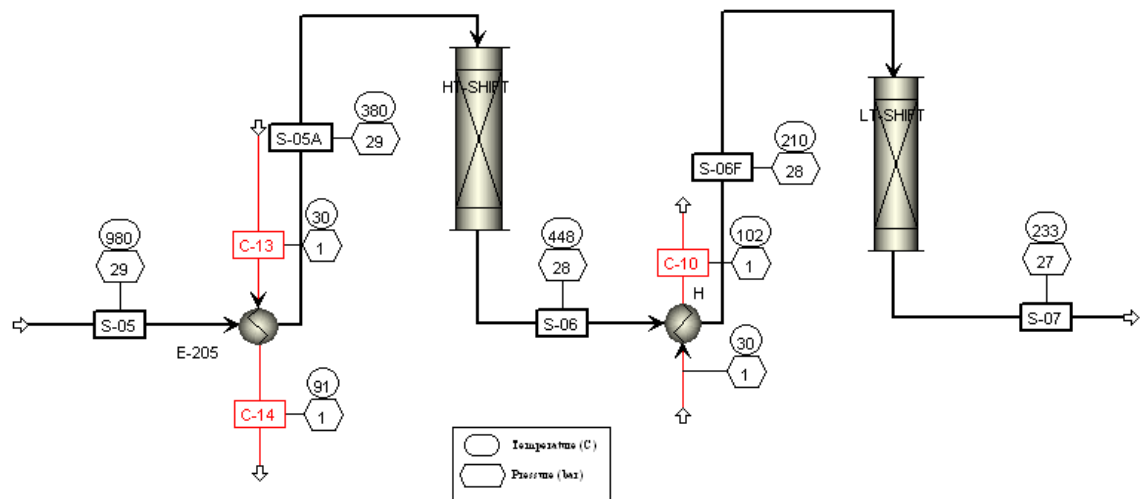
Figure 13 Process model of carbon monoxide conversion section

Table 11 Operating condition of each streams of carbon monoxide conversion
section

Stream no.	Description	T (^{o}C)	P (bar)
C-09	Water input in E-205 block	30	1
C-10	Water output in E-205 block	102.1	1
C-13	Water input in H block	30	1
C-14	Water output in H block	91.5	1
S-05	Stream feed from reforming section	980.3	28.7
S-05A	Process stream is fed HT-SHIFT block	380	28.7
S-06	Reacted stream with HT-SHIFT block	447.9	28
S-06F	Process stream is fed LT-SHIFT block	210	28
S-07	Reacted stream with LT-SHIFT block	232.8	26.8

The process flow diagram and the condition of each streams of carbon dioxide
removal section were shown in Figure 14 and Table 12. The carbon dioxide was
removed from the converted gas in the CO_2 removal. CO_2 was captured by NH_3 and it
also generates an ammonium hydrogen carbonate as byproduct. The purified gas with
about 0.1 vol% CO_2 is called synthesis gas.

The carbon dioxide removal section was composed of ABSORBER and
STRIPPER blocks. The carbon dioxide removal was used Flash2 because this model
used rigorous vapor liquid equilibrium. The input parameters of ABSORBER and
STRIPPER blocks were temperature and pressure. The temperature of ABSORBER
and STRIPPER were 30 and 60 ^{o}C. The pressure of ABSORBER and STRIPPER
were 25.6 and 1 bar.

There were 3 blocks in the carbon dioxide removal. One heat exchanger
heated up stream and two separators were separation streams. From, the stream S-07
from the carbon monoxide conversion section was fed to the carbon dioxide removal
section. The stream S-07 is heated up from 232.8 to 40 ^{o}C with E210 block. The

stream S-RE2 was removed carbon dioxide by absorption technique. The absorption in liquid phase was often used to get more complete removal of a solute from gas mixture. In this case, a dilute carbon dioxide can be used to scrub water and ammonia (S-RE1) from streams S-RE2. The removed gas (S-RE3) was delivered to methanation section. The stream S-RE4 was rich carbon dioxide that was removed by desorption technique. The stream S-RE4 that was absorbed from a gas mixture was desorbed from the liquid to recover the solute in more concentrated form and regenerate the absorbing solution. The stream S-RE3 was delivered to mathanation section. Simulation result in process stream line S-RE3 was contained carbon dioxide 18.98 kmol/hr.
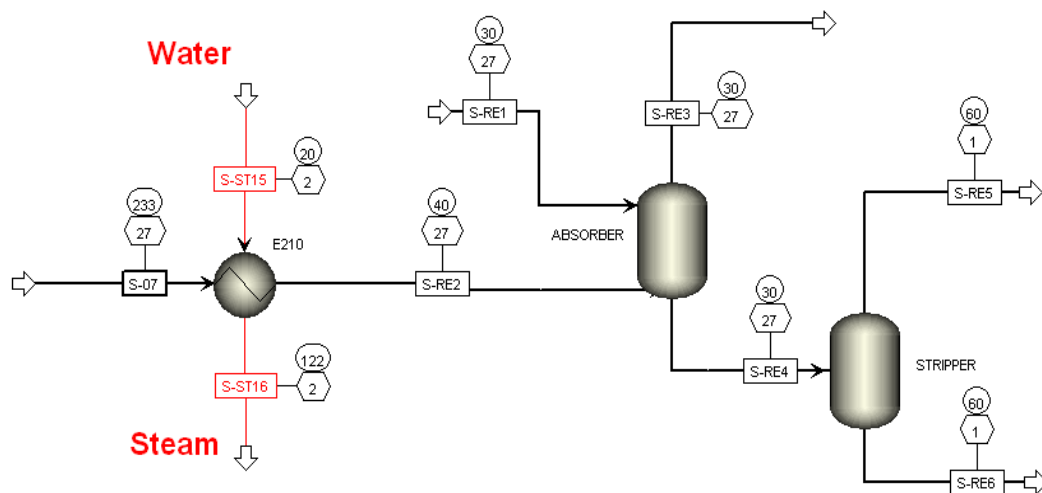
Figure 14 Process model of carbon dioxide removal section

Table 12 Operating condition of each streams of carbon dioxide removal section

Stream no.	Description	T (^{o}C)	P (bar)
S-07	Stream feed from carbon dioxide removal section	232.8	26.8
S-RE1	Solvent solution	30	26.5
S-RE2	Process stream is fed ABSORBER block	40	26.8
S-RE3	Process stream is separated CO_2 gas	30	26.5
S-RE4	Process stream is stripped with STRIPPER block	30	26.5
S-RE5	Process stream is rich CO_2 gas	60	1
S-RE6	Process stream is removed CO_2 gas	60	1
S-ST15	Water input in E210 block	20	2
S-ST16	Water output in E210 block	122	2

The process flow diagram and the condition of each streams of methanation section were shown in Figure 15 and Table 13. Even small quantities of CO (0.1 vol%) and CO_2 (0.3 vol%) were poisons for the ammonia synthesis catalyst. Thus they were reacted to methane over a nickel catalyst. The residual content of CO and CO_2 was less than 10 ppm.

The methanation section was composed of reactor and separation. The methanation reaction was used RPLUG reactor because rigorous plug flow reactor with rate-controlled reactions based on knows kinetics. The separation was used Sep2 because separate compositions into 2 outlet streams based on flows and purities. The input parameters of METH block composed of reactor type, configuration and reaction. The reactor type of METH block was reactor with specified temperature. The configuration of METH block composed of number of tube, length and diameter equal to 30, 3 meter and 0.11 meter. The input parameters of SPLIT-1 were split fraction. The methanation reaction was written external fortran code from Yadav (1993) reaction.

There were 2 blocks in the methanation section that composed one reactor and one separation. From the carbon dioxide removal section, the stream S-9 was fed to the mathanation section. The stream S-9 was reformed carbon monoxide and carbon dioxide to methane with METH block. The stream S-9A was separated hydrogen, nitrogen and water in stream S-9B. The stream S-1 was delivered to synthesis and refrigeration section. Simulation result in process stream line S-1 did not have carbon dioxide and carbon monoxide.
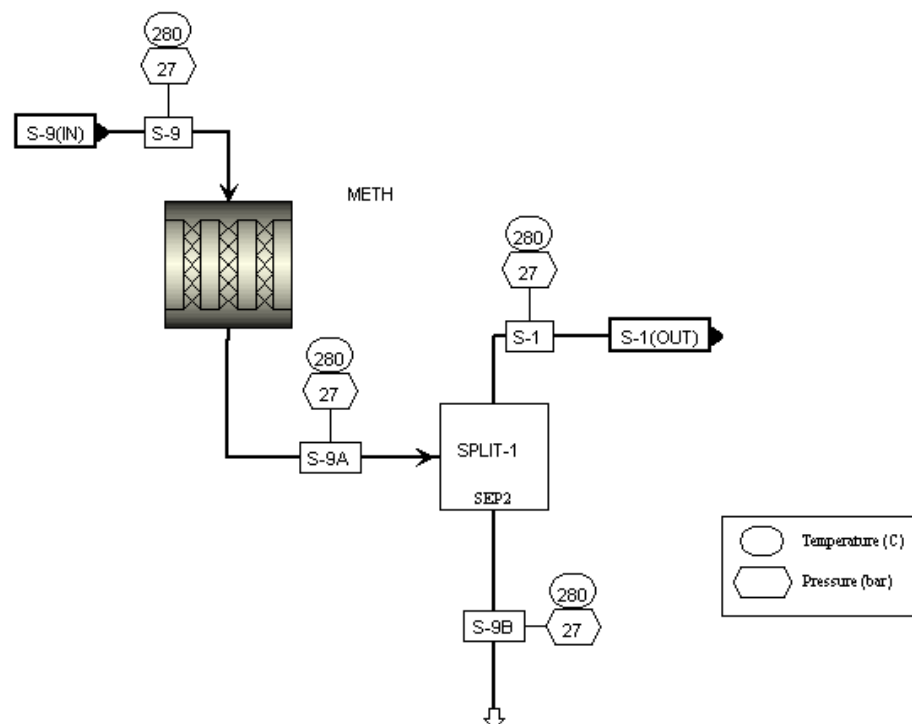
Figure 15 Process model of methanation section

Table 13 Operating condition of each streams of methanation section

Stream no.	Description	T (^{o}C)	P (bar)
S-1	Main process stream	280	26.5
S-9	Stream feed from methanation section	280	26.5
S-9A	Reacted stream with METH block	280	26.5
S-9B	Removed gas	280	26.5

A typical ammonia production process consists of (a) production of the synthesis gas, (b) compression of the gas to the required pressure, and (c) synthesis loop in which its conversion to ammonia takes place. Although the first two sections have their own importance, the converter which is part of the synthesis loop is crucial in the overall control strategy of the plant.

The process flow diagram and the conditions of each stream of synthesis and refrigeration sections were shown in Figure 16 and Table 14. The synthesis gas was pressurized by a centrifugal compressor to approximately 300 bar and hydrogen and nitrogen were catalytically converted to ammonia. Simulation result in process stream line S-3 composed of ammonia 4182.36 kmol/hr. The ammonia in the purge gas from the ammonia unit was recovered in the tailgas scrubbing unit and fed to a refrigeration unit. The treated purge gas was used as fuel for the primary reformer. Simulation result in process stream line S-14 and S-15 composed of ammonia 3096.63 and 10.25 kmol/hr. The results of ammonia process model from ASPEN PLUS were shown in APPENDIX A.

Figure 16 Process model of synthesis and refrigeration section

Table 14 Operating condition of each streams of synthesis and refrigeration section

Stream no.	Description	T (^{o}C)	P (bar)
S-1	Stream feed from methanation section	280	26.5
S-2	Compressed stream with COMPR-A block	5	275
S-2B	Compressed stream with COMPR-B block	30.1	292
S-2V	Stream feed to SYNTH block	180	292
S-3	Stream output from SYNTH block	444.1	284
S-3A	Heated stream with E001A block	240	281
S-3B	Heated stream with E002 block	83.9	278
S-3C	Heated stream with E003 block	39.4	275
S-3E	Separated stream with F002 block	39.4	275
S-3F	Separated stream with F001 block	8.1	274.5
S-3G	Heated stream with E004 block	22.6	274.5
S-3H	Heated stream with E004 block	30.7	275
S-3I	Separated stream with PURGEVL block	15	275
S-3J	Mixed stream with MIX6-1 block	8.1	275
S-3K	Separated stream with PURGEVL block	15	275
S-3L	Separated stream with PURGE-S block	15	275
S-3M	Stream output from REFRIG1 block	15	275
S-4	Mixed stream with D001M block	33.7	30
S-4A	Separated stream with D001 block	33.8	30
S-4B	Separated stream with D001 block	33.8	30
S-4C	Stream output from REFRIG2 block	25.6	30
S-4D	Separated stream with 08-E007F block	25.6	30
S-5	Separated stream with PURGE-S block	15	275
S-6	Separated stream with 08-E007F block	25.6	30
S-7	Water input in E001A block	105	48.5
S-8	Water output in E001A block	323.7	45
S-12	Separated stream with SPLIT6-1 block	33.7	30
S-12A	Separated stream with SPLIT6-1 block	33.7	30
S-14	Separated stream with D002 block	33.3	20
S-15	Separated stream with D002 block	33.3	20
S-18	Separated stream with F002 block	39.4	275
S-19	Separated stream with F001 block	8.1	274.5

2. Heat integration process of ammonia production

Energy conservation is important in the process design. In industrial process, the calculation of the minimum heating and cooling requirements reveal significant energy savings. The first step in the energy integration analysis is the calculation of the minimum heating and cooling requirements for a heat-exchanger network. In the ammonia process flow sheet, there are four streams that need to be heated, are five streams that need to be cooled. There are two laws for heat integration analysis. The first laws states that the difference between the heat available in the hot streams. The heat required for the cold streams is the net amount of heat that must be removed or supplied.

According to nine streams in the proposed ammonia process, five streams need to be cooled and four streams need to be heated up were chosen. Figures 17, 18 and Table 15 show the descriptions of the chosen streams.
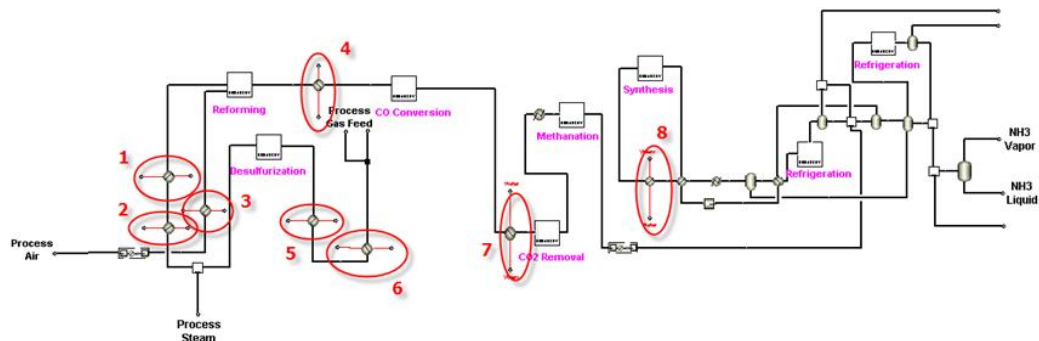
Figure 17 Schematic Diagram of Ammonia Production Plant
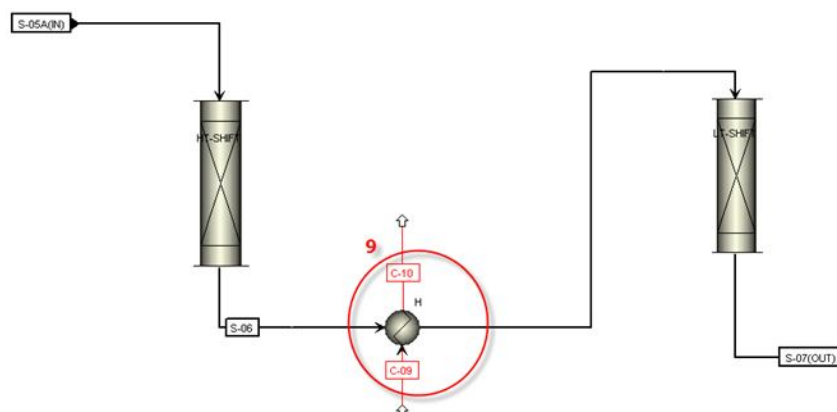
Figure 18 Schematic Diagram in CO conversion section

Table 15 Description of Streams for heat integration

Stream No.	Name heat exchanger	Description
1	HLOSS1	Desufurized gas going in Reforming
2	E-201	Desufurized gas going in Reforming
3	E-202	Process air going in Reforming
4	E-205	Reformed gas going in CO conversion
5	E-204A	Process gas going in Desulfurization
6	E-204B	Process gas going in Desulfurization
7	E210	Reacted gas going from CO conversion to CO_2 Removal
8	E001A	Synthesis gas going to separation
9	H	Reacted gas going from high shift temperature to low shift temperature

Table 16 First Law Calculation

Stream No.	Condition	MCp (kJ/°C.hr)	Tin (°C)	Tout (°C)	Enthalpy (kJ/hr)
1	Hot	333,198.43	513.5	503.3	3,411,950.87
2	Cold	324,562.25	347.9	513.5	-53,773,192.55
3	Cold	72,588.39	133.1	482.3	-25,348,969.84
4	Hot	444,436.17	980.3	380.0	266,800,364.59
5	Cold	87,032.44	253.5	344.2	-7,894,414.80
6	Cold	74,103.43	46.9	253.5	-15,305,495.62
7	Hot	1,192,402.00	232.8	40.0	229,859,741.89
8	Hot	653,237.56	444.1	240.0	133,349,151.02
9	Hot	423,210.08	447.9	210.0	100,699,700.43
				Total	63,178,836

As shown in the Table 16, 63,178,836 kJ/hr must be supplied from utilities if no restrictions on temperature-driving forces are present. However, the calculation for the first law does not consider the fact that heat can only be transferred from a hot stream to a cold stream if the temperature of the hot stream surpasses that of the cold stream. Therefore, a second law states that a positive temperature driving force must exist between the hot and the cold streams. For any heat-networks, the second law must be satisfied as well as the first law.

A simple way to encompass the second law was presented by Hohmann and Umeda (1971), and Linhoff and Flower (1979). A description of their analysis is shown in accordingly. The minimum driving force of 10 °C between the hot and the cold streams is chosen, a graph can be established showing two temperature scales that are shifted by 10 °C, one for the hot streams and the other for the cold streams. Then, stream data is plotted on this graph (Figure 19). Next a series of temperature intervals are generated corresponding to the heads and the tails of the arrows on the graph.
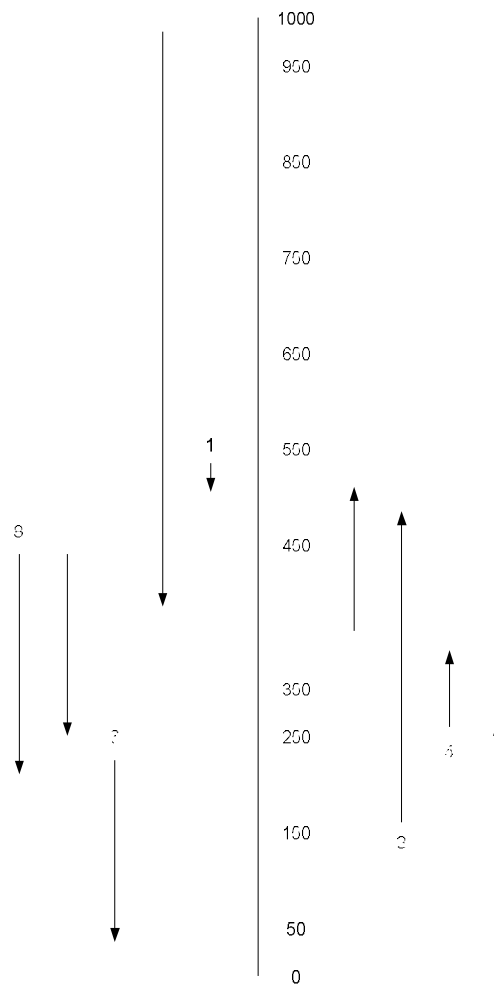
Figure 19 Shifted Temperature Scale

To construct a temperature-enthalpy diagram, the minimum heating and cooling loads must first be calculated using the procedure above. Therefore, the cumulative H will be plotted versus T (Figure 20). This is called composite a curve for the hot streams because it includes the effect of all hot streams. Likewise, the composite curve for the cold streams can be created by calculating the cumulative enthalpy of each cold stream. In this case, composite curve from ASPEN HX-NET simulator is shown in Figure 20. For this Figure, the composite curve is added the minimum heating and cooling requirements.
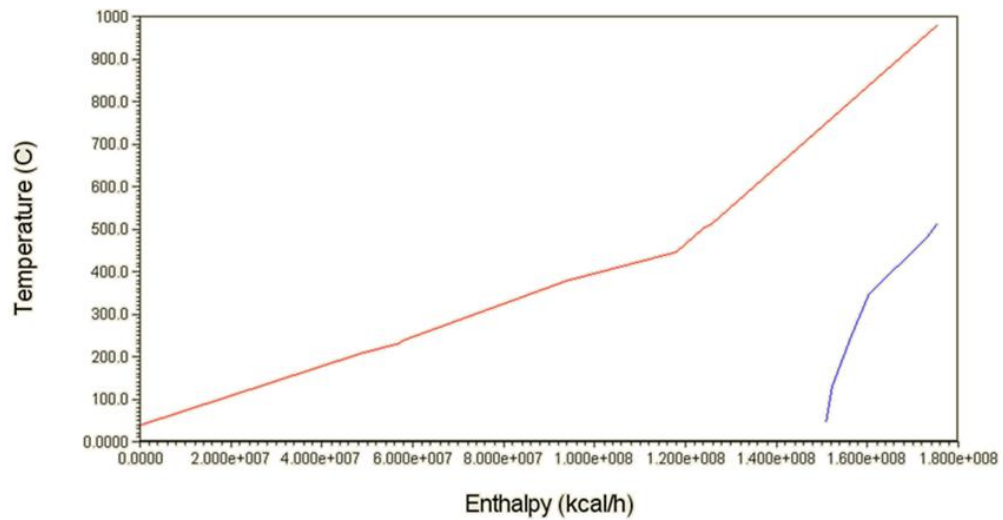
Figure 20 Temperature-Enthalpy Diagram (Composite curve)

From composite curve (Figure 20), the structure of heat integration that is maximum energy recovery (MER) can be constructed by ASPEN HX-NET simulator. The results from ASPEN HX-NET proposed ten structures (See in Appendix B). They are called superstructures because the structures of heat integration are MER. From ten superstructures, number tenth structure (See Figure 21) is chosen for using in the process.

The efficiency of super structure from ASPEN HX-NET were shown amount of spliter, heat exchanger, and total cost index in Table 17. In this structure (Figure 21), Tenth structure is chosen because the amount of split and heat exchanger are the least in the other structures and the least total capital cost index. Tenth structure is used in ammonia process that is shown in Figure 22. The energy is decrease 24.5 percent (energy in heat integration process 630,638,082 kJ/hr and original process 835,282,228 kJ/hr) in heat integration process.

Table 17 Efficiency of super structure from ASPEN HX-NET

Number of structure	Amount of spliter	Amount of heat exchanger	Total Cost Index (Cost/s)
Structure 1	5	13	0.103
Structure 2	4	13	7.26e-002
Structure 3	4	13	8.42e-002
Structure 4	3	12	9.00e-002
Structure 5	5	13	9.19e-002
Structure 6	3	11	9.72e-002
Structure 7	4	12	0.103
Structure 8	2	11	0.109
Structure 9	3	12	9.71e-002
Structure 10	2	11	7.26e-002
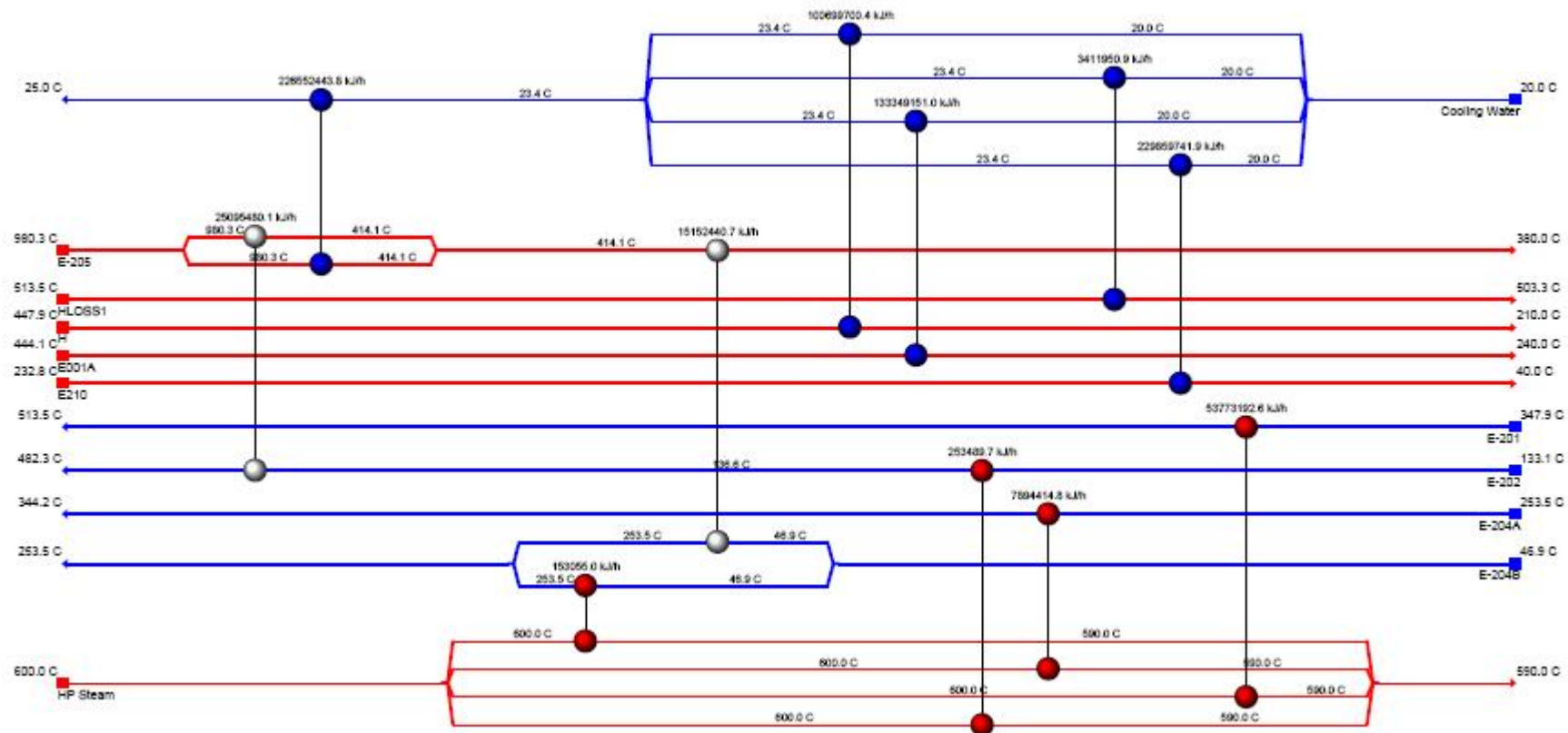
Figure 21 The superstructure number 10 from ASPEN HX-NET
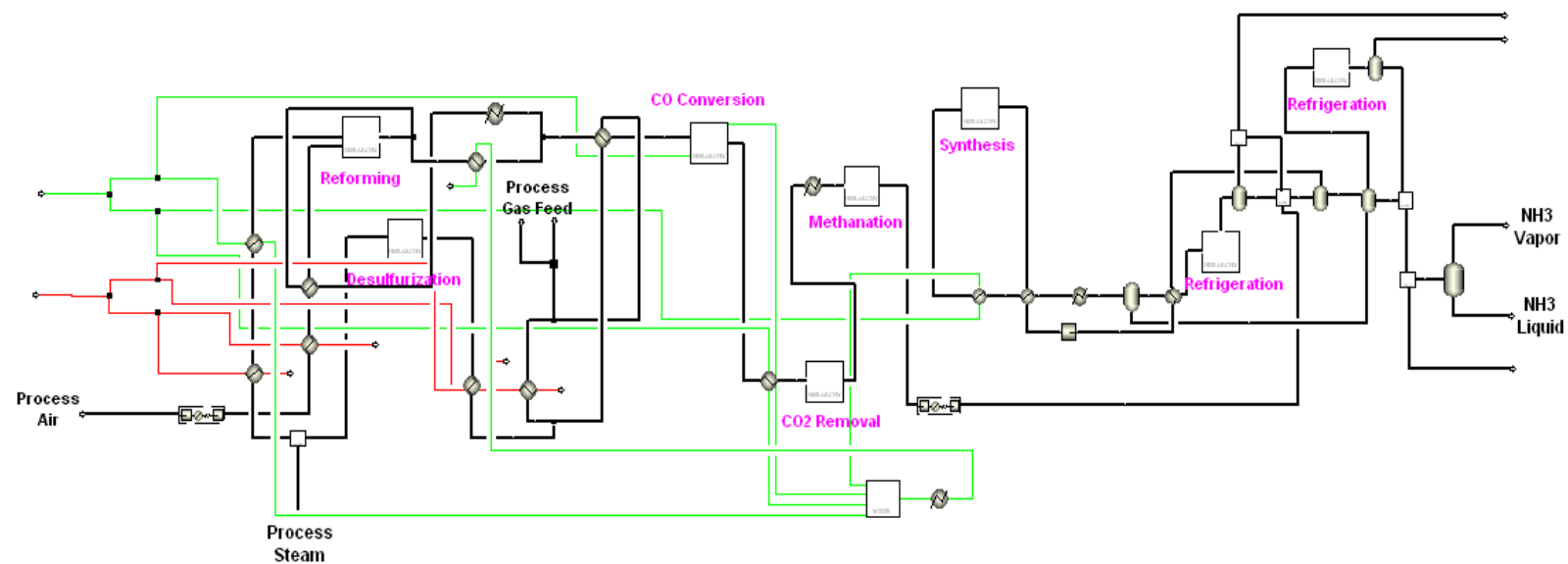
Figure 22 The ammonia process model combined heat integration

3. Test of controllability for ammonia process

In this part, the steady-state simulations from the previous part were exported into dynamic simulation files. At first, the ASPEN DYNAMIC 2006.5 was used to run the simulations. The test can be performed by changing the feed temperature to observe the dynamic responses of the process. The process variables should be reached the design setpoint or new steady-state point after changing of feed temperature. The purity of the process has not lower than the limitation of 99.82 wt%. To test the controllability of the control system, the feed temperature of each section was changed to plus or minus 10 % of original steady-state designed value. The results of the test were divided into 2 parts which were the test results of plus and minus 10 % of feed temperature for each section. The results of tuning parameter based on Tyreus-Luyben are shown in Table 18 for ammonia process model.

Table 18 Results of tuning parameter from ammonia process model

Controller	Name	Type of controller	Tuned parameter K_C	τ_i
Temperature controller at E-204B	TC-01	PI	1.09	0.90
Temperature controller at E-204A	TC-02	PI	1.83	2.00
Temperature controller at E-201	TC-03	PI	0.46	6.00
Temperature controller at HLOSS1	TC-04	PI	0.60	1.21
Temperature controller at E-202	TC-05	PI	677.23	0.95
Temperature controller at PREF-T	TC-06	PI	0.83	2.00
Temperature controller at SREF-R	TC-07	PI	7.03	4.00
Temperature controller at ABSORBER	TC-08	PI	0.27	4.00
Temperature controller at STRIPPER	TC-09	PI	0.27	2.00
Temperature controller at H	TC-10	PI	9.08	4.00
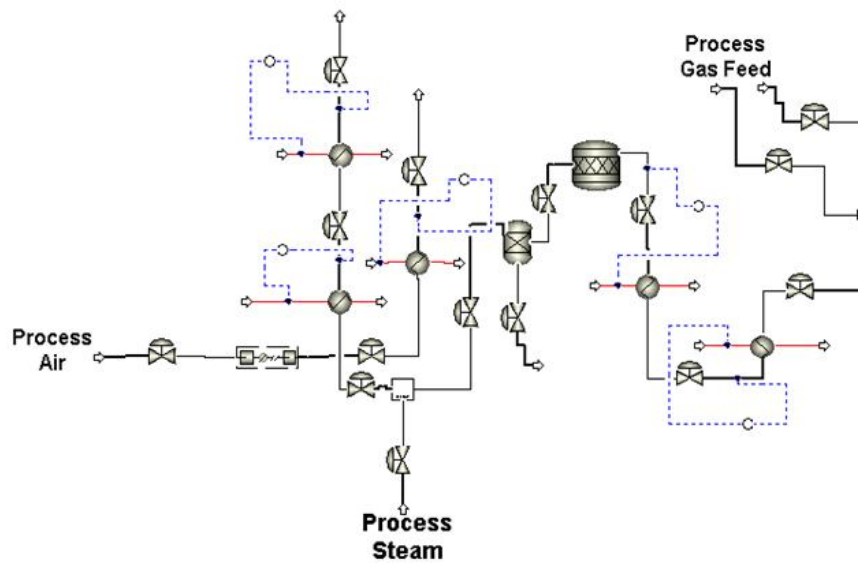
Figure 23 The desulfurization section control temperature system

3.1 Increasing 10 % of Reactant Feed Temperature for desulfurization section

For the part of desulfurization section process (Figure 23), the temperature of the feed natural gas was changed to 10 % higher than the value of the steady-state condition at 1 hour of the simulation time, shown in Figures 24, 25. The previous steady-state value of temperature feed natural gas was 45 ^{o}C. At the new steady-state, the value of each temperature was 49.5 ^{o}C.
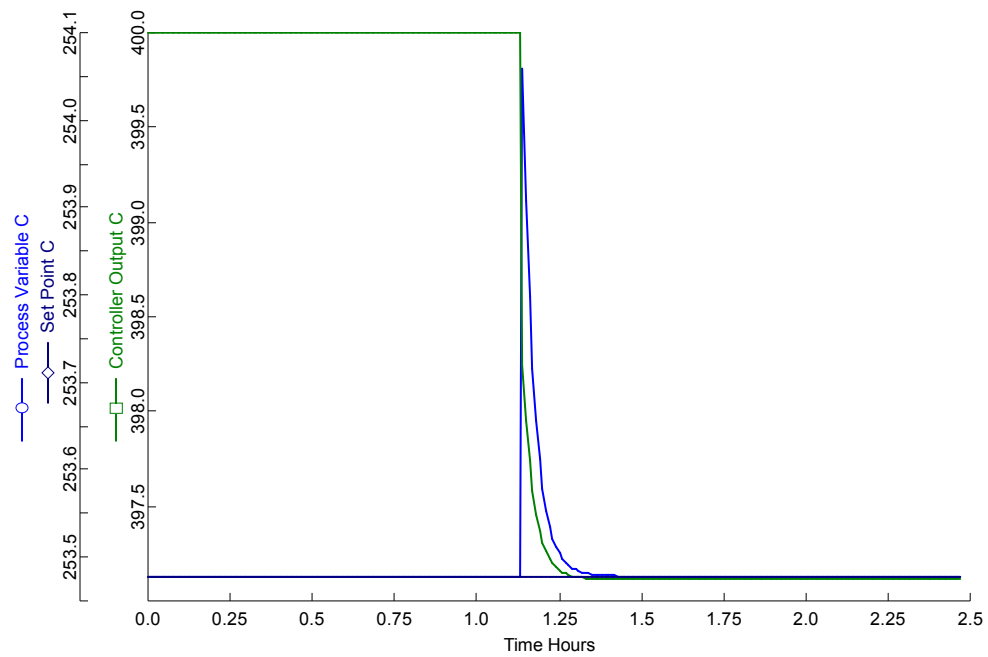
(a)
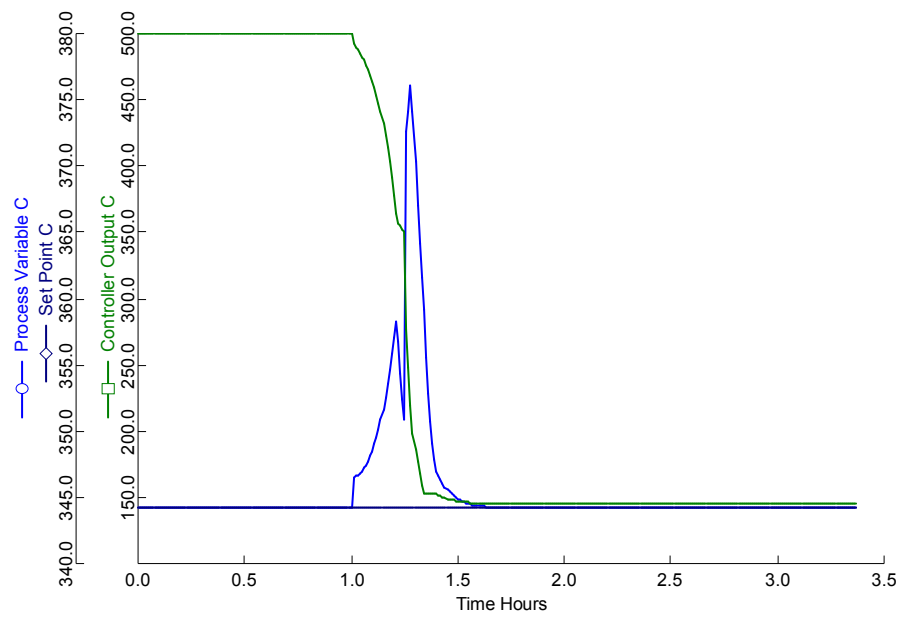
(b)

Figure 24 Responses of TC-01, TC-02 controller for increasing 10 % of feed temperature of desulfurization section (a) TC-01 (b) TC-02
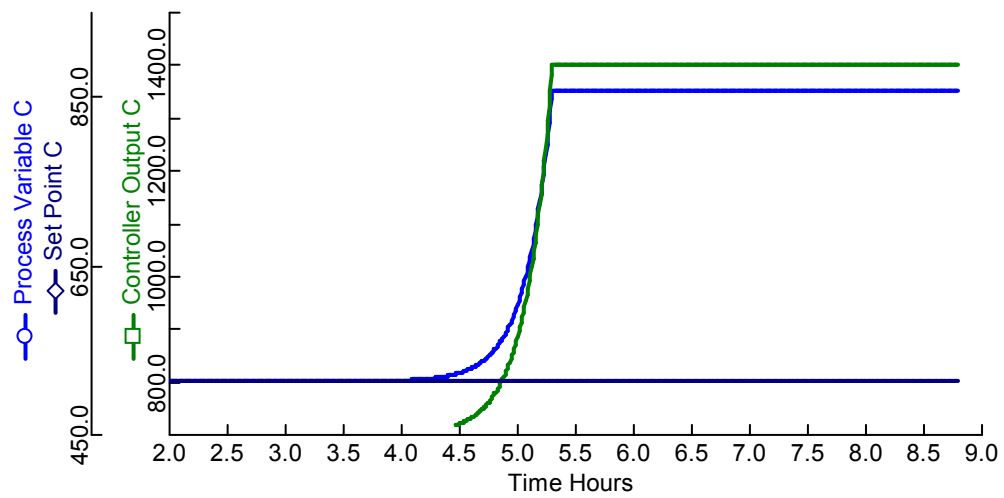
(a)
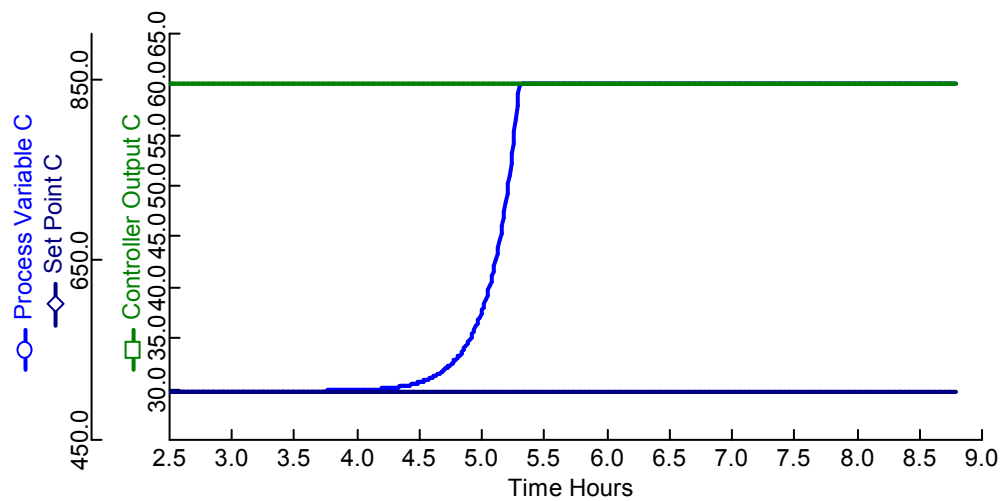
(b)

Figure 25 Responses of TC-03, TC-05 controller for increasing 10 % of feed
temperature of desulfurization section (a) TC-03 (b) TC-05

From the Figure 24, the response of TC-01 and TC-02 for increasing 10 %
feed temperature of desulfurization section is increase at 1 hour and the responses are
stable at 1.5 and 2 hour. From the Figure 25, the responses of TC-03 and TC-05 for
increasing 10 % feed temperature of desulfurization section is increase response of the
process and the process can reach to the new steady-state condition at 4 hour.

3.2 Increasing 10 % of Reactant Feed Temperature for reforming section

For the part of reforming section process (Figure 26), the temperature of the desulfurized gas was changed to 10 % higher than the value of the steady-state condition at 1 hour of the simulation time, shown in Figure 27.
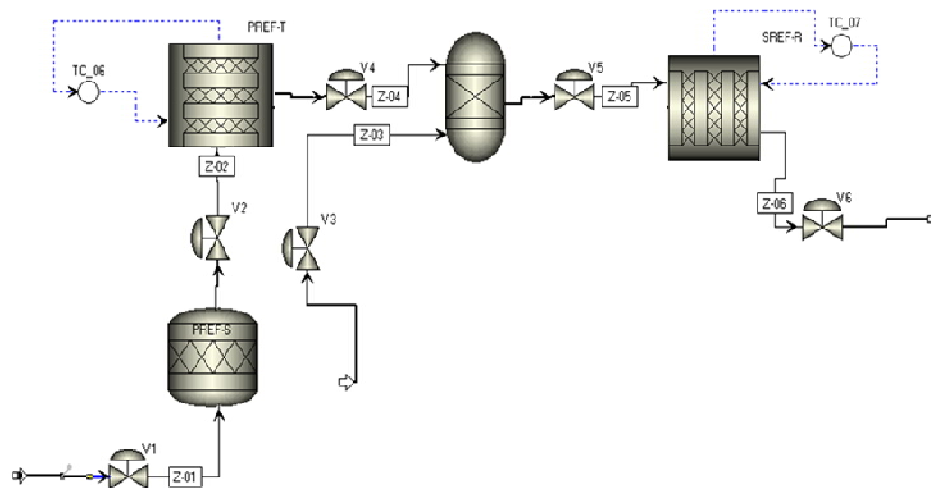
Figure 26 The reforming section control temperature system

(a)

(b)
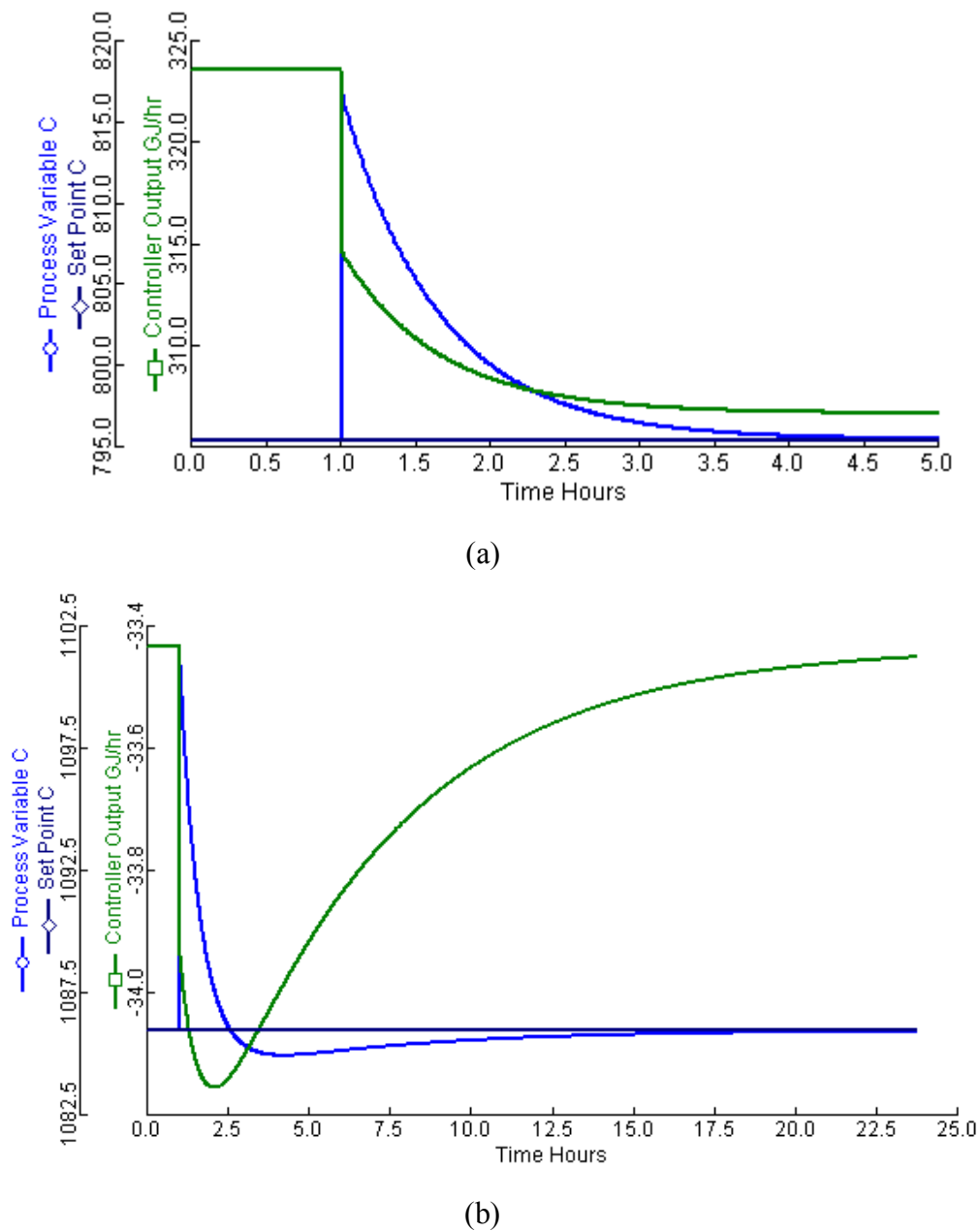
Figure 27 Responses of TC-06, TC-07 controller for increasing 10 % of feed temperature of reforming section (a) TC-06 (b) TC-07

From Figure 27 (a), the response of TC-06 for increasing 10 % feed temperature of reforming section is increase at 1 hour and the response is stable at 4 hour. From the Figure 27 (b) the response of TC-07 for increasing 10 % feed

temperature of reforming section is increase at 1 hour and the response is stable at 22.5 hour.

3.3 Increasing 10 % of Reactant Feed Temperature for CO_2 removal section

For the part of CO_2 removal section process (Figure 28), the temperature of the reformed gas was changed to 10 % higher than the value of the steady-state condition at 1 hour of the simulation time, shown in Figure 29.
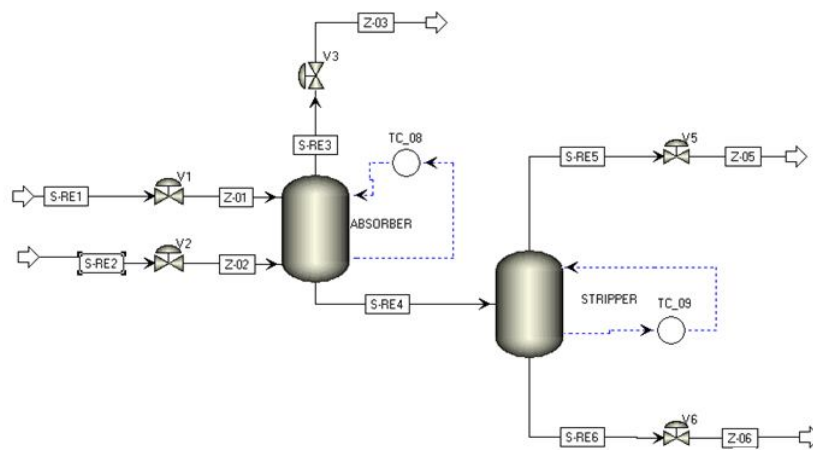
Figure 28 The CO_2 removal section control temperature system
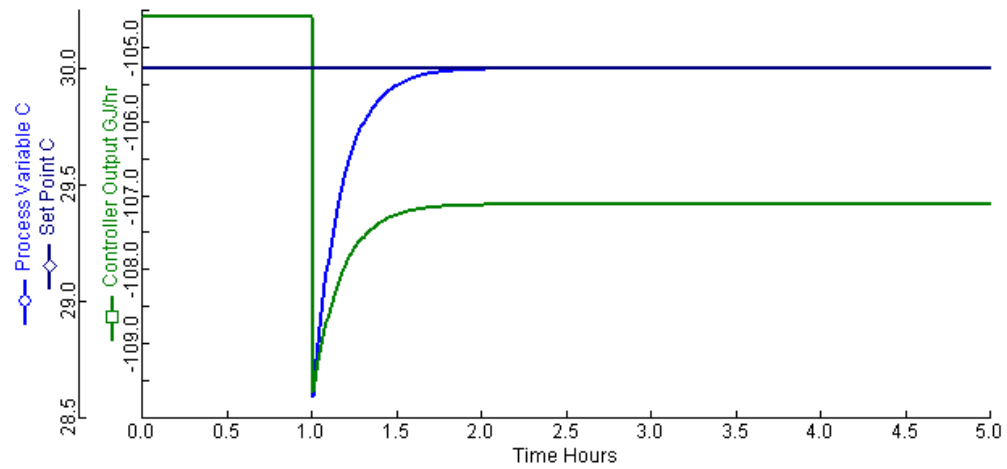
(a)
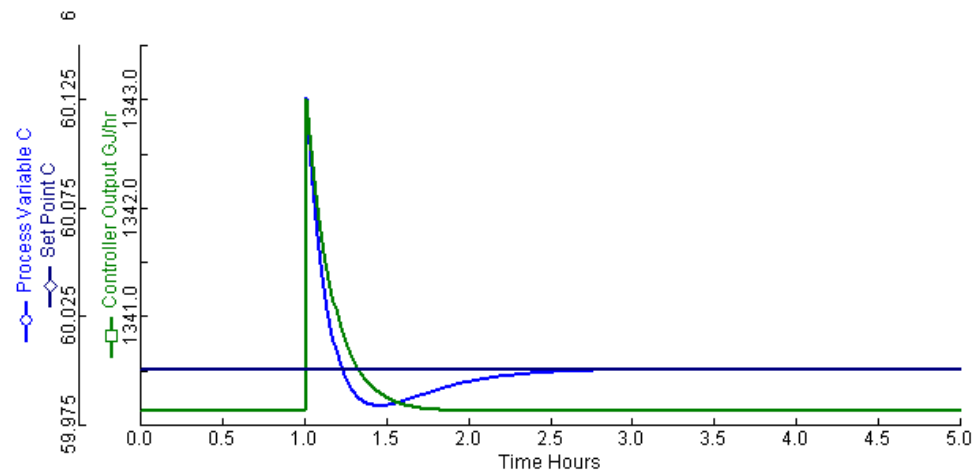
(b)

Figure 29 Responses of TC-08, TC-09 controller for increasing 10 % of feed
temperature of CO_2 removal section (a) TC-08 (b) TC-09

From the Figure 29, the responses of TC-08 and TC-09 for increasing 10
% feed temperature of CO_2 removal section disturb the response of the process and
the process can reach to the new steady-state condition at 2 and 2.5 hour, respectively.

3.4 Increasing 10 % of Reactant Feed Temperature for CO Conversion
section

For the part of CO Conversion section process (Figure 30), the
temperature of the reformed gas was changed to 10 % higher than the value of the
steady-state condition at 1 hour of the simulation time, shown in Figure 31.
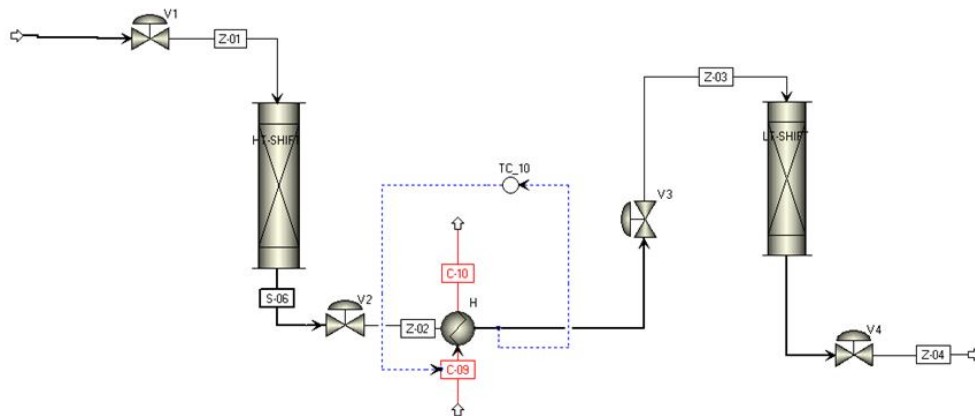
Figure 30 The CO conversion section control temperature system
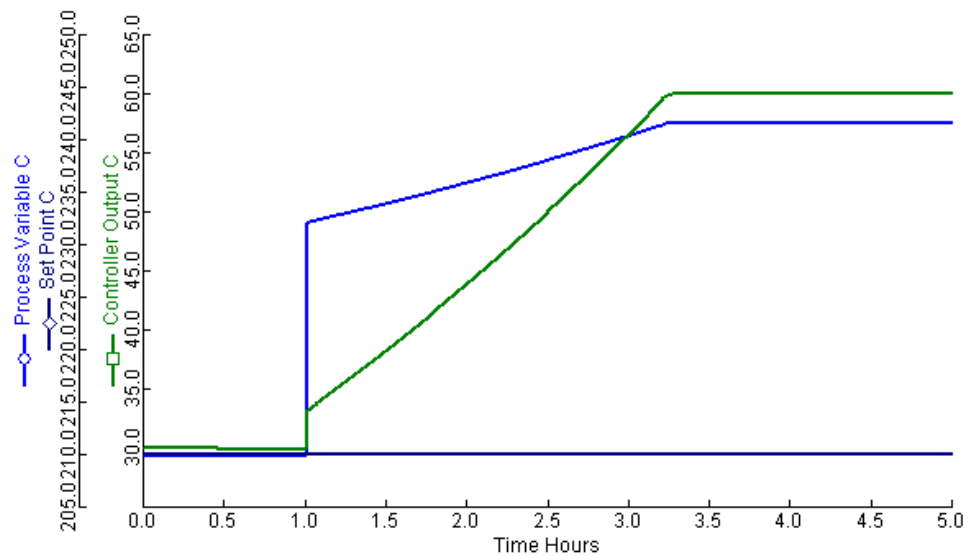
Figure 31 Response of TC-10 controller for increasing 10 % of feed
temperature of CO Conversion section

From the Figure 31, the response of TC-10 for increasing 10 % feed temperature of CO Conversion section disturb the response of the process and the process can reach to the new steady-state condition at 3 hour.

3.5 Decreasing 10 % of Reactant Feed Temperature for desulfurization section

For the part of desulfurization section process, the temperature of the feed natural gas was changed to 10 % lower than the value of the steady-state condition at 1 hour of the simulation time. For testing of controllability for desulfurization section process, the feed temperature of reactants was tried to decrease about 10 % of the designed value. After about 10 minutes of simulation time have passed, the simulation shows error message of calculations. The responses of each controller were checked to find the cause of this problem. However, there is not an uncontrolled parameter which leads to this problem. Therefore, the 10 % decreasing of reactant temperature in steady-state simulation was performed to investigate the problem. After the feed temperature of reactants was decreased and the simulation was run, the flowsheet is not converged. Therefore, this is a problem of steady-state calculation. It is not a controllability problem.

3.6 Decreasing 10 % of Reactant Feed Temperature for reforming section

For the part of reforming section process (Figure 26), the temperature of the desulfurized gas was changed to 10 % lower than the value of the steady-state condition at 1 hour of the simulation time, shown in Figure 32.
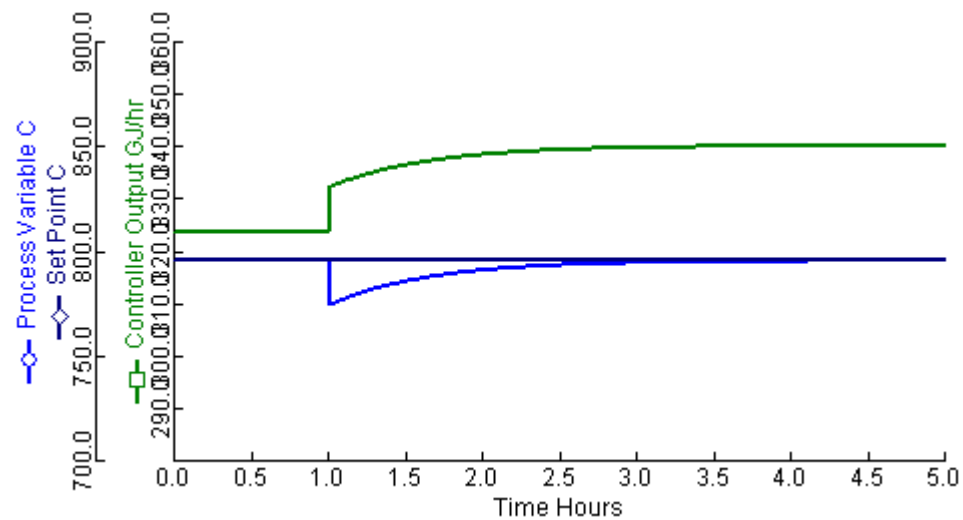
(a)
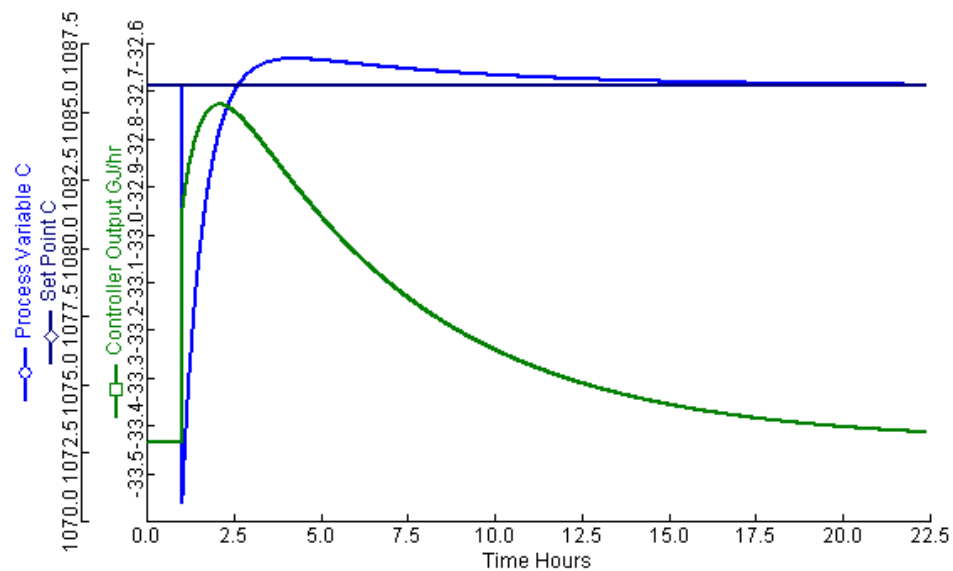
(b)

Figure 32 Responses of TC-06, TC-07 controller for decreasing 10 % of feed
temperature of reforming section (a) TC-06 (b) TC-07

From the Figure 32 (a), the response of TC-06 for decreasing 10 % feed
temperature of reforming section is increase at 1 hour and the response is stable at 3
hour. From the Figure 32 (b) the response of TC-07 for decreasing 10 % feed
temperature of reforming section is decrease at 1 hour and the response is stable at
22.5 hour.

3.7 Decreasing 10 % of Reactant Feed Temperature for CO_2 removal section

For the part of CO_2 removal section process (Figure 28), the temperature of the desulfurized gas was changed to 10 % lower than the value of the steady-state condition at 1 hour of the simulation time, shown in Figure 33.
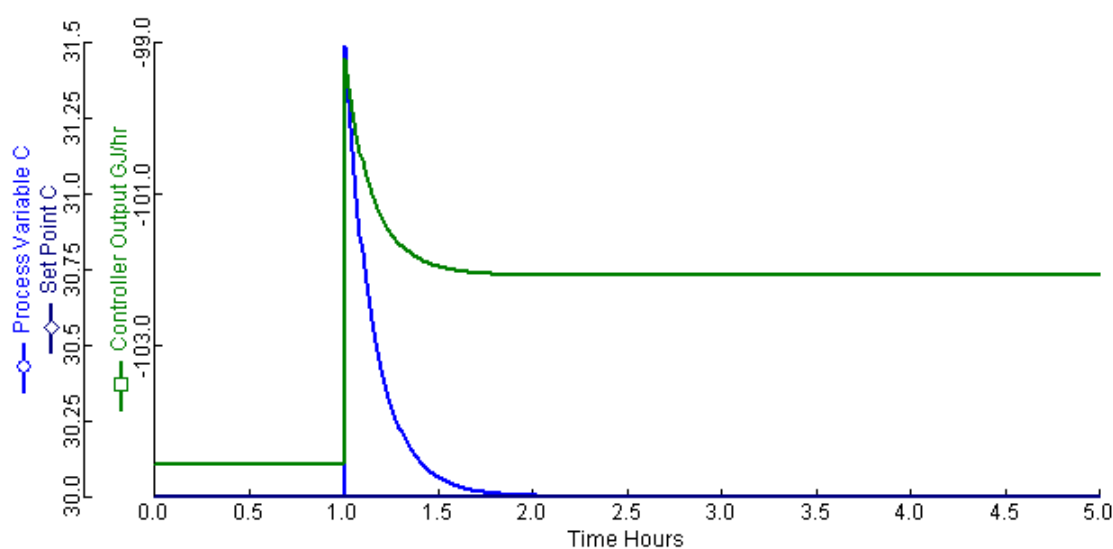
(a)
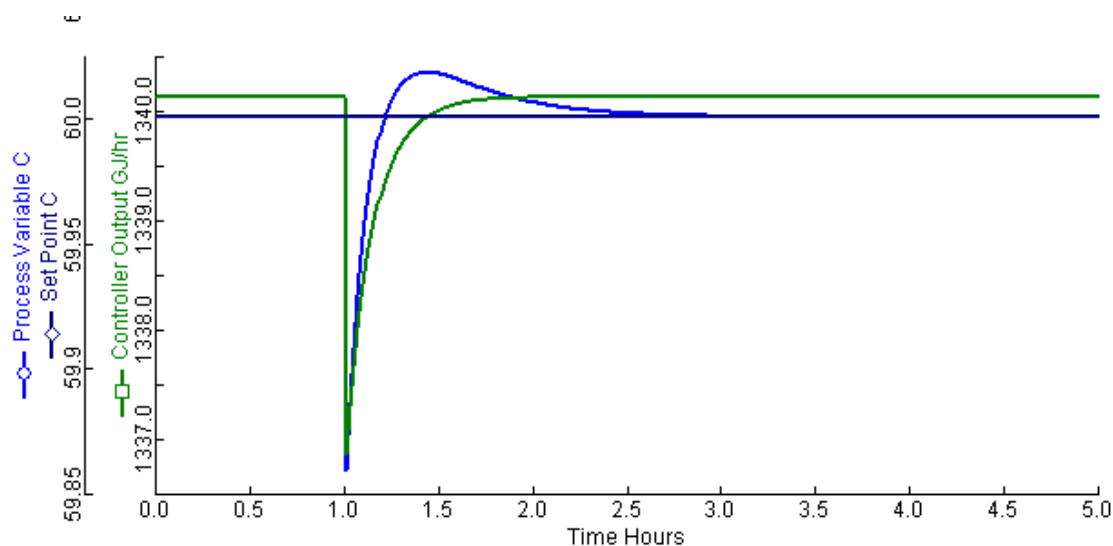
(b)

Figure 33 Responses of TC-08, TC-09 controller for decreasing 10 % of feed temperature of CO_2 removal section (a) TC-08 (b) TC-09

From the Figure 33, the responses of TC-08 and TC-09 for decreasing 10 % feed temperature of CO_2 removal section disturb the response of the process and the process can reach to the new steady-state condition at 2 and 2.5 hour, respectively.

3.8   Decreasing 10 % of Reactant Feed Temperature for CO Conversion section

For the part of CO Conversion section process (Figure 30), the temperature of the reformed gas was changed to 10 % lower than the value of the steady-state condition at 1 hour of the simulation time, shown in Figure 34.
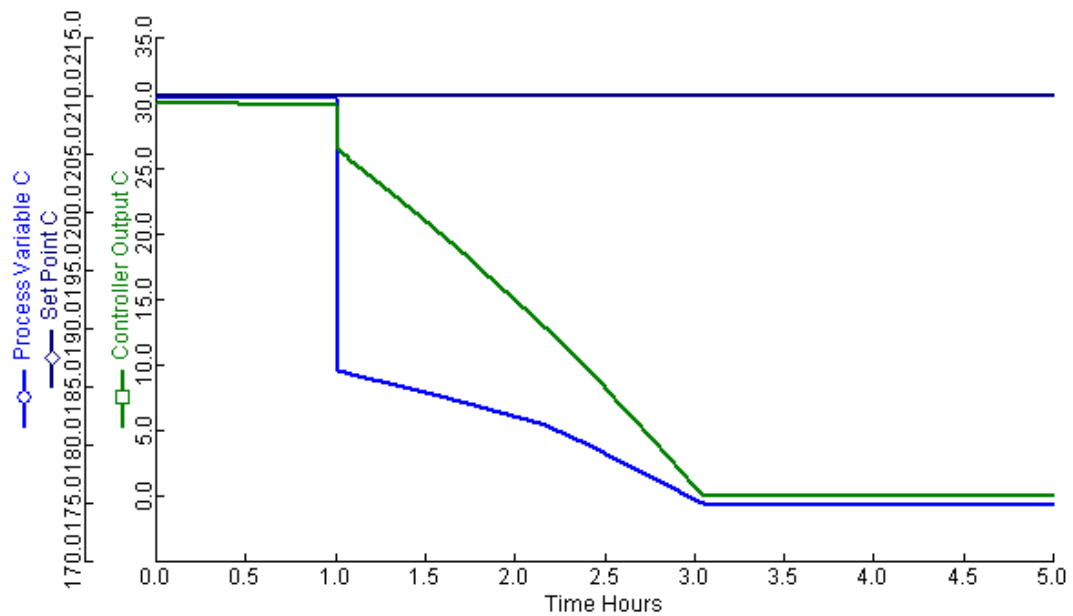
Figure 34 Responses of TC-10 controller for decreasing 10 % of feed temperature of CO Conversion section

From the Figure 34, the response of TC-10 for decreasing 10 % feed temperature of CO Conversion section disturb the response of the process and the process can reach to the new steady-state condition at 3 hour.

4. Model Predictive Control (MPC)

Model predictive control offers several important advantages: (1) The process model captures the dynamic and static interactions between input, output and disturbance variables; (2) constraints on inputs and outputs are considered in a systematic manner; (3) the control calculations can be coordinated with the calculation of optimum set points, and (4) accurate model predictions can provide early warnings of potential problems. The model predictive control is feed forward control. Previously, the state space model was created to use in model predictive control. In this case, the CSTR with a recirculating jacket (Figure 36) is considered at the desulfurization section. This reactor is the DESULF-R block. From B. Wayne et.al, (2002) the state space model can be created for simulating by MATLAB simulator. The MPC control for in this case has three steps. First, the CSTR with a recirculating jacket is created by ASPEN PLUS simulator. Second, the ASPEN PLUS model is exported to ASPEN DYNAMIC. Third, ASPEN DYNAMIC and MATLAB are linked by AM Simulation block for simulating model predictive control.

Based on the following assumptions:

1. Perfect mixing.

2. The inlet and outlet flow rates are equal.

3. The density ρ and heat capacity C of the liquid are assumed to be constant.

Conservation of Mass

$$\{\text{rate of mass accumulation}\} = \{\text{rate of mass in}\} - \{\text{rate of mass out}\} \qquad (75)$$

$$\frac{d(\rho V)}{dt} = \rho q_i - \rho q \qquad (76)$$

Because V and ρ are constant,

$$0 = q_i - q \qquad (77)$$

$$q_i = q \tag{78}$$

Conservation of Component i

$$\begin{Bmatrix} \text{rate of component i} \\ \text{accumulation} \end{Bmatrix} = \begin{Bmatrix} \text{rate of component i} \\ \text{in} \end{Bmatrix} - \begin{Bmatrix} \text{rate of component i} \\ \text{out} \end{Bmatrix} + \\ \begin{Bmatrix} \text{rate of component i} \\ \text{produced} \end{Bmatrix}$$

$$V\frac{dc_A}{dt} = q_i c_{Ai} - q_i c_A - Vkc_A \tag{79}$$

$$V\frac{dc_A}{dt} = q_i(c_{Ai} - q_i c_A) - Vkc_A \tag{80}$$

Conservation of Energy

Assumptions:

1. Changes in potential energy and kinetic energy can be neglected because they are small in comparison with changes in internal energy.

2. The net rate of work can be neglected because it is small compared to the rates of heat transfer and convection.

$$\therefore \quad \frac{dU_{int}}{dt} = -\Delta(w\hat{H}) + Q \tag{81}$$

$$U_{int} = \hat{H} \tag{82}$$

Assume that: $U_{int} = \hat{H}$ and $\hat{U}_{int} = \hat{H}$

$$\frac{dU_{int}}{dt} = \frac{d(\rho V\hat{U}_{int})}{dt} = \rho V\frac{d\hat{H}}{dt} = \rho VC\frac{dT}{dt} \tag{83}$$

$$-\Delta(w\hat{H}) = w[C(T_i - T_{ref})] - w[C(T - T_{ref})] = wC(T_i - T) \tag{84}$$

$$\therefore \rho VC \frac{dT}{dt} = wC(T_i - T) + Q \qquad (85)$$

Make five additional assumptions

1. The thermal capacitances of the coolant and the cooling coil wall are negligible compared to the thermal capacitances of the liquid in the tank.

2. All of coolant is at a uniform temperature, T_C

3. $Q = UA(T_c - T)$

4. The heat of mixing is negligible compared to the heat of reaction.

5. Shaft work and heat losses can be neglected.

$$\left\{ \begin{array}{c} \text{rate of energy} \\ \text{accumulation} \end{array} \right\} = \left\{ \begin{array}{c} \text{rate of energy in} \\ \text{by convection} \end{array} \right\} - \left\{ \begin{array}{c} \text{rate of energy out} \\ \text{by convection} \end{array} \right\}$$
$$+ \left\{ \begin{array}{c} \text{net rate of heat addition} \\ \text{to the system from} \\ \text{the surrounding} \end{array} \right\} + \left\{ \begin{array}{c} \text{net rate of work} \\ \text{performed on the system} \\ \text{by the surrounding} \end{array} \right\} \qquad (86)$$

$$\therefore \rho VC \frac{dT}{dt} = wC(T_i - T) + (-\Delta H_R)Vkc_A + UA(Tc - T) \qquad (87)$$

$$V \frac{dc_A}{dt} = q(c_{Ai} - c_A) - Vk_{cA} \qquad (88)$$

$$\rho VC \frac{dT}{dt} = wC(T_i - T) + (-\Delta HR)Vkc_A + U_A(T_c - T) \qquad (89)$$

Input variable: T_C

Output variable: c_A, T_C

q, inlet condition assumed to be constant

From

$$\frac{dy}{dt} = f(y,u) \tag{90}$$

The resulting linearization model is in the form of

$$\frac{dy'}{dt} = \frac{\partial f}{\partial y}\Big|_s y' + \frac{\partial f}{\partial u}\Big|_s u' + \frac{\partial f}{\partial z}\Big|_s z' \tag{91}$$

Where y is the output, u is the input and z is another input variable.

$$f_1 = \frac{1}{V}[q(c_{Ai} - c_A) - Vkc_A \ ] \tag{92}$$

$$f_2 = \frac{1}{\rho VC} \ [wC(Ti - T) + (-\Delta H_R)Vkc_A + UA(T_c - T)] \tag{93}$$

$$\therefore \frac{dc_A'}{dt} = \frac{\partial f_1}{\partial c_A}\Big|_s y' + \frac{\partial f_1}{\partial T_c}\Big|_s T_C' + \frac{\partial f_1}{\partial T}\Big|_s T' \tag{94}$$

$$= \left(-\frac{q}{v} - k_0 e^{-\frac{E}{R\overline{T}}}\right) c_A' + (-\overline{c}_A k_0 (\frac{E}{R\overline{T}^2}) e^{-\frac{E}{R\overline{T}}}) T' \tag{95}$$

$$= a_{11} c_A' + a_{12} \ T' \tag{96}$$

$$\therefore \frac{dT'}{dt} = \frac{\partial f_2}{\partial c_A}\Big|_s c_A' + \frac{\partial f_2}{\partial T_c}\Big|_s T_C' + \frac{\partial f_2}{\partial T}\Big|_s T' \tag{97}$$

$$= \left(\frac{-\Delta H k_0 e^{-\frac{E}{R\overline{T}}}}{\rho C} \right) c_A' + \frac{1}{V\rho C} \left[-(wC + UA) - (\Delta H)V\overline{c}_A k_0 (\frac{E}{R\overline{T}^2})e^{-\frac{E}{R\overline{T}}} \right] T' + \left(\frac{UA}{V\rho C} \right) T_c'$$

$$= a_{21} c_A' + a_{22} T' + b_2 T_c'$$

$$\begin{bmatrix} \dfrac{dc_A'}{dt} \\ \dfrac{dT'}{dt} \end{bmatrix} = \begin{bmatrix} a_{11} & a_{12} \\ a_{21} & a_{22} \end{bmatrix} \begin{bmatrix} c_A' \\ T' \end{bmatrix} + \begin{bmatrix} 0 \\ b_2 \end{bmatrix} T_c' \qquad (98)$$

Where;

$$a_{11} = -\frac{q}{V} - k_0 e^{-E/R\overline{T}}$$

$$a_{12} = -k_0 e^{-E/R\overline{T}} \overline{c}_A \left(\frac{E}{R\overline{T}^2} \right)$$

$$a_{21} = \frac{(-\Delta H)k_0 e^{-E/R\overline{T}}}{\rho C}$$

$$a_{22} = \frac{1}{V\rho C} \left[-(wC + UA) + (-\Delta H)V\overline{c}_A k_0 e^{-E/R\overline{T}} \left(\frac{E}{R\overline{T}^2} \right) \right]$$

$$b_2 = \frac{UA}{V\rho C}$$

This system has the following parameter values (the kinetic and heat of reaction values are from Fogler, 1992, based on studies by Furusawa *er al.,* 1969)

$E_a = 32,400 \text{ Btu/lbmol}$

$k_0 = 16.96 \times 10^{12} \text{ hr}^{-1}$

$-\Delta H = 39,000 \text{ Btu/lbmol}$

$U = 75 \text{ Btu/hr.ft}^2.^\circ F$

$\rho C_p = 53.25 \text{Btu/ft}^3.^\circ F$

$R = 1.987 \text{Btu/lbmol}.^\circ F$

Assume that the reactor is to be operated with the following residence time and feed concentration

$V/F = 15 \text{ minutes} = 0.25 \text{hr}$

$C_{Af} = 0.132 \text{lbmol/ft}^3$

The stability criterion for state-space models is metric A and B.

$$A = \begin{bmatrix} a_{11} & a_{12} \\ a_{21} & a_{22} \end{bmatrix} = \begin{bmatrix} -7.9909 & -0.013674 \\ 2922.9 & 4.5564 \end{bmatrix}$$

$$B = \begin{bmatrix} b_1 \\ b_2 \end{bmatrix} = \begin{bmatrix} 0 \\ 1.458 \end{bmatrix}$$

In Figure 35, the process model was simulated from ASPEN DYNAMIC. The temperature of reactor was control variable and temperature of cooling water was manipulated variable. The AM Simulation block was process model from ASPEN DYNAMIC and MPC block was Model Predictive Control. The state-space model was input the model predictive control block in Matlab Simulink. The set-point of state-space was 50 $^\circ$C. The output process from AM Simulation and set-point of state-space model were input in MPC block. The control variable was tuning in MPC block and sent manipulated variable into the AM Simulation block.
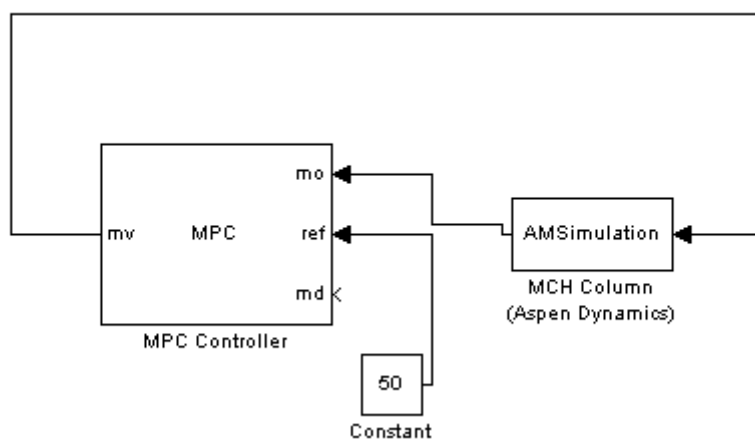
Figure 35 Block diagram model predictive control linked ASPEN DYNAMIC

The results from model predictive control are shown in Figure 37. At time 0.1 hr, the temperature of cooling water is decrease 5 ^{o}C. The process stream in the reactor is decrease from 145.2 to 144.6 ^{o}C.
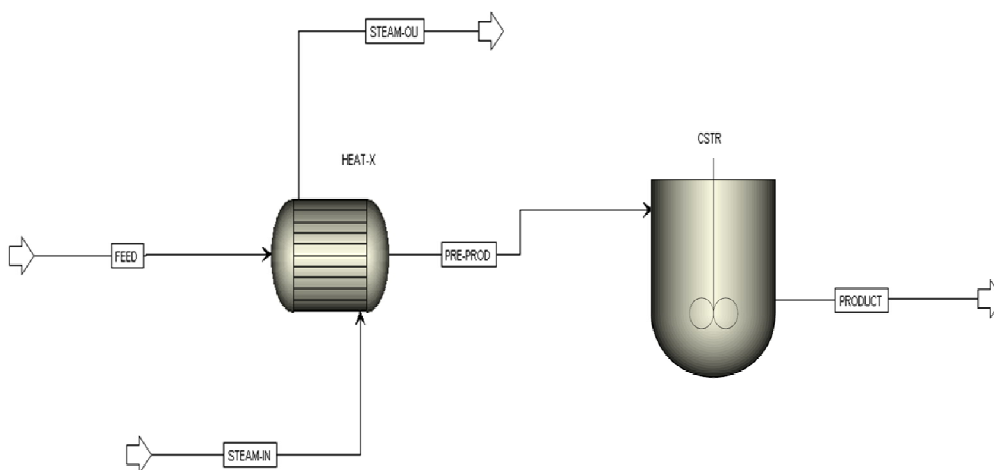
Figure 36 The CSTR with a recirculating jacket by ASPEN PLUS simulator
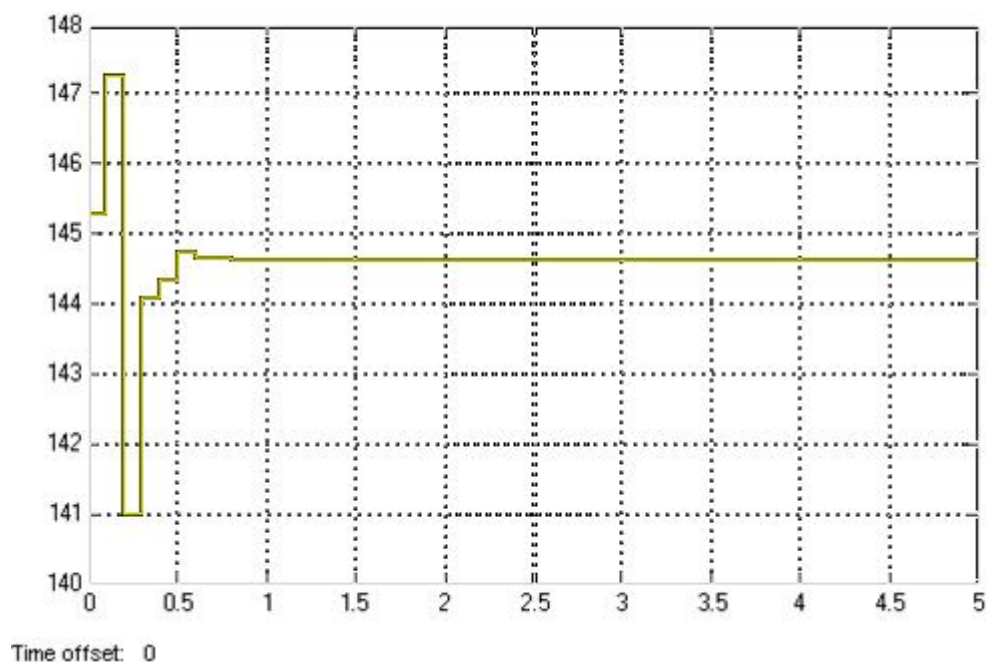
Figure 37 Responses of temperature in reactor for decreasing 5 ^{o}C of cooling water

For the temperature in the reactor, the responses of temperature were shown in Figure 37. The temperature in the reactor is changed when the temperature of cooling water was changed. From the results in Figure 37, the temperature in the reactor approaches to new steady state in 0.7 hr. The model predictive control was preliminary studied in this thesis.

5. Preliminary Process Design

The ASPEN ICARUS was used for evaluating capital projects such as renovations, revamps, expansions, and retrofits for the Chemical Process Industries. The ASPEN ICARUS is applicable to virtually any kind of in-plant process project, worldwide. The ASPEN ICARUS contains design procedures and cost data for hundreds of types of materials of construction for general process equipment, vessel shells and internals, tubing, castings, linings, packing, clad plates, piping, steel, and electrical bulks.

In this work, the ammonia process is evaluated preliminary design by ASPEN ICARUS simulator. The preliminary design for ammonia process is contained liquid volume, vessel diameter, vessel tangent to tangent height, agitator power, impeller speed, design temperature, design gauge pressure, base material thickness, fluid depth, jacket type, jacket design gauge pressure, and total weight in the Table 19.

Table 19 General design equipment data from ASPEN ICARUS

General Design Data	E007F	ABSORBER	STRIPPER	D001	D002	DESULE-R
Liquid volume (GALLONS)	634.5	2,932.6	11,037.25	634.5	2,843.7	1,043.6
Vessel diameter (Feet)	3.0	5.5	8.5	3.0	5.5	3.50
Vessel tangent to tangent height (Feet)	12.0	16.5	26.0	12.0	16.0	14.5
Agitator power (HP)	-	-	-	-	-	25.0
Impeller speed (RPM)	-	-	-	-	-	758.0
Design temperature (DEG F)	250.0	250.0	250.0	250.0	250.0	702.6
Design gauge pressure (PSIG)	35.3	35.3	35.3	35.3	35.3	774.
Base material thickness	0.3125	0.3125	0.3125	0.3125	0.3125	1.5
Fluid depth (Feet)	-	-	-	-	-	13.5
Jacket type	-	-	-	-	-	FULL
Jacket design gauge pressure (PSIG)	-	-	-	-	-	90.0
Total weight	2,600	16,500	16,500	2,600	5,500	18,400

Table 19 General design equipment data from ASPEN ICARUS (Continue)

General Design Data	DESULE-F	F-001	F-002	SPLIT-1	PURGEVIL
Liquid volume (GALLONS)	634.5	1,128.1	2,276.7	2,932.6	6,045.9
Vessel diameter (Feet)	3.0	4.0	5.0	5.5	7.0
Vessel tangent to tangent height (Feet)	12.0	12.0	15.5	16.5	21.0
Agitator power (HP)	-	-	-	-	-
Impeller speed (RPM)	-	-	-	-	-
Design temperature (DEG F)	250.0	250.0	250.0	250.0	250.0
Design gauge pressure (PSIG)	35.3	35.3	35.3	35.3	35.3
Base material thickness	0.3125	0.3125	0.3125	0.3125	0.3125
Fluid depth (Feet)	-	-	-	-	-
Jacket type	-	-	-	-	-
Jacket design gauge pressure (PSIG)	-	-	-	-	-
Total weight	2,600	3,400	4,900	5,600	8,700

CONCLUSIONS AND RECOMMENDATIONS

Conclusion

The ammonia is produced basically from water, air, and energy. The energy source is usually hydrocarbons, thus providing hydrogen as well, but may also be coal or electricity. A model was developed for the production of ammonia from natural gas reforming using ASPEN PLUS 2006.5 simulator based on real process. The capacity of this process is 461,205 metricton/year. To provide the model, several ASPEN PLUS unit operation blocks were combined and, where necessary, kinetic expressions and hydrodynamic models were developed using external FORTRAN and models from the literature. The overall process model composed desulfurization, reforming, CO conversion, CO_2 removal, methanation, synthesis and refrigeration. The simulation results in this process, the feed stream composed process air, natural gas, process steam and combustion air equal to 53000, 32000, 102041 and 178220 scmh, respectively. The product stream is the liquid ammonia equal to 3097 kmol/hr. The purity of liquid ammonia is 99.8 %.

Energy conservation is considered to be the critical stage in process design. In industrial process, the calculation of the minimum heating and cooling requirements reveal significant energy savings. The first step in the energy integration analysis is the calculation of the minimum heating and cooling requirements for a heat-exchanger network. From composite curve, the structure of heat integration that is maximum energy recovery (MER) can be constructed by ASPEN HX-NET simulator. There are 10 superstructures for heat integration. The number tenth structure is chosen in this thesis. The heat integration process reduced the energy 24.5 percent from existing process.

To analyze the controllability of hydrogen and nitrogen purity, the responses mass fractions of hydrogen and nitrogen is changed when the temperature of reactant feeds was changed. The test controllability is good responses of the process and the process can reach to the original steady-state condition.

The model predictive control is feedback control. At time 0.1 hr, the temperature of cooling water is decrease 5 ^{o}C. The process stream in the reactor is decrease from 145.2 to 144.6 ^{o}C. The temperature in the reactor approaches to new steady state in 0.7 hr. The model predictive control is preliminary studied in this thesis.

In this thesis, the ammonia process is evaluated preliminary design by ASPEN ICARUS simulator. The preliminary design for ammonia process is contained liquid volume, vessel diameter, vessel tangent to tangent height, agitator power, impeller speed, design temperature, design gauge pressure, base material thickness, fluid depth, jacket type, jacket design gauge pressure, and total weight in each reactor.

Recommendations

1. The heat integration of process can be determined by computing the minimum usage of heating and cooling utilities. Moreover, the number of heat exchanges can be reduced by breaking the heat loops. These calculations can be performed by ASPEN HX-NET.

2. In this research, only controllability of feed disturbances was considered. The process control should also investigate to provide an economic advantage by enabling closer operation to optimization constraints, decreasing the number of shut-downs and by reducing the amount of off-specification products.

3. The future works, the controllability of ammonia process model combined with heat integration process.

LITERATURE CITED

Douglas, J. M. 1988. Conceptual Design of Chemical Processes, Singapore, **McGraw Hill**, pp. 216-288.

Fogler, H. S. 1992. Elements of Chemical Reaction Eneineerinq, **2nd** ed., Prentice Hall .

Furusawa, T., H. Nishimura and T. Miyauchi 1969. "Experimental Study of a Bistable Continuous Stirred-Tank Reactor, *J. Chem. Eng. Japan,* 2(1), 95-100.

Hyman, M.H. 1967, Computational Study of a Refinery Hydrogen Plant, **H.S. Thesis**, Univ. of Calif., Berkeley,.

Linnhoff, B. 1993. "Pinch analysis—A State-of-The-Art Overview," **Trans. IchemE**., 71 Part A, p. 503.

Luyben, W.L., Tyreus B.D. and Luyben, M.L. 1999. **Plantwide Process Control**. New York, McGraw-Hill.

Martin L. 2005. "Monte Carlo adiabatic simulation of equilibrium reacting systems: The ammonia synthesis reaction" Volume 235, Issue 1, 18 August 2005, Pages 50-57

Miles D.H., Wilson G.M. 1974, "Vapor liquid Equilibrium Data for Design of Sour Water Strippers", **Annual Report to the API**.

Moe, J.H. and Gerhard, E.R. 1965, Preprint 36d, 56th National Meeting, **AIChE**, May,.

Mok, L-F1982, Sensitivity Study of Energy Consumption in Ammonia Plant Operation, **H.S. Thesis**, Univ. of California, Berkeley,.

Nielsen, A. 1968, An Investigation on Promoted Iron Catalysts for the Synthesis of Ammonia, 3rd ed., Jul. **Gjellerups Forlag**,.

Pinsent B. R., Pearson L., Roughton F. J. 1956, "The Kinetics of Combination of Carbon Dioxide with Ammonia", **Trans. Faraday Soc**., Vol. 52, 1594.

Slack, A.V. and G.R. James, ed. 1974, Ammonia, Marcel Dekker, Inc., New York,.

Trypuc M., Kielkowska U. 1996, "Solubility in the NH4HCO3 + NH4VO3 + H2O System", **J. Chem. Eng. Data**, Vol. 41, 1005.

Twygg, Martyn V. 1989. Catalyst Handbook (2nd Edition ed.). Oxford University Press. ISBN 1-874545-36-7.

Yadav, R. and R.G. Rinker 1993, Steady-State Methanation Kinetics Over a Ni/Al2O3 Catalyst, **Can. J. of Chem. Eng**., 71, 202.

APPENDICES

Appendix A

Results from ASPEN PLUS Simulation

Table A1 Results from ASPEN PLUS simulation in Desulfurization section

	C-01	C-02	C-03	C-04	C-05	C-06	C-07	C-08	C-11
Total Flow (kmol/hr)	4,000	4,000	4,000	4,000	4,000	4,000	4,000	4,000	20,000
Temperature (^{o}C)	700	367.36	600	454.58	500	465.61	400	326.92	30
Pressure (bar)	5	5	5	32.36	5	32.30	5	35.94	1
Vapor Fraction	1	1	1	1	1	1	1	1	0
Liquid Fraction	0	0	0	0	0	0	0	0	1
Solid Fraction	0	0	0	0	0	0	0	0	0

Table A1 (Continued)

	C-01	C-02	C-03	C-04	C-05	C-06	C-07	C-08	C-11
Enthalpy (cal/mol)	-51,825.81	-54,930.40	-52,792.15	-54,306.80	-53,729.48	-54,201.18	-54,639.10	-55,553.63	-68,889.63
Entropy (cal/mol-K)	-3.56	-7.45	-4.61	-10.18	-5.75	-10.03	-7.01	-12.26	-40.46
Mole Flow (kmol/hr)									
CO_2	0	0	0	0	0	0	0	0	0
CO	0	0	0	0	0	0	0	0	0
H_2	0	0	0	0	0	0	0	0	0
N_2	0	0	0	0	0	0	0	0	0
CH_4	0	0	0	0	0	0	0	0	0
AR	0	0	0	0	0	0	0	0	0
NH_3	0	0	0	0	0	0	0	0	0
H_2O	4,000	4,000	4,000	4,000	4,000	4,000	4,000	4,000	20,000
O_2	0	0	0	0	0	0	0	0	0

Table A1 (Continued)

	C-01	C-02	C-03	C-04	C-05	C-06	C-07	C-08	C-11
C2H6	0	0	0	0	0	0	0	0	0
C3H8	0	0	0	0	0	0	0	0	0
N-BUTANE	0	0	0	0	0	0	0	0	0
I-BUTANE	0	0	0	0	0	0	0	0	0
I-PENTAN	0	0	0	0	0	0	0	0	0
Mole Flow (kmol/hr)									
N-PENTAN	0	0	0	0	0	0	0	0	0
N-HEXANE	0	0	0	0	0	0	0	0	0
N-HEPTNE	0	0	0	0	0	0	0	0	0
SULFUR	0	0	0	0	0	0	0	0	0
H2S	0	0	0	0	0	0	0	0	0
H3O+	0	0	0	0	0	0	0	0	0
OH-	0	0	0	0	0	0	0	0	0

Table A1 (Continued)

	C-01	C-02	C-03	C-04	C-05	C-06	C-07	C-08	C-11
NH4+	0	0	0	0	0	0	0	0	0
NH2COO-	0	0	0	0	0	0	0	0	0
HCO3-	0	0	0	0	0	0	0	0	0
CO3--	0	0	0	0	0	0	0	0	0
NH4HCO3S	0	0	0	0	0	0	0	0	0
NH4HCO3	0	0	0	0	0	0	0	0	0

Table A1 (Continued)

	C-12	S-01	S-01A	S-01B	S-01C	S-01D	S-01E	S-01F	S-01G
Total Flow (kmol/hr)	20,000	1,427.70	1,512.47	1,512.47	1,512.47	1,512.47	1,512.46	7,176.60	7,176.60
Temperature (°C)	31.97	45	46.94	253.48	344.18	344.76	344.76	353.58	513.54
Pressure (bar)	1	38.25	38.25	38.25	38.25	51	51	35.30	35.30
Vapor Fraction	0	1	1	1	1	1	1	1	1
Liquid Fraction	1	0	0	0	0	0	0	0	0
Solid Fraction	0	0	0	0	0	0	0	0	0
Enthalpy (cal/mol)	-68,848.9	-18,141.27	-17,096.00	-14,677.37	-13,429.87	-13,429.88	-13,429.97	-46,419.63	-44,689.23
Entropy (cal/mol-K)	-40.33	-29.57	-27.75	-21.98	-19.79	-20.37	-20.37	-12.36	-9.90

Table A1 (Continued)

	C-12	S-01	S-01A	S-01B	S-01C	S-01D	S-01E	S-01F	S-01G
Mole Flow (kmol/hr)									
CO2	0	0	0	0	0	0	0	0	0
CO	0	0	0	0	0	0	0	0	0
H2	0	0	62.87	62.87	62.87	62.86	62.86	62.86	62.86
N2	0	11.29	32.31	32.31	32.31	32.31	32.31	32.31	32.31
CH4	0	1,142.87	1,143.49	1,143.49	1,143.49	1,143.49	1,143.49	1,143.49	1,143.49
AR	0	0	0.25	0.25	0.25	0.25	0.25	0.25	0.25
NH3	0	0	0	0	0	0	0	0	0
H2O	20000	0	0	0	0	0	0	5,664.14	5,664.14
O2	0	2.85	2.85	2.85	2.85	2.85	2.85	2.85	2.85
C2H6	0	252.92	252.92	252.92	252.92	252.92	252.92	252.92	252.92
C3H8	0	13.41	13.41	13.41	13.41	13.41	13.41	13.41	13.41

Table A1 (Continued)

	C-12	S-01	S-01A	S-01B	S-01C	S-01D	S-01E	S-01F	S-01G
Mole Flow (kmol/hr)									
N-BUTANE	0	0.85	0.85	0.85	0.85	0.85	0.85	0.85	0.85
I-BUTANE	0	0	0	0	0	0	0	0	0
I-PENTAN	0	0	0	0	0	0	0	0	0
N-PENTAN	0	2.67	2.67	2.67	2.67	2.67	2.67	2.67	2.67
N-HEXANE	0	0.85	0.85	0.85	0.85	0.85	0.85	0.85	0.85
N-HEPTNE	0	0	0	0	0	0	0	0	0
SULFUR	0	0.001	0.001	0.001	0.001	0	0	0	0
H2S	0	0	0	0	0	0.01	0	0	0
H3O+	0	0	0	0	0	0	0	0	0
OH-	0	0	0	0	0	0	0	0	0

Table A1 (Continued)

	C-12	S-01	S-01A	S-01B	S-01C	S-01D	S-01E	S-01F	S-01G
NH4+	0	0	0	0	0	0	0	0	0
NH2COO-	0	0	0	0	0	0	0	0	0
HCO3-	0	0	0	0	0	0	0	0	0
CO3--	0	0	0	0	0	0	0	0	0
NH4HCO3S	0	0	0	0	0	0	0	0	0
NH4HCO3	0	0	0	0	0	0	0	0	0

Table A1 (Continued)

	S-01H	S-02	S-03	S-DS01	S-PA01	S-PA2	S-PS1
Total Flow (kmol/hr)	7,176.60	84.77	2,364.63	0.01	2,364.63	2,364.63	5,664.14
Temperature (^{o}C)	503.30	116	133.12	344.76	33	482.34	360
Pressure (bar)	35.30	38.25	32.36	51	2.94	32.36	35.30
Vapor Fraction	1	1	1	1	1	1	1
Liquid Fraction	0	0	0	0	0	0	0
Solid Fraction	0	0	0	0	0	0	0
Enthalpy (cal/mol)	-44,802.86	508.64	712.19	-2,318.97	23.17	3,274.35	-55,228.67
Entropy (cal/mol-K)	-10.05	-4.29	-3.66	8.55	-0.82	0.88	-11.70

Table A1 (Continued)

	S-01H	S-02	S-03	S-DS01	S-PA01	S-PA2	S-PS1
Mole Flow (kmol/hr)							
CO2	0	0	0.71	0	0.71	0.71	0
CO	0	0	0	0	0	0	0
H2	62.86	62.87	0	0	0	0	0
N2	32.31	21.02	1,845.12	0	1,845.12	1,845.12	0
CH4	1,143.49	0.63	0	0	0	0	0
AR	0.25	0.25	22.46	0	22.46	22.46	0
NH3	0	0	0	0	0	0	0
H2O	5,664.14	0	0	0	0	0	5,664.14
O2	2.85	0	496.34	0	496.34	496.34	0
C2H6	252.92	0	0	0	0	0	0
C3H8	13.41	0	0	0	0	0	0
N-BUTANE	0.85	0	0	0	0	0	0

Table A1 (Continued)

	S-01H	S-02	S-03	S-DS01	S-PA01	S-PA2	S-PS1
Mole Flow (kmol/hr)							
I-BUTANE	0	0	0	0	0	0	0
I-PENTAN	0	0	0	0	0	0	0
N-PENTAN	2.67	0	0	0	0	0	0
N-HEXANE	0.85	0	0	0	0	0	0
N-HEPTNE	0	0	0	0	0	0	0
SULFUR	0	0	0	0	0	0	0
H2S	0	0	0	0.01	0	0	0
H3O+	0	0	0	0	0	0	0
OH-	0	0	0	0	0	0	0
NH4+	0	0	0	0	0	0	0
NH2COO-	0	0	0	0	0	0	0
HCO3-	0	0	0	0	0	0	0

Table A1 (Continued)

	S-01H	S-02	S-03	S-DS01	S-PA01	S-PA2	S-PS1
Mole Flow (kmol/hr)							
CO3--	0	0	0	0	0	0	0
NH4HCO3S	0	0	0	0	0	0	0
NH4HCO3	0	0	0	0	0	0	0

Table A2 Results from ASPEN PLUS simulation in reforming section

	S-01H	S-01I	S-04	S-04A	S-05	S-PA2
Total Flow (kmol/hr)	7,176.60	7,374.74	9,370.82	11,239.12	11,865.91	2,364.63
Temperature (°C)	503.30	502.16	795.41	1,263.74	1,085.94	482.34
Pressure (bar)	35.30	33.40	30.69	30.69	28.73	32.36
Vapor Fraction	1	1	1	1	1	1
Liquid Fraction	0	0	0	0	0	0
Solid Fraction	0	0	0	0	0	0
Enthalpy (cal/mol)	-44,802.86	-43,599.11	-26,446.00	-21,360.94	-20,522.36	3,274.35
Entropy (cal/mol-K)	-10.05	-9.05	1.85	5.69	5.71	0.88

Table A2 (Continued)

	S-01H	S-01I	S-04	S-04A	S-05	S-PA2
Mole Flow (kmol/hr)						
CO_2	0	1.43	589.16	589.87	541.42	0.71
CO	0	99.07	509.38	509.38	871.22	0
H_2	62.86	62.86	3644.71	2,652.04	3,543.78	0
N_2	32.31	32.31	32.31	1,877.43	1,877.43	1,845.12
CH_4	1,143.49	1,610.91	612.87	612.87	299.47	0
AR	0.25	0.25	0.25	22.72	22.72	22.46
NH_3	0	0	0	0	0	0
H_2O	5,664.14	5,567.92	3,982.14	4,974.82	4,709.87	0
O_2	2.85	0	0	0	0	496.34
C_2H_6	252.92	0	0	0	0	0
C_3H_8	13.41	0	0	0	0	0
N-BUTANE	0.85	0	0	0	0	0

Table A2 (Continued)

	S-01H	S-01I	S-04	S-04A	S-05	S-PA2
Mole Flow (kmol/hr)						
I-BUTANE	0	0	0	0	0	0
I-PENTAN	0	0	0	0	0	0
N-PENTAN	2.67	0	0	0	0	0
N-HEXANE	0.85	0	0	0	0	0
N-HEPTNE	0	0	0	0	0	0
SULFUR	0	0	0	0	0	0
H2S	0	0	0	0	0	0
H3O+	0	0	0	0	0	0
OH-	0	0	0	0	0	0
NH4+	0	0	0	0	0	0
NH2COO-	0	0	0	0	0	0
HCO3-	0	0	0	0	0	0

Table A2 (Continued)

	S-01H	S-01I	S-04	S-04A	S-05	S-PA2
Mole Flow (kmol/hr)						
CO3--	0	0	0	0	0	0
NH4HCO3S	0	0	0	0	0	0
NH4HCO3	0	0	0	0	0	0

Table A3 Results from ASPEN PLUS simulation in carbon monoxide conversion section

	C-09	C-10	C-13	C-14	S-05	S-05A	S-06	S-06F	S-07
Total Flow (kmol/hr)	10,000	10,000	50,000	50,000	11,865.91	12,375.30	12,375.30	12,375.30	12,375.30
Temperature (°C)	30	102.11	30	91.48	1085.94	380	447.94	210	232.77
Pressure (bar)	1	1	1	1	28.73	28.73	28.04	28.04	26.77
Vapor Fraction	0	0.09	0	0	1	1	1	1	1
Liquid Fraction	1	0.91	1	1	0	0	0	0	0
Solid Fraction	0	0	0	0	0	0	0	0	0
Enthalpy (cal/mol)	-68,889.6	-66,482.84	-68,889.6	-67,614.29	-20,522.36	-24,737.06	-24,737.06	-26,681.89	-26,681.89
Entropy (cal/mol-K)	-40.46	-33.61	-40.47	-36.63	5.71	0.13	0.39	-2.88	-2.70

Table A3 (Continued)

	C-09	C-10	C-13	C-14	S-05	S-05A	S-06	S-06F	S-07
Mole Flow (kmol/hr)									
CO_2	0	0	0	0	541.42	625.045	1,394.23	1,394.23	1,639.98
CO	0	0	0	0	871.22	1042.29	273.11	273.11	27.35
H_2	0	0	0	0	3,543.78	4,391.48	5,160.67	5,160.67	5,406.42
N_2	0	0	0	0	1,877.43	1,877.43	1,877.43	1,877.43	1,877.43
CH_4	0	0	0	0	299.47	44.78	44.78	44.78	44.78
AR	0	0	0	0	22.72	22.72	22.72	22.72	22.72
NH_3	0	0	0	0	0	0	0	0	0
H_2O	10,000	10,000	50,000	50,000	4,709.87	4,371.55	3,602.37	3,602.37	3,356.62
O_2	0	0	0	0	0	0	0	0	0
C_2H_6	0	0	0	0	0	0	0	0	0
C_3H_8	0	0	0	0	0	0	0	0	0
N-BUTANE	0	0	0	0	0	0	0	0	0

Table A3 (Continued)

	C-09	C-10	C-13	C-14	S-05	S-05A	S-06	S-06F	S-07
Mole Flow (kmol/hr)									
I-BUTANE	0	0	0	0	0	0	0	0	0
I-PENTAN	0	0	0	0	0	0	0	0	0
N-PENTAN	0	0	0	0	0	0	0	0	0
N-HEXANE	0	0	0	0	0	0	0	0	0
N-HEPTNE	0	0	0	0	0	0	0	0	0
SULFUR	0	0	0	0	0	0	0	0	0
H2S	0	0	0	0	0	0	0	0	0
H3O+	0	0	0	0	0	0	0	0	0
OH-	0	0	0	0	0	0	0	0	0
NH4+	0	0	0	0	0	0	0	0	0
NH2COO-	0	0	0	0	0	0	0	0	0
HCO3-	0	0	0	0	0	0	0	0	0

Table A3 (Continued)

	C-09	C-10	C-13	C-14	S-05	S-05A	S-06	S-06F	S-07
Mole Flow (kmol/hr)									
CO3--	0	0	0	0	0	0	0	0	0
NH4HCO3S	0	0	0	0	0	0	0	0	0
NH4HCO3	0	0	0	0	0	0	0	0	0

Table A4 Results from ASPEN PLUS simulation in carbon dioxide removal section

	S-07	S-ST15	S-ST16	S-RE1	S-RE2	S-RE3	S-RE4	S-RE5	S-RE6
Total Flow (kmol/hr)	12,375.30	10,000	10,000	10,850	12,375.30	7,267.65	13,296.52	172.21	13,124.32
Temperature (^{o}C)	232.77	20	122.06	30	40	30	30	60	60
Pressure (bar)	26.77	2	2	26.52	26.77	26.52	26.52	1.01	1.01
Vapor Fraction	1	0	0.34	0	0.73	1	0	1	0
Liquid Fraction	0	1	0.66	1	0.27	0	0.92	0	1
Solid Fraction	0	0	0	0	0	0	0.08	0	0
Enthalpy (cal/mol)	-26,681.89	-69,096.5	-63,602.70	-59,961.58	-31,121.21	-467.46	-80,597.96	-16,834.31	-57,046.01
Entropy (cal/mol-K)	-2.70	-41.16	-26.42	-37.53	-13.74	-5.13	-49.02	-0.07	-5.13

Table A4 (Continued)

	S-07	S-ST15	S-ST16	S-RE1	S-RE2	S-RE3	S-RE4	S-RE5	S-RE6
Mole Flow (kmol/hr)									
CO_2	1,639.98	0	0	0	1,639.98	18.98	16.80	10.62	6.18
CO	27.35	0	0	0	27.35	25.09	2.27	2.13	0.14
H_2	5,406.42	0	0	0	5,406.42	5,406.42	0	0	0
N_2	1,877.43	0	0	0	1,877.43	1,756.71	120.72	113.85	6.87
CH_4	44.78	0	0	0	44.78	28.59	16.19	14.16	2.03
AR	22.72	0	0	0	22.72	19.47	3.25	3.03	0.21
NH_3	0	0	0	1,627.19	0	0.50	1.77	0.09	1.68
H_2O	3,356.62	10,000	10,000	9,222.19	3,356.62	11.90	10,977.27	28.33	10,948.95
O_2	0	0	0	0	0	0	0	0	0
C_2H_6	0	0	0	0	0	0	0	0	0
C_3H_8	0	0	0	0	0	0	0	0	0
N-BUTANE	0	0	0	0	0	0	0	0	0

Table A4 (Continued)

	S-07	S-ST15	S-ST16	S-RE1	S-RE2	S-RE3	S-RE4	S-RE5	S-RE6
Mole Flow (kmol/hr)									
I-BUTANE	0	0	0	0	0	0	0	0	0
I-PENTAN	0	0	0	0	0	0	0	0	0
N-PENTAN	0	0	0	0	0	0	0	0	0
N-HEXANE	0	0	0	0	0	0	0	0	0
N-HEPTNE	0	0	0	0	0	0	0	0	0
SULFUR	0	0	0	0	0	0	0	0	0
H2S	0	0	0	0	0	0	0	0	0
H3O+	0	0	0	7.29e-12	0	0	2.72e-05	0	2.72e-05
OH-	0	0	0	0.31	0	0	0.0002	0	0.0002
NH4+	0	0	0	0.31	0	0	554.06	0	554.06
NH2COO-	0	0	0	0	0	0	14.26	0	14.26
HCO3-	0	0	0	0	0	0	526.25	0	526.25

Table A4 (Continued)

	S-07	S-ST15	S-ST16	S-RE1	S-RE2	S-RE3	S-RE4	S-RE5	S-RE6
Mole Flow (kmol/hr)									
CO3--	0	0	0	0	0	0	6.77	0	6.77
NH4HCO3S	0	0	0	0	0	0	1,056.92	2.02e-78	1,056.92
NH4HCO3	0	0	0	0	0	0	0	0	0

Table A5 Results from ASPEN PLUS simulation in methanation section

	S-1	S-9	S-9A	S-9B
Total Flow (kmol/hr)	6,996.34	7,267.65	7,179.59	183.25
Temperature (^{o}C)	280	280	280	280
Pressure (bar)	26.52	26.52	26.52	26.52
Vapor Fraction	1	1	1	1
Liquid Fraction	0	0	0	0
Solid Fraction	0	0	0	0
Enthalpy (cal/mol)	1,614.50	1,293.01	1,016.61	-21,841.76
Entropy (cal/mol-K)	-1.10	-0.90	-1.10	-4.42

Table A5 (Continued)

	S-1	S-9	S-9A	S-9B
Mole Flow (kmol/hr)				
CO2	0	18.98	0.02	0.02
CO	0	25.09	0.02	0.02
H2	5,166.03	5,406.42	5,255.37	89.34
N2	1,739.14	1,756.71	1,756.71	17.57
CH4	71.90	28.59	72.62	0.73
AR	19.27	19.47	19.47	0.19
NH3	0	0.50	0.50	0.50
H2O	0	11.90	74.89	74.89
O2	0	0	0	0
C2H6	0	0	0	0
C3H8	0	0	0	0

Table A5 (Continued)

	S-1	S-9	S-9A	S-9B
Mole Flow (kmol/hr)				
N-BUTANE	0	0	0	0
I-BUTANE	0	0	0	0
I-PENTAN	0	0	0	0
N-PENTAN	0	0	0	0
N-HEXANE	0	0	0	0
N-HEPTNE	0	0	0	0
SULFUR	0	0	0	0
H2S	0	0	0	0
H3O+	0	0	0	0
OH-	0	0	0	0
NH4+	0	0	0	0
NH2COO-	0	0	0	0

Table A5 (Continued)

	S-1	S-9	S-9A	S-9B
Mole Flow (kmol/hr)				
HCO3-	0	0	0	0
CO3--	0	0	0	0
NH4HCO3S	0	0	0	0
NH4HCO3	0	0	0	0

Table A6 Results from ASPEN PLUS simulation in synthesis and refrigeration section

	S-1	S-2	S-2B	S-2V	S-3	S-3A	S-3B	S-3C	S-3E
Total Flow (kmol/hr)	1,427.70	6,996.33	20,722.10	20,722.10	17,473.10	17,473.10	17,473.10	17,473.10	14,861.06
Temperature (°C)	45	5	30.10	180	444.14	240	83.93	39.36	39.36
Pressure (bar)	38.25	275	292	292	284	281	278	275	275
Vapor Fraction	1	1	1	1	1	1	1	0.85	1
Liquid Fraction	0	0	0	0	0	0	0	0.15	0
Solid Fraction	0	0	0	0	0	0	0	0	0
Enthalpy (cal/mol)	-18,141.27	-302.89	-1,815.86	-639.36	-758.38	-2,582.39	-3,977.66	-4,859.96	-3,056.35
Entropy (cal/mol-K)	-29.57	-10.83	-11.95	-8.79	-9.06	-12.03	-15.25	-17.89	-13.48

Table A6 (Continued)

	S-1	S-2	S-2B	S-2V	S-3	S-3A	S-3B	S-3C	S-3E
Mole Flow (kmol/hr)									
CO2	0	0	0	0	0	0	0	0	0
CO	0	0	0	0	0	0	0	0	0
H2	0	5,166.03	12,986.97	12,986.97	8,113.24	8,113.24	8,113.24	8,113.24	8,069.41
N2	11.29	1,739.14	4,772.28	4,772.28	3,147.78	3,147.78	3,147.78	3,147.78	3,129.54
CH4	1,142.87	71.90	1,540.15	1,540.15	1,540.27	1,540.27	1,540.27	1,540.27	1,516.33
AR	0	19.27	489.49	489.49	489.45	489.45	489.45	489.45	485.23
NH3	0	0	933.22	933.22	4,182.36	4,182.36	4,182.36	4,182.36	1,660.55
H2O	0	0	0	0	0	0	0	0	0
O2	2.85	0	0	0	0	0	0	0	0
C2H6	252.92	0	0	0	0	0	0	0	0
C3H8	13.41	0	0	0	0	0	0	0	0

Table A6 (Continued)

	S-1	S-2	S-2B	S-2V	S-3	S-3A	S-3B	S-3C	S-3E
Mole Flow (kmol/hr)									
N-BUTANE	0.85	0	0	0	0	0	0	0	0
I-BUTANE	0	0	0	0	0	0	0	0	0
I-PENTAN	0	0	0	0	0	0	0	0	0
N-PENTAN	2.67	0	0	0	0	0	0	0	0
N-HEXANE	0.85	0	0	0	0	0	0	0	0
N-HEPTNE	0	0	0	0	0	0	0	0	0
SULFUR	0.001	0	0	0	0	0	0	0	0
H2S	0	0	0	0	0	0	0	0	0
H3O+	0	0	0	0	0	0	0	0	0
OH-	0	0	0	0	0	0	0	0	0
NH4+	0	0	0	0	0	0	0	0	0

Table A6 (Continued)

	S-1	S-2	S-2B	S-2V	S-3	S-3A	S-3B	S-3C	S-3E
Mole Flow (kmol/hr)									
NH2COO-	0	0	0	0	0	0	0	0	0
HCO3-	0	0	0	0	0	0	0	0	0
CO3--	0	0	0	0	0	0	0	0	0
NH4HCO3S	0	0	0	0	0	0	0	0	0
NH4HCO3	0	0	0	0	0	0	0	0	0

Table A6 (Continued)

	S-3F	S-3G	S-3H	S-3I	S-3J	S-3K	S-3L	S-3M	S-4
Total Flow (kmol/hr)	20,722.03	20,722.03	14,861.06	870.82	21,437.89	13,990.24	13,570.53	14,861.06	3,179.49
Temperature (°C)	8.13	22.64	30.71	14.98	8.14	14.98	14.98	14.98	33.70
Pressure (bar)	274.5	274.5	275	275	275	275	275	275	30
Vapor Fraction	1	1	0.97	0	0.97	1	1	0.94	0
Liquid Fraction	0	0	0.03	1	0.03	0	0	0.06	1
Solid Fraction	0	0	0	0	0	0	0	0	0
Enthalpy (cal/mol)	-1,994.02	-1,877.07	-3,219.43	-15,766.62	-2,459.37	-2,717.05	-2,717.05	-3,481.72	-1,5734.52
Entropy (cal/mol-K)	-12.41	-12.01	-14.01	-44.98	-13.53	-13.03	-13.03	-14.90	-44.03

Table A6 (Continued)

	S-3F	S-3G	S-3H	S-3I	S-3J	S-3K	S-3L	S-3M	S-4
Mole Flow (kmol/hr)									
CO_2	0	0	0	0	0	0	0	0	0
CO	0	0	0	0	0	0	0	0	0
H_2	12,987.00	12,987.00	8,069.41	8.88	12,993.60	8,060.54	7,818.72	8,069.41	3.08
N_2	4,772.26	4,772.26	3,129.54	3.77	4,774.97	3,125.77	3,032.00	3,129.54	1.56
CH_4	1,540.08	1,540.08	1,516.33	5.80	1,543.05	1,510.54	1,465.22	1,516.33	5.66
AR	489.51	489.51	485.23	0.93	489.96	484.30	469.77	485.23	0.53
NH_3	933.18	933.18	1,660.55	851.45	1,636.29	809.1	784.82	1,660.55	3,168.66
H_2O	0	0	0	0	0	0	0	0	0
O_2	0	0	0	0	0	0	0	0	0

Table A6 (Continued)

	S-3F	S-3G	S-3H	S-3I	S-3J	S-3K	S-3L	S-3M	S-4
Mole Flow (kmol/hr)									
C2H6	0	0	0	0	0	0	0	0	0
C3H8	0	0	0	0	0	0	0	0	0
N-BUTANE	0	0	0	0	0	0	0	0	0
I-BUTANE	0	0	0	0	0	0	0	0	0
I-PENTAN	0	0	0	0	0	0	0	0	0
N-PENTAN	0	0	0	0	0	0	0	0	0
N-HEXANE	0	0	0	0	0	0	0	0	0
N-HEPTNE	0	0	0	0	0	0	0	0	0
SULFUR	0	0	0	0	0	0	0	0	0
H2S	0	0	0	0	0	0	0	0	0
H3O+	0	0	0	0	0	0	0	0	0

Table A6 (Continued)

	S-3F	S-3G	S-3H	S-3I	S-3J	S-3K	S-3L	S-3M	S-4
Mole Flow (kmol/hr)									
OH-	0	0	0	0	0	0	0	0	0
NH4+	0	0	0	0	0	0	0	0	0
NH2COO-	0	0	0	0	0	0	0	0	0
HCO3-	0	0	0	0	0	0	0	0	0
CO3--	0	0	0	0	0	0	0	0	0
NH4HCO3S	0	0	0	0	0	0	0	0	0
NH4HCO3	0	0	0	0	0	0	0	0	0

Table A6 (Continued)

	S-4A	S-4B	S-4C	S-4D	S-5	S-6	S-7	S-8	S-12
Mole Flow (kmol/hr)									
Total Flow (kmol/hr)	3151.66	176.24	176.24	27.83	419.71	148.41	2886.44	2886.44	62.00
Temperature (^{o}C)	33.77	33.77	25.56	25.56	14.98	25.56	105	323.67	33.70
Pressure (bar)	30	30	30	30	275	30	48.5	45	30
Vapor Fraction	0	1	0.84	0	1	1	0	1	0
Liquid Fraction	1	0	0.16	1	0	0	1	0	1
Solid Fraction	0	0	0	0	0	0	0	0	0
Enthalpy (cal/mol)	-15,733.02	-7,469.62	-8,259.52	-15,904.02	-2,717.05	-6,826.015	-66,852.14	-55,810.42	-15,734.52

Table A6 (Continued)

	S-4A	S-4B	S-4C	S-4D	S-5	S-6	S-7	S-8	S-12
Mole Flow (kmol/hr)									
CO2	0	0	0	0	0	0	0	0	0
CO	0	0	0	0	0	0	0	0	0
H2	3.05	47.38	47.38	0.03	241.82	47.35	0	0	0.06
N2	1.54	19.41	19.41	0.01	93.77	19.39	0	0	0.03
CH4	5.61	21.31	21.31	0.05	45.32	21.25	0	0	0.11
AR	0.52	4.16	4.16	0.005	14.53	4.15	0	0	0.01
NH3	3140.93	84	84	27.73	24.27	56.26	0	0	61.79
H2O	0	0	0	0	0	0	2886.44	2886.44	0
O2	0	0	0	0	0	0	0	0	0
C2H6	0	0	0	0	0	0	0	0	0
C3H8	0	0	0	0	0	0	0	0	0

Table A6 (Continued)

	S-4A	S-4B	S-4C	S-4D	S-5	S-6	S-7	S-8	S-12
Mole Flow (kmol/hr)									
N-BUTANE	0	0	0	0	0	0	0	0	0
I-BUTANE	0	0	0	0	0	0	0	0	0
I-PENTAN	0	0	0	0	0	0	0	0	0
N-PENTAN	0	0	0	0	0	0	0	0	0
N-HEXANE	0	0	0	0	0	0	0	0	0
N-HEPTNE	0	0	0	0	0	0	0	0	0
SULFUR	0	0	0	0	0	0	0	0	0
H2S	0	0	0	0	0	0	0	0	0
H3O+	0	0	0	0	0	0	0	0	0
OH-	0	0	0	0	0	0	0	0	0
NH4+	0	0	0	0	0	0	0	0	0

Table A6 (Continued)

	S-4A	S-4B	S-4C	S-4D	S-5	S-6	S-7	S-8	S-12
Mole Flow (kmol/hr)									
NH2COO-	0	0	0	0	0	0	0	0	0
HCO3-	0	0	0	0	0	0	0	0	0
CO3--	0	0	0	0	0	0	0	0	0
NH4HCO3S	0	0	0	0	0	0	0	0	0
NH4HCO3	0	0	0	0	0	0	0	0	0

Table A6 (Continued)

	S-12A	S-14	S-15	S-18	S-19
Total Flow (kmol/hr)	3117.49	3102.20	15.29	2612.04	715.86
Temperature (^{o}C)	33.70	33.27	33.27	39.36	8.13
Pressure (bar)	30	20	20	275	274.5
Vapor Fraction	0	0	1	0	0
Liquid Fraction	1	1	0	1	1
Solid Fraction	0	0	0	0	0
Enthalpy (cal/mol)	-15,734.52	-15,764.83	-9,584.82	-15,121.52	-15,929.88
Entropy (cal/mol-K)	-44.03	-44.11	-22.25	-42.93	-45.58

Table A6 (Continued)

	S-12A	S-14	S-15	S-18	S-19
Mole Flow (kmol/hr)					
CO2	0	0	0	0	0
CO	0	0	0	0	0
H2	3.02	1	2.02	43.83	6.60
N2	1.53	0.58	0.95	18.24	2.71
CH4	5.55	3.74	1.81	23.94	2.97
AR	0.52	0.25	0.26	4.22	0.45
NH3	3106.88	3096.63	10.25	2521.81	703.11
H2O	0	0	0	0	0
O2	0	0	0	0	0
C2H6	0	0	0	0	0
C3H8	0	0	0	0	0
N-BUTANE	0	0	0	0	0

Table A6 (Continued)

	S-12A	S-14	S-15	S-18	S-19
Mole Flow (kmol/hr)					
I-BUTANE	0	0	0	0	0
I-PENTAN	0	0	0	0	0
N-PENTAN	0	0	0	0	0
N-HEXANE	0	0	0	0	0
N-HEPTNE	0	0	0	0	0
SULFUR	0	0	0	0	0
H2S	0	0	0	0	0
H3O+	0	0	0	0	0
OH-	0	0	0	0	0
NH4+	0	0	0	0	0
NH2COO-	0	0	0	0	0
HCO3-	0	0	0	0	0

Table A6 (Continued)

	S-12A	S-14	S-15	S-18	S-19
Mole Flow (kmol/hr)					
CO3--	0	0	0	0	0
NH4HCO3S	0	0	0	0	0
NH4HCO3	0	0	0	0	0

Table A7 Results from ASPEN PLUS simulation in synthesis section

	S-2V	S-3	S-20	S-R3	S-R5	S-R6	S-R7	S-R9	S-RAI
Total Flow (kmol/hr)	20,722.10	17,473.11	18,625.83	20,307.66	414.44	20,307.64	20,307.72	20,307.66	20,722.16
Temperature (^{o}C)	180	444.14	348.22	289	180	379.58	448.08	180	442.79
Pressure (bar)	292	284	285	292	292	292	292	292	292
Vapor Fraction	1	1	1	1	1	1	1	1	1
Liquid Fraction	0	0	0	0	0	0	0	0	0
Solid Fraction	0	0	0	0	0	0	0	0	0
Enthalpy (cal/mol)	-639.36	-758.38	-711.44	205.21	-639.36	910.98	1,450.03	-639.36	1,408.25
Entropy (cal/mol-K)	-8.79	-9.06	-8.67	-7.12	-8.79	-5.96	-5.17	-8.79	-5.23

Table A7 (Continued)

	S-2V	S-3	S-20	S-R3	S-R5	S-R6	S-R7	S-R9	S-RAI
Mole Flow (kmol/hr)									
CO2	0	0	0	0	0	0	0	0	0
CO	0	0	0	0	0	0	0	0	0
H2	12,986.97	8,113.24	9,842.33	12,727.20	259.74	12,727.21	12,727.2	12,727.23	12,986.94
N2	4,772.28	3,147.78	3,724.14	4,676.84	95.45	4,676.84	4,676.87	4,676.83	4,772.32
CH4	1,540.15	1,540.27	1,540.27	1,509.38	30.80	1,509.35	1,509.41	1,509.34	1,540.22
AR	489.49	489.45	489.45	479.68	9.79	479.68	479.67	479.70	489.46
NH3	933.22	4,182.36	3,029.63	914.55	18.66	914.56	914.56	914.55	933.23
H2O	0	0	0	0	0	0	0	0	0
O2	0	0	0	0	0	0	0	0	0
C2H6	0	0	0	0	0	0	0	0	0
C3H8	0	0	0	0	0	0	0	0	0
N-BUTANE	0	0	0	0	0	0	0	0	0

Table A7 (Continued)

	S-2V	S-3	S-20	S-R3	S-R5	S-R6	S-R7	S-R9	S-RAI
Mole Flow (kmol/hr)									
I-BUTANE	0	0	0	0	0	0	0	0	0
I-PENTAN	0	0	0	0	0	0	0	0	0
N-PENTAN	0	0	0	0	0	0	0	0	0
N-HEXANE	0	0	0	0	0	0	0	0	0
N-HEPTNE	0	0	0	0	0	0	0	0	0
SULFUR	0	0	0	0	0	0	0	0	0
H2S	0	0	0	0	0	0	0	0	0
H3O+	0	0	0	0	0	0	0	0	0
OH-	0	0	0	0	0	0	0	0	0
NH4+	0	0	0	0	0	0	0	0	0
NH2COO-	0	0	0	0	0	0	0	0	0
HCO3-	0	0	0	0	0	0	0	0	0

Table A7 (Continued)

	S-2V	S-3	S-20	S-R3	S-R5	S-R6	S-R7	S-R9	S-RAI
Mole Flow (kmol/hr)									
CO3--	0	0	0	0	0	0	0	0	0
NH4HCO3S	0	0	0	0	0	0	0	0	0
NH4HCO3	0	0	0	0	0	0	0	0	0

Table A7 (Continued)

	S-RAO	S-RBT	S-RBO	S-RCI	S-RCO
Total Flow (kmol/hr)	19,676.85	19,676.85	19,157.26	19,157.26	18,625.76
Temperature (^{o}C)	526.14	459.20	501.21	412.50	456.06
Pressure (bar)	290	290	288	288	285
Vapor Fraction	1	1	1	1	1
Liquid Fraction	0	0	0	0	0
Solid Fraction	0	0	0	0	0
Enthalpy (cal/mol)	1,483.06	926.66	951.80	203.63	209.44
Entropy (cal/mol-K)	-5.33	-6.06	-6.16	-7.18	-7.30

Table A7 (Continued)

	S-RAO	S-RBT	S-RBO	S-RCI	S-RCO
Mole Flow (kmol/hr)					
CO2	0	0	0	0	0
CO	0	0	0	0	0
H2	11,418.96	11,418.96	10,639.59	10,639.59	9,842.34
N2	4,249.66	4,249.66	3,989.87	3,989.87	3,724.12
CH4	1,540.22	1,540.22	1,540.22	1,540.22	1,540.22
AR	489.46	489.46	489.46	489.46	489.46
NH3	1,978.54	1,978.54	2,498.13	2,498.13	3,029.63
H2O	0	0	0	0	0
O2	0	0	0	0	0
C2H6	0	0	0	0	0
C3H8	0	0	0	0	0
N-BUTANE	0	0	0	0	0

Table A7 (Continued)

	S-RAO	S-RBT	S-RBO	S-RCI	S-RCO
Mole Flow (kmol/hr)					
I-BUTANE	0	0	0	0	0
I-PENTAN	0	0	0	0	0
N-PENTAN	0	0	0	0	0
N-HEXANE	0	0	0	0	0
N-HEPTNE	0	0	0	0	0
SULFUR	0	0	0	0	0
H2S	0	0	0	0	0
H3O+	0	0	0	0	0
OH-	0	0	0	0	0
NH4+	0	0	0	0	0
NH2COO-	0	0	0	0	0
HCO3-	0	0	0	0	0

Table A7 (Continued)

	S-RAO	S-RBT	S-RBO	S-RCI	S-RCO
Mole Flow (kmol/hr)					
CO3--	0	0	0	0	0
NH4HCO3S	0	0	0	0	0
NH4HCO3	0	0	0	0	0

Table A8 Results from ASPEN PLUS simulation in refrigeration (REFRIG1) section

	S-3H	S-3M	S-10	S-10A	S-11
Total Flow (kmol/hr)	14,861.06	14,861.06	822.05	822.05	822.05
Temperature (°C)	30.71	14.98	20	-2.71	-2.71
Pressure (bar)	275	275	8.6	3.9	3.9
Vapor Fraction	0.97	0.94	0	0.09	1
Liquid Fraction	0.03	0.06	1	0.91	0
Solid Fraction	0	0	0	0	0
Enthalpy (cal/mol)	-3,219.43	-3,481.72	-16,053.40	-16,053.40	-11,311.65
Entropy (cal/mol-K)	-14.01	-14.90	-45.07	-44.99	-27.45

Table A8 (Continued)

	S-3H	S-3M	S-10	S-10A	S-11
Mole Flow (kmol/hr)					
CO2	0	0	0	0	0
CO	0	0	0	0	0
H2	8,069.41	8,069.41	0	0	0
N2	3,129.54	3,129.54	0	0	0
CH4	1,516.33	1,516.33	0	0	0
AR	485.23	485.23	0	0	0
NH3	1,660.55	1,660.55	822.05	822.05	822.05
H2O	0	0	0	0	0
O2	0	0	0	0	0
C2H6	0	0	0	0	0
C3H8	0	0	0	0	0
N-BUTANE	0	0	0	0	0

Table A8 (Continued)

	S-3H	S-3M	S-10	S-10A	S-11
Mole Flow (kmol/hr)					
I-BUTANE	0	0	0	0	0
I-PENTAN	0	0	0	0	0
N-PENTAN	0	0	0	0	0
N-HEXANE	0	0	0	0	0
N-HEPTNE	0	0	0	0	0
SULFUR	0	0	0	0	0
H2S	0	0	0	0	0
H3O+	0	0	0	0	0
OH-	0	0	0	0	0
NH4+	0	0	0	0	0
NH2COO-	0	0	0	0	0
HCO3-	0	0	0	0	0

Table A8 (Continued)

	S-3H	S-3M	S-10	S-10A	S-11
Mole Flow (kmol/hr)					
CO3--	0	0	0	0	0
NH4HCO3S	0	0	0	0	0
NH4HCO3	0	0	0	0	0

Table A9 Results from ASPEN PLUS simulation in refrigeration (REFRIG2) section

	S-4B	S-4C	S-16	S-16A	S-17
Total Flow (kmol/hr)	176.24	176.24	29.36	29.36	29.36
Temperature (°C)	33.77	25.56	20	-2.71	-2.71
Pressure (bar)	30	30	8.6	3.9	3.9
Vapor Fraction	1	0.84	0	0.09	1
Liquid Fraction	0	0.16	1	0.91	0
Solid Fraction	0	0	0	0	0
Enthalpy (cal/mol)	-7,469.62	-8,259.52	-16,053.40	-16,053.40	-11,311.65
Entropy (cal/mol-K)	-17.93	-20.54	-45.07	-44.99	-27.45

Table A9 (Continued)

	S-4B	S-4C	S-16	S-16A	S-17
Mole Flow (kmol/hr)					
CO2	0	0	0	0	0
CO	0	0	0	0	0
H2	47.38	47.38	0	0	0
N2	19.41	19.41	0	0	0
CH4	21.31	21.31	0	0	0
AR	4.16	4.16	0	0	0
NH3	84	84	29.36	29.36	29.36
H2O	0	0	0	0	0
O2	0	0	0	0	0
C2H6	0	0	0	0	0
C3H8	0	0	0	0	0
N-BUTANE	0	0	0	0	0

Table A9 (Continued)

	S-4B	S-4C	S-16	S-16A	S-17
Mole Flow (kmol/hr)					
I-BUTANE	0	0	0	0	0
I-PENTAN	0	0	0	0	0
N-PENTAN	0	0	0	0	0
N-HEXANE	0	0	0	0	0
N-HEPTNE	0	0	0	0	0
SULFUR	0	0	0	0	0
H2S	0	0	0	0	0
H3O+	0	0	0	0	0
OH-	0	0	0	0	0
NH4+	0	0	0	0	0
NH2COO-	0	0	0	0	0
HCO3-	0	0	0	0	0

Table A9 (Continued)

	S-4B	S-4C	S-16	S-16A	S-17
Mole Flow (kmol/hr)					
CO3--	0	0	0	0	0
NH4HCO3S	0	0	0	0	0
NH4HCO3	0	0	0	0	0

Appendix B
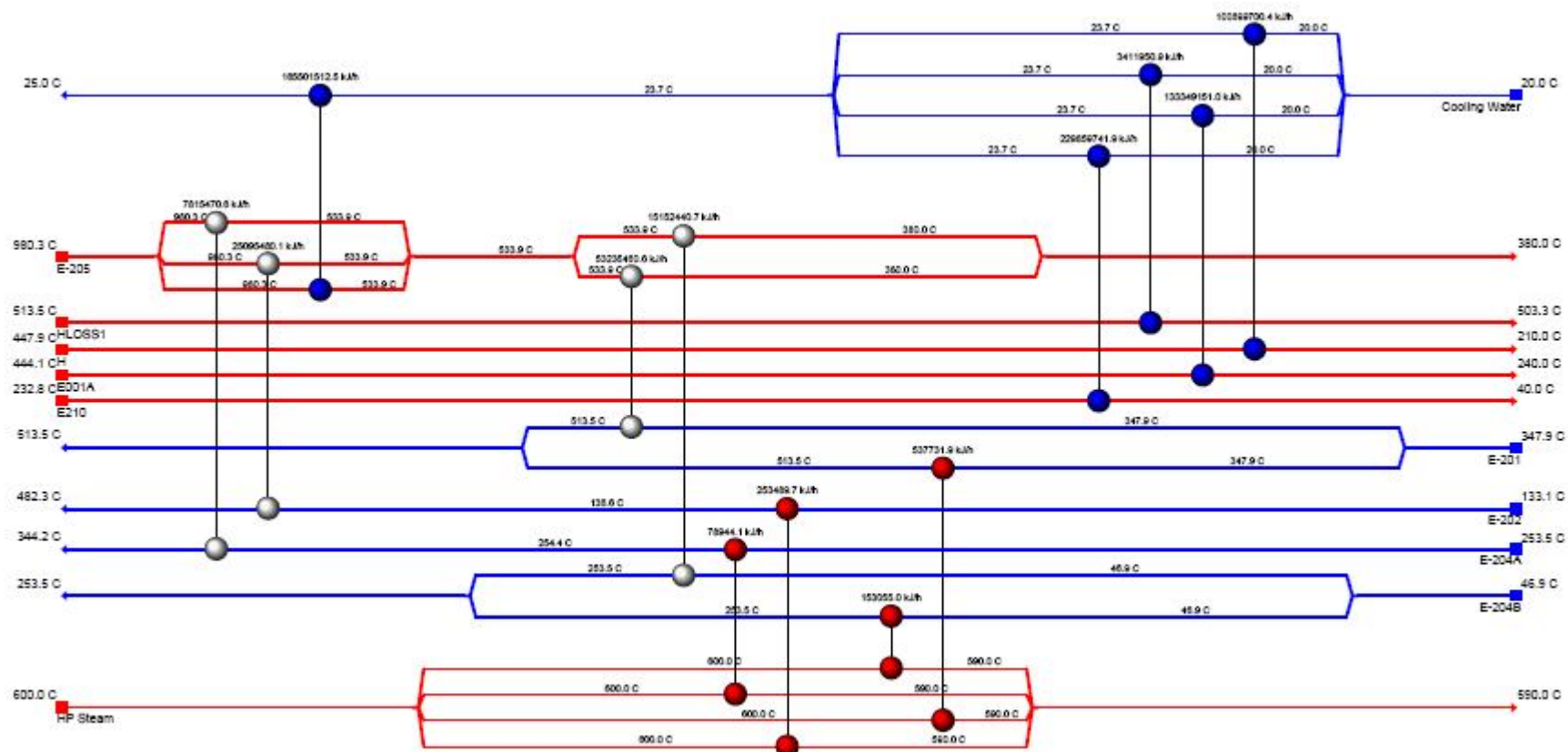
Results from ASPEN HX-NET Simulation
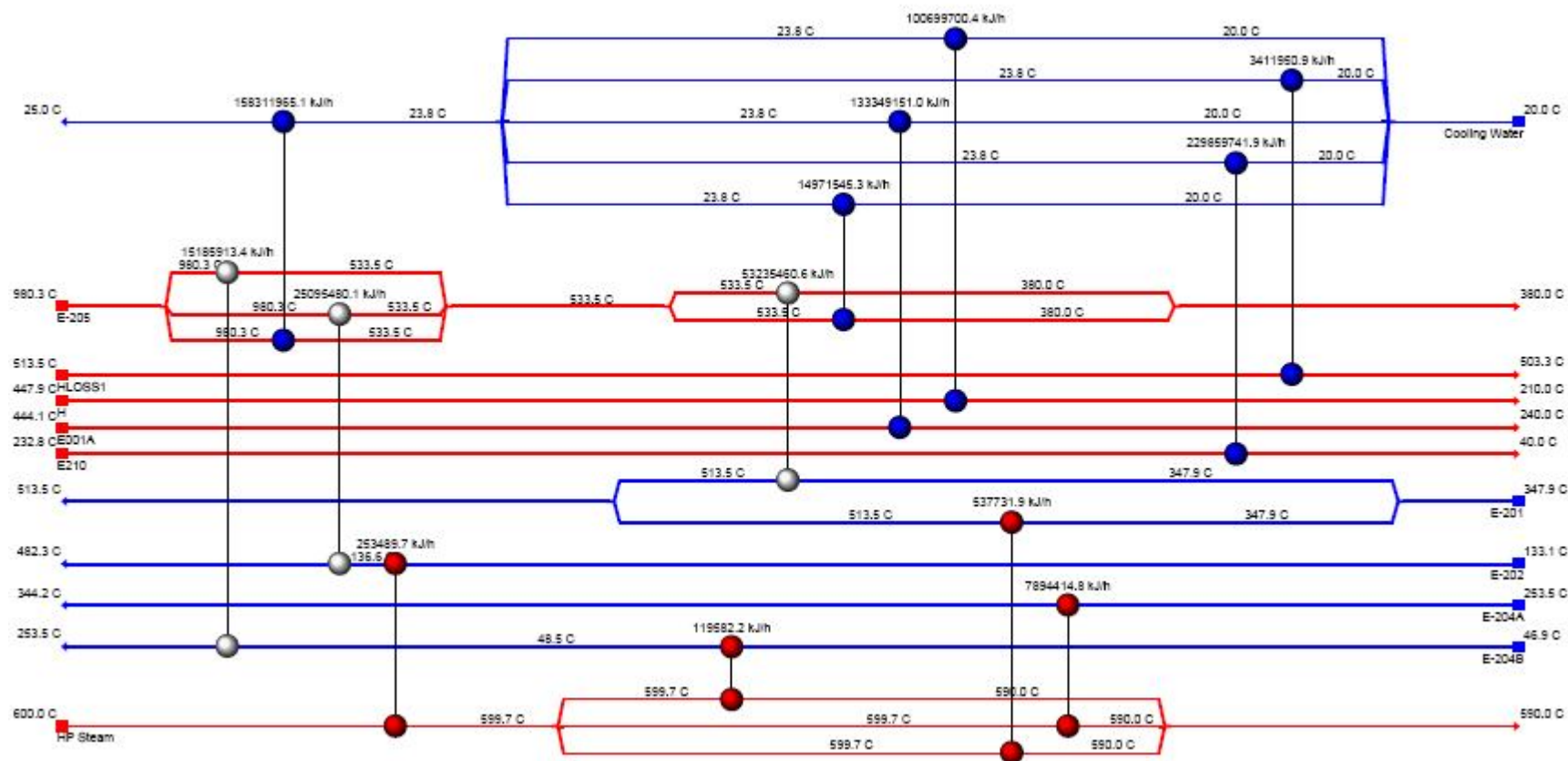
Figure B1 The superstructure number 1
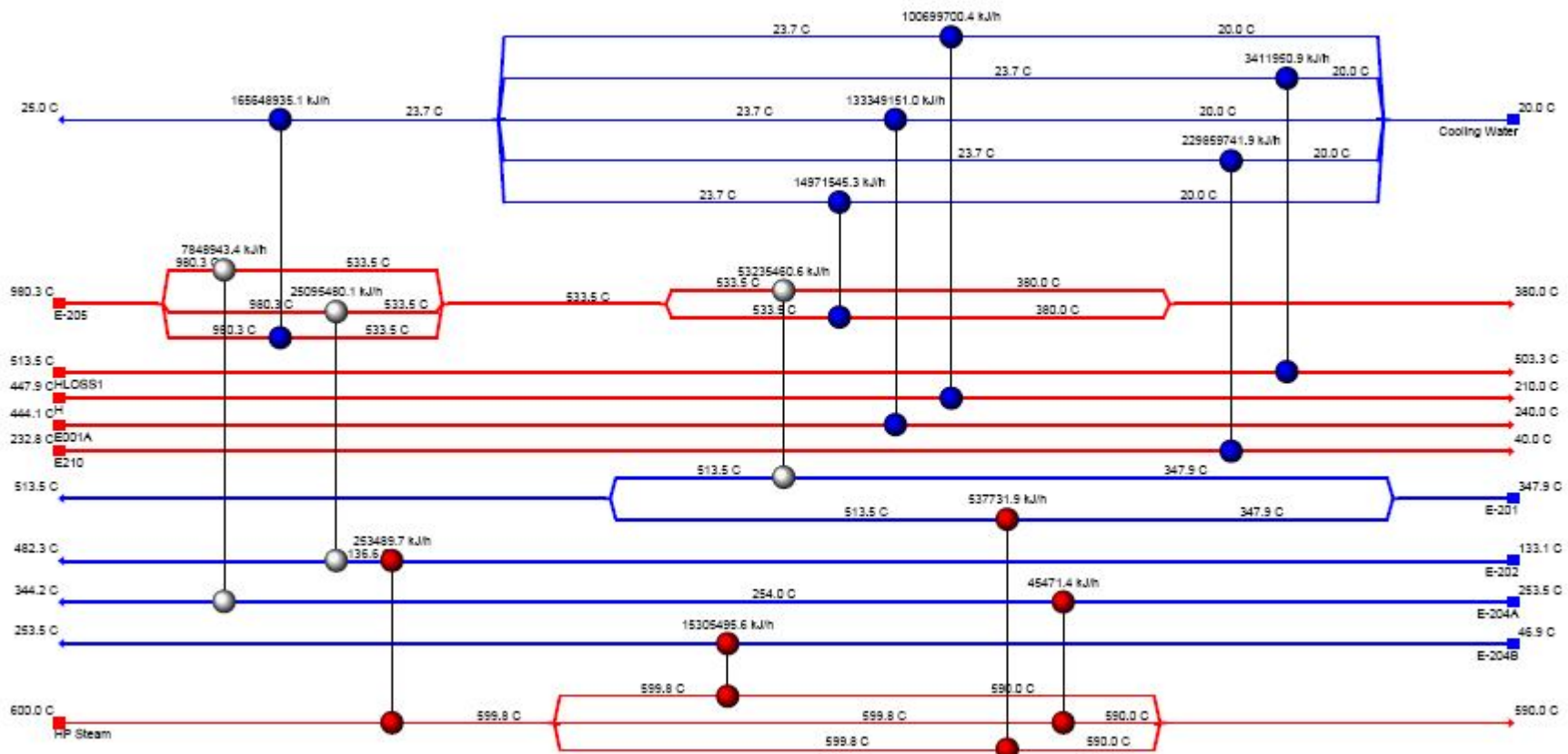
Figure B2 The superstructure number 2
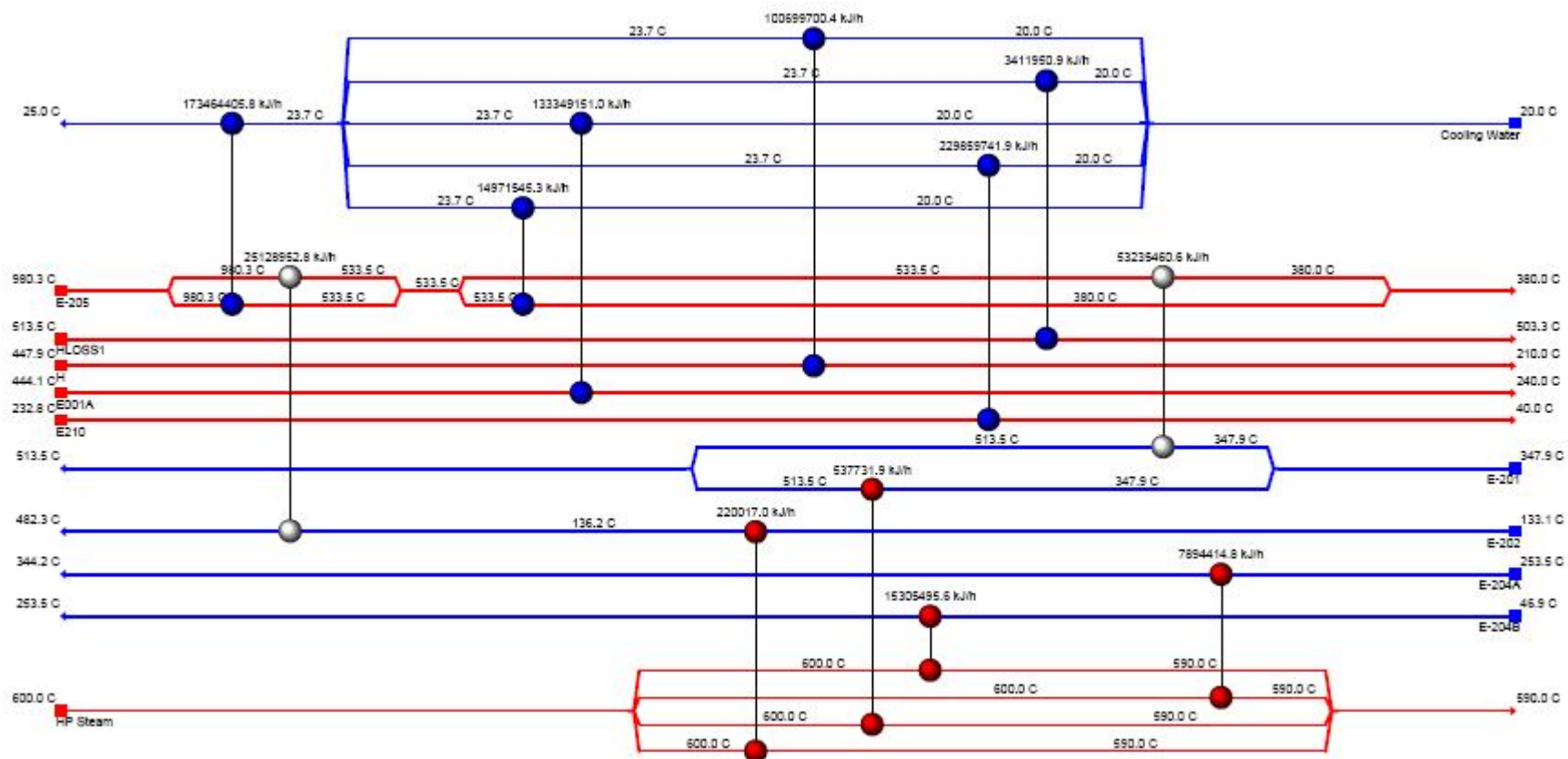
Figure B3 The superstructure number 3
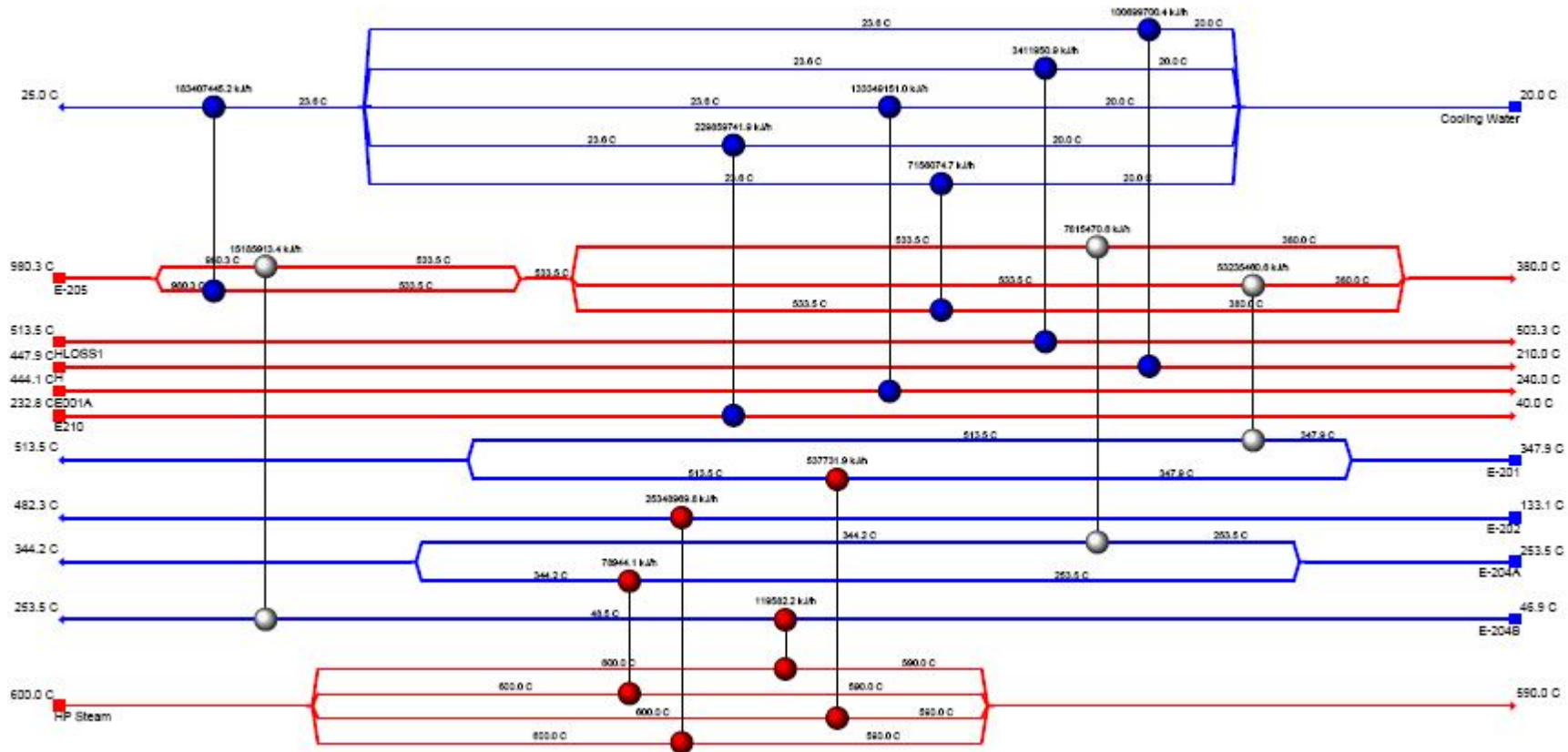
Figure B4 The superstructure number 4

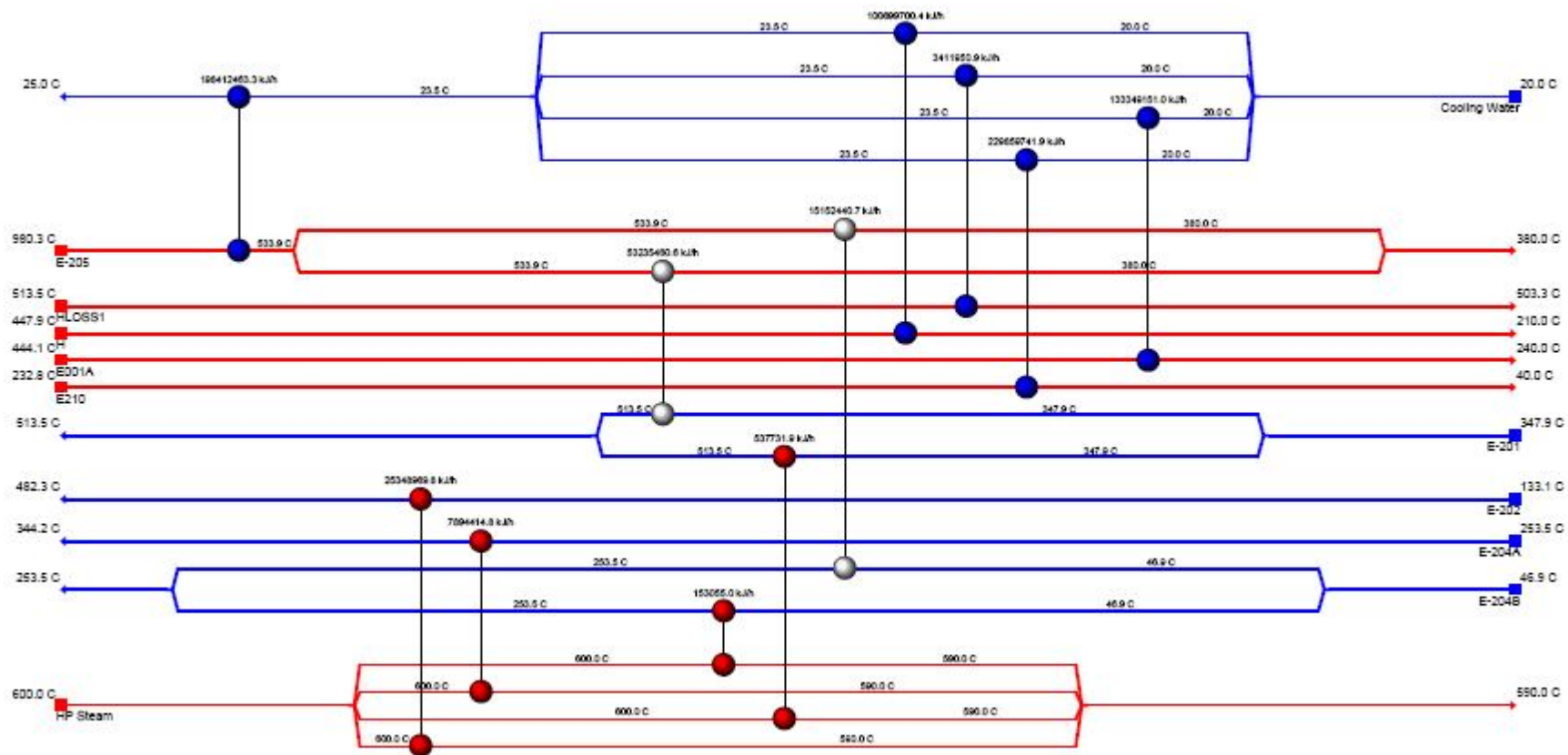**Figure B5** The superstructure number 5

Figure B6 The superstructure number 6
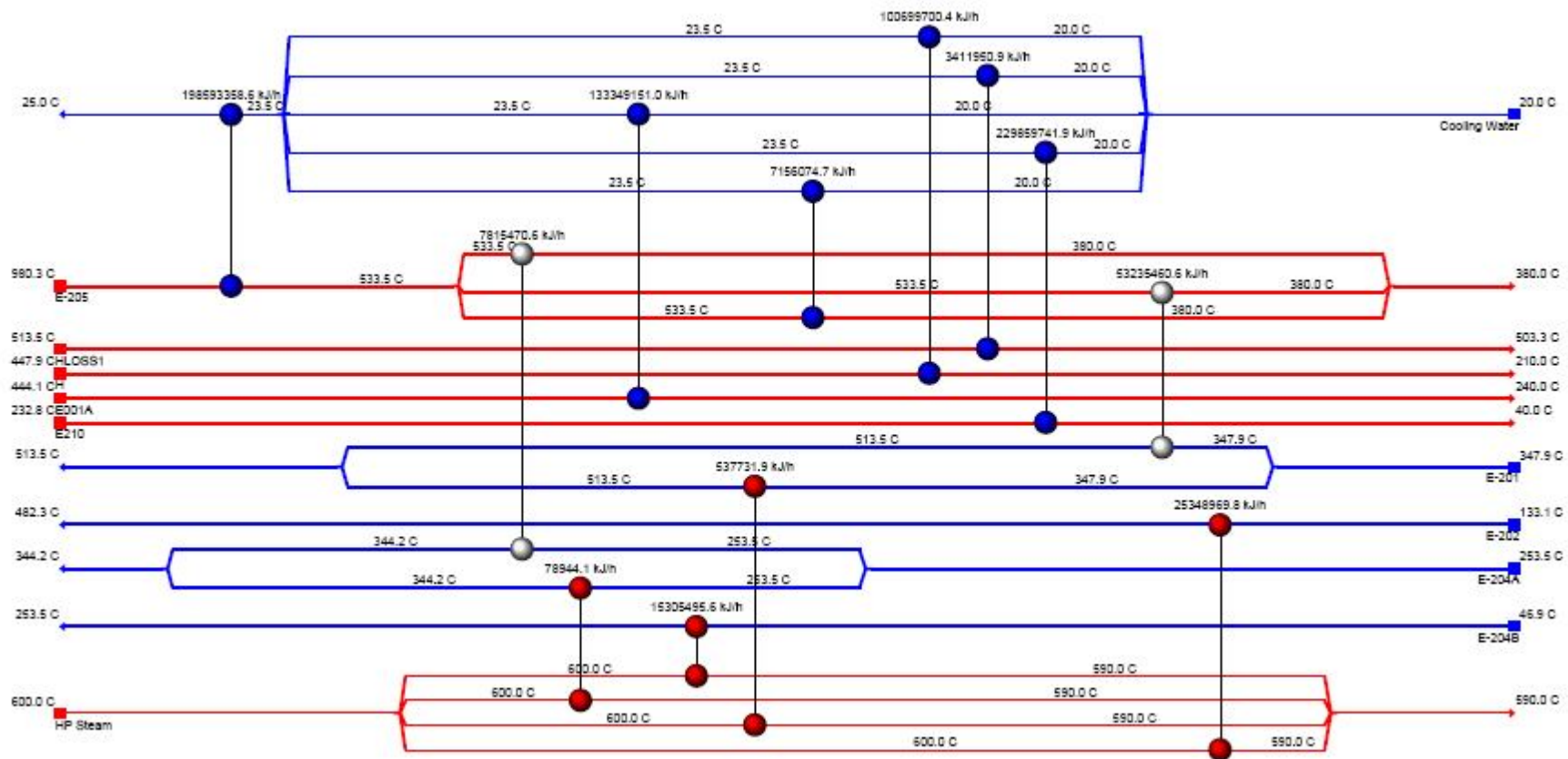
Figure B7 The superstructure number 7
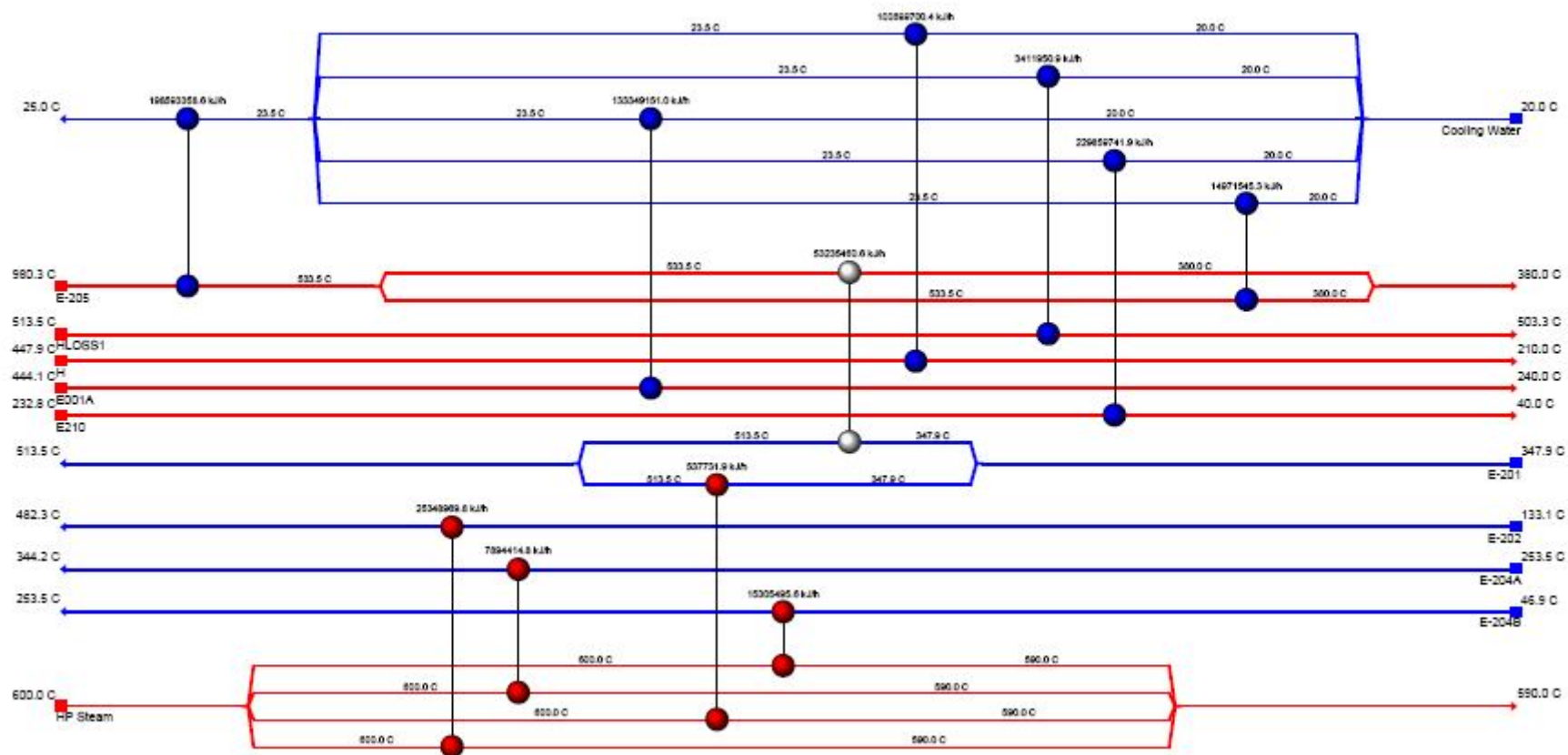
Figure B8 The superstructure number 8
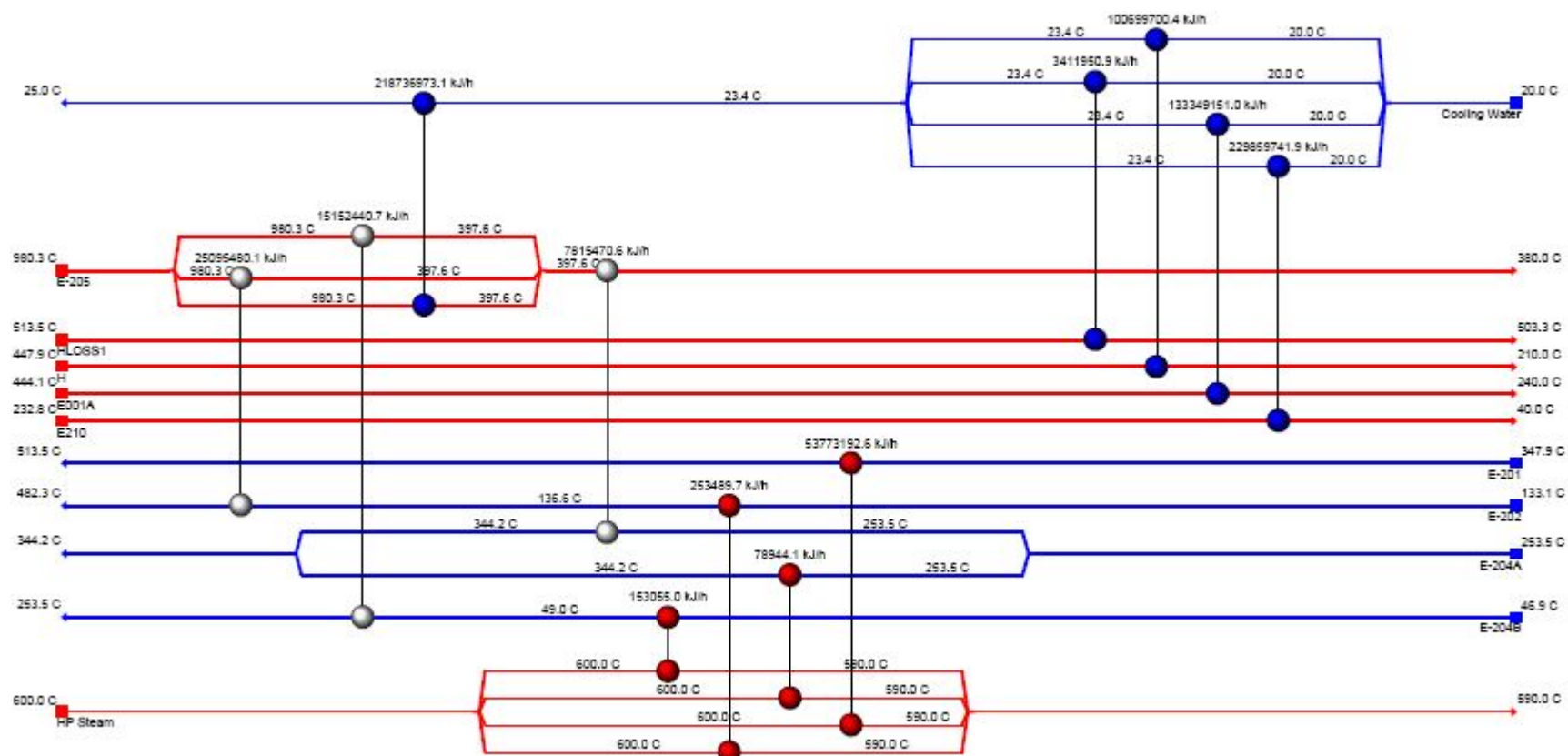
Figure B9 The superstructure number 9
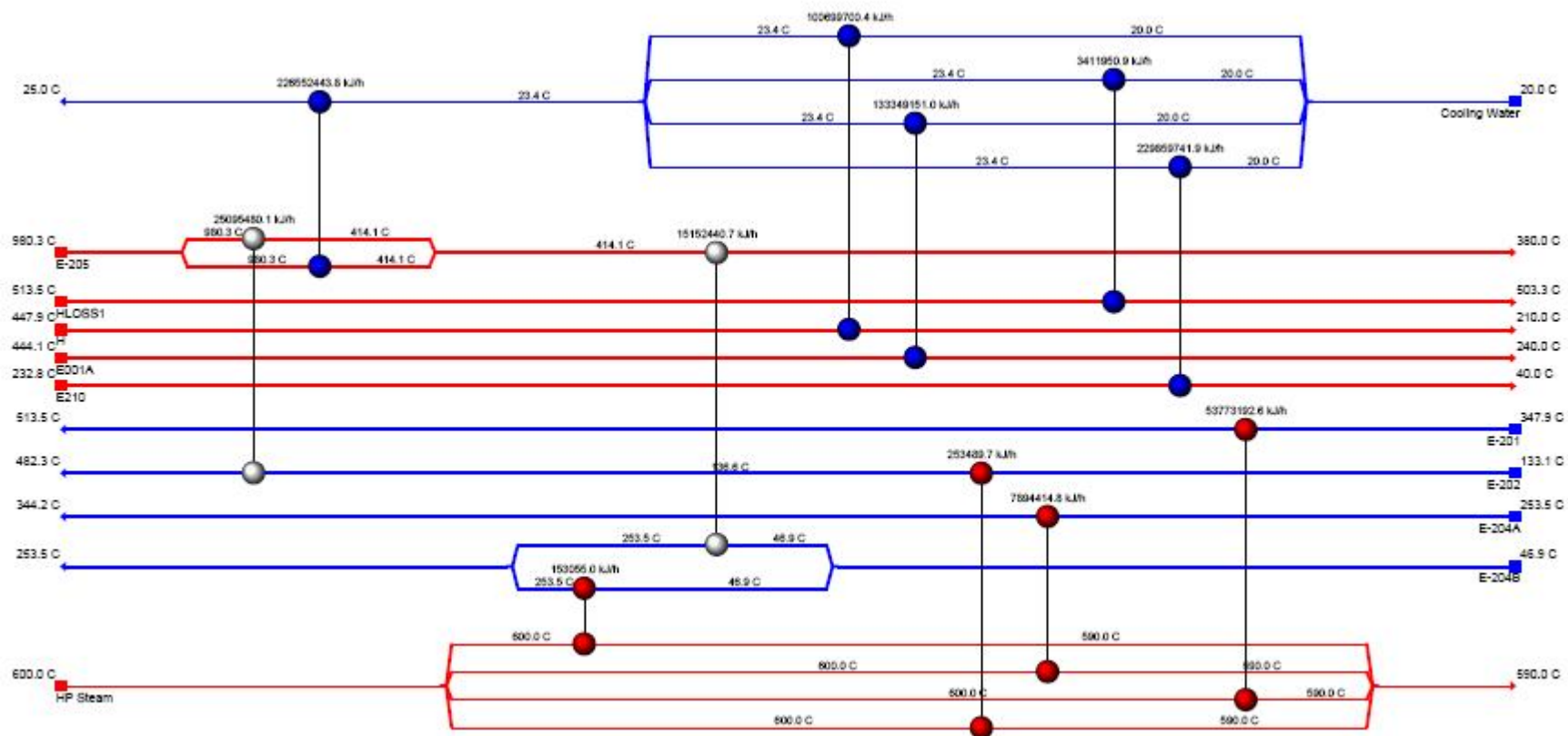
Figure B10 The superstructure number 10

Appendix C

Input condition in ASPEN PLUS

Table C1 Input conditions in ASPEN PLUS simulation

	C-01	C-03	C-05	C-07	C-11	C-13	S-01	S-01B	S-01G
Total Flow (kmol/hr)	4,000	4,000	4,000	4,000	20,000	50,000	1,427.70	1,512.47	7,176.60
Temperature (°C)	700	600	500	400	30	30	45	253.48	513.54
Pressure (bar)	5	5	5	5	1	1	38.25	38.25	35.30
Mole Flow (kmol/hr)									
CO2	0	0	0	0	0	0	0	0	0
CO	0	0	0	0	0	0	0	0	0
H2	0	0	0	0	0	0	0	62.87	62.86
N2	0	0	0	0	0	0	11.29	32.31	32.31
CH4	0	0	0	0	0	0	1,142.87	1,143.49	1,143.49

Table C1 (Continued)

	C-01	C-03	C-05	C-07	C-11	C-13	S-01	S-01B	S-01G
Mole Flow (kmol/hr)									
AR	0	0	0	0	0	0	0	0.25	0.25
NH3	0	0	0	0	0	0	0	0	0
H2O	4,000	4,000	4,000	4,000	20,000	50,000	0	0	5664.14
O2	0	0	0	0	0	0	2.85	2.85	2.85
C2H6	0	0	0	0	0	0	252.92	252.92	252.92
C3H8	0	0	0	0	0	0	13.41	13.41	13.41
N-BUTANE	0	0	0	0	0	0	0.85	0.85	0.85
I-BUTANE	0	0	0	0	0	0	0	0	0
I-PENTAN	0	0	0	0	0	0	0	0	0
N-PENTAN	0	0	0	0	0	0	2.67	2.67	2.67
N-HEXANE	0	0	0	0	0	0	0.85	0.85	0.85
N-HEPTNE	0	0	0	0	0	0	0	0	0

Table C1 (Continued)

	C-01	C-03	C-05	C-07	C-11	C-13	S-01	S-01B	S-01G
Mole Flow (kmol/hr)									
SULFUR	0	0	0	0	0	0	0.001	0.001	0
H2S	0	0	0	0	0	0	0	0	0
H3O+	0	0	0	0	0	0	0	0	0
OH-	0	0	0	0	0	0	0	0	0
NH4+	0	0	0	0	0	0	0	0	0
NH2COO-	0	0	0	0	0	0	0	0	0
HCO3-	0	0	0	0	0	0	0	0	0
CO3--	0	0	0	0	0	0	0	0	0
NH4HCO3S	0	0	0	0	0	0	0	0	0
NH4HCO3	0	0	0	0	0	0	0	0	0

Table C1 (Continued)

	S-02	S-2B	S-3J	S-7	S-PA01	S-PS1	S-ST15
Total Flow (kmol/hr)	84.77	20,722.1	21,437.89	2,886.44	2,364.63	5,664.14	10,000
Temperature (^{o}C)	116	30.1	8.14	105	33	360	20
Pressure (bar)	38.25	292	275	48.5	2.94	35.30	2
Mole Flow (kmol/hr)							
CO_2	0	0	0	0	0.71	0	0
CO	0	0	0	0	0	0	0
H_2	62.87	12,986.97	12,993.60	0	0	0	0
N_2	21.02	4,772.28	4,774.97	0	1,845.12	0	0
CH_4	0.63	1,540.15	1,543.05	0	0	0	0
AR	0.25	489.49	489.96	0	22.46	0	0
NH_3	0	933.22	1,636.29	0	0	0	0

Table C1 (Continued)

	S-02	S-2B	S-3J	S-7	S-PA01	S-PS1	S-ST15
Mole Flow (kmol/hr)							
H2O	0	0	0	2,886.44	0	5,664.14	10,000
O2	0	0	0	0	496.34	0	0
C2H6	0	0	0	0	0	0	0
C3H8	0	0	0	0	0	0	0
N-BUTANE	0	0	0	0	0	0	0
I-BUTANE	0	0	0	0	0	0	0
I-PENTAN	0	0	0	0	0	0	0
N-PENTAN	0	0	0	0	0	0	0
N-HEXANE	0	0	0	0	0	0	0
N-HEPTNE	0	0	0	0	0	0	0
SULFUR	0	0	0	0	0	0	0
H2S	0	0	0	0	0	0	0

Table C1 (Continued)

	S-02	S-2B	S-3J	S-7	S-PA01	S-PS1	S-ST15
Mole Flow (kmol/hr)							
H3O+	0	0	0	0	0	0	0
OH-	0	0	0	0	0	0	0
NH4+	0	0	0	0	0	0	0
NH2COO-	0	0	0	0	0	0	0
HCO3-	0	0	0	0	0	0	0
CO3--	0	0	0	0	0	0	0
NH4HCO3S	0	0	0	0	0	0	0
NH4HCO3	0	0	0	0	0	0	0

Input condition in ASPEN PLUS units

1. Desulfurization section

    DESULF-R (RStoic)

    Pressure = 51 bar

    Heat duty = 0 cal/sec

    Reaction $S_8 + 8H_2 \rightarrow 8H_2S$ fractional conversion 1 of S_8

    DESULF-S

    Remove H_2S

2. Reforming Section

    PREF-T (RPlug)

    Reactor type: Reactor with constant coolant temperature

    Specify heat transfer parameters 70 kcal/hr.sqm.K

    Multitubes: Number of tubes 280

    Length 10 meter

    Diameter 0.1 meter

    SREF-R (RPlug)

    Reactor type: Reactor with constant coolant temperature

    Specify heat transfer parameters 70 kcal/hr.sqm.K

    Length 4 meter

    Diameter 3 meter

3. Carbon monoxide conversion section

    HT-SHIFT (RPlug)

    Reactor type: Adiabatic reactor

    Length 15 meter

    Diameter 2 meter

    LT-SHIFT (RPlug)

    Reactor type: Adiabatic reactor

    Length 7 meter

    Diameter 3 meter

4. Carbon dioxide removal section

    ABSORBER (Flash2)

    Temperature 30 ^{o}C

    Pressure 26.5 bar

    STRIPPER (Flash2)

    Temperature 140 ^{o}F

    Pressure 1 atm

5. Methanation section

    Reactor type: Reactor with specified temperature

    Multitubes: Number of tubes 30

    Length 3 meter

    Diameter 0.1 meter

6. Ammonia synthesis

Reactor type: Adiabatic rector

Length 3.5 meter

Diameter 4 meter

CURRICULUM VITAE

NAME   : Mr. Nithi Russamee

BIRTH DATE   : March 22, 1985

BIRTH PLACE   : Bangkok, Thailand

EDUCATION   : **YEAR**   **INSTITUTE**   **DEGREE**

                2009   Kasetsart Univ.   B.Eng (Chem Eng)

SCHOLARSHIP   : Department of Chemical Engineering Kasetsart University